

**DEVELOPMENT OF A MELATONIN MEDIATED THERAPEUTIC
APPROACH IN THE TREATMENT OF INFLAMMATORY BOWEL
DISEASE**

SONI JIGNESH MOHANBHAI

*A thesis submitted for the partial fulfillment of
the degree of Doctor of Philosophy*



Institute of Nano Science and Technology
Sector-81, Knowledge City, Sahibzada Ajit Singh Nagar, Punjab, 140306
Indian Institute of Science Education and Research Mohali
Knowledge city, Sector 81, SAS Nagar, Manauli PO, Mohali 140306, Punjab, India.

March 2023

Dedicated to my beloved
parents and friends.....

Declaration

The work presented in this thesis has been carried out by me under the guidance of Prof. Surajit Karmakar at the Institute of Nano Science and Technology Mohali. This work has not been submitted in part or in full for a degree, a diploma, or a fellowship to any other university or institute. Whenever contributions of others are involved, every effort is made to indicate this clearly, with due acknowledgement of collaborative research and discussions. This thesis is a bona fide record of original work done by me and all sources listed within have been detailed in the bibliography.

SONI JIGNESH MOHANBHAI

In my capacity as the supervisor of the candidate's thesis work, I certify that the above statements by the candidate are true to the best of my knowledge.

PROF. SURAJIT KARMAKAR

Acknowledgements

I am thankful to my Ph.D. supervisor, Prof. Surajit Karmakar, for his valuable guidance and constant support during my tenure at the Institute of Nano Science and Technology-Mohali. I express my humble gratitude towards him for being a great mentor and having a wonderful personality.

I am thankful to Prof. Amitava Patra (Director, INST-Mohali) and Prof. H.N. Ghosh (Former Officiating Director, INST-Mohali) for their contestant support and encouragement. I express my sincere thanks to our collaborators, Dr. Subhasree Roy Choudhury (INST-Mohali), Prof. Shyam Sunder Sharma (NIPER-Mohali), and Prof. Prasenjit Guchhait (RCB-Faridabad).

I am thankful to the doctoral committee members, Prof. Prakash P. Neelakandan, and Prof. Ehesan Ali for their valuable suggestions and timely reviews of my progress during the Ph.D. program. I am also grateful to Prof. Sharmistha Sinha, Prof. Abir De Sarkar, Dr. Shyamlal M., and the academics department for their constant support.

I am extremely thankful to my lab members Dr. Arpit, Dr. Atul Dev, Dr. Anup, Dr. Ankur Sood, Mr. Nadim, Mr. Avinash, Mr. Vinayak, Mr. Shakti, Mr. Paras, Ms. Babita Kaundal, Ms. Shiwangi, Ms. Babita Bhatt, Mr. Mahendran, Mr. Devraj, Mr. Liku, Mrs. Angela, Ms. Nedhi, Mr. Biswaroop, Mr. Apurba, Mr. Aritra, Mr. Anirban, Ms. Priya, Ms. Sushmita, Ms. Devangi and Mr. Ayoub for their kind support.

I would like to express my thanks to Dr. Harsimran, Dr. Pooja, Dr. Vijay, Dr. Kalpesh, Dr. Ruby, Dr. Pranjali, Dr. Jijo, Dr. Vianni, Dr. Rakesh Mr. Krishna, Mr. Raghuraj, Mr. Prem, Mr. Anand, Mr. Himashu, Mr. Gaurav, Mr. Navin, Mr. Naushad, Mr. SM Rose, Mr. Shumile, Ms. Archana, Ms. Silky, Mrs. Harpreet, Ms. Simer, Mrs. Ankush, Mr. Ajay. Ms. Tashmeen, Ms. Archita, Ms. Jigmat, and Ms. Mimansa, who were kind and helpful during my tenure at INST-Mohali.

I would like to thank my parents and other family members for their kind support and encouragement throughout my journey. I would also like to thank MAA Foundation Vapi for helping financially during my tough days.

Finally, I'd like to express my heartfelt gratitude and appreciation to the animals that gave their lives to help me complete this thesis.

SONI JIGNESH MOHANBHAI

List of Publications

Relevant to thesis

1. M.N. Sardoiwala, **S.J. Mohanbhai**, A.C. Kushwaha, A. Dev, L. Biswal, S.S. Sharma, S.R. Choudhury, S. Karmakar, Melatonin mediated inhibition of EZH2-NOS2 crosstalk attenuates inflammatory bowel disease in preclinical in vitro and in vivo models, Life Sciences, 302 (2022) 120655.
2. **S.J. Mohanbhai**, M.N. Sardoiwala, S. Gupta, N. Shrimali, S.R. Choudhury, S.S. Sharma, P. Guchhait, S. Karmakar, Colon targeted chitosan-melatonin nanotherapy for preclinical Inflammatory Bowel Disease, Biomaterials Advances, 136 (2022) 212796.
3. **S.J. Mohanbhai**, M.N. Sardoiwala, S.R. Choudhury, S.S. Sharma, S. Karmakar, Melatonin-loaded chitosan nanoparticles endows nitric oxide synthase 2 mediated anti-inflammatory activity in inflammatory bowel disease model, Mater Sci Eng C Mater Biol Appl, 124 (2021) 112038.

Other publications

4. A. Dev, M.N. Sardoiwala, A. Sharma, **S.J. Mohanbhai**, S. Karmakar, S.R. Choudhury, Nanoacetylated N -(4-Hydroxyphenyl) Retinamide Modulates Histone Acetylation–Methylation Epigenetic Disparity to Restrict Epithelial–Mesenchymal Transition in Neuroblastoma, ACS Medicinal Chemistry Letters, 13 (2022).
5. A. Dev, M.N. Sardoiwala, B. Mrunalini, **S.J. Mohanbhai**, S.R. Choudhury, S. Karmakar, 4-Oxo-fenretinide-Loaded Human Serum Albumin Nanoparticles for the Inhibition of Epithelial–Mesenchymal Transition in Neuroblastoma Xenografts, ACS Applied Nano Materials, 5 (2022).
6. M.N. Sardoiwala, **S.J. Mohanbhai**, S. Karmakar, S.R. Choudhury, Hytrin loaded polydopamine-serotonin nanohybrid induces IDH2 mediated neuroprotective effect to alleviate Parkinson's disease, Materials Science and Engineering: C, (2021) 112602.
7. A. Bhargava, A. Dev, **S.J. Mohanbhai**, V. Pareek, N. Jain, S.R. Choudhury, J. Panwar, S. Karmakar, Pre-coating of protein modulate patterns of corona formation, physiological stability and cytotoxicity of Silver nanoparticles, Science of The Total Environment, 772 (2021) 144797.
8. A. Kushwaha, Kaundal, A. Dev, A. Srivastava, **S.J. Mohanbhai**, S. Karmakar, S.R. Choudhury, PRT4165 nanocomposite promoting epigenetic retardation through proteasomal depletion of polycomb in acute myeloid leukemia, Applied Materials Today, 21 (2020) 100847.

9. A. Kushwaha, **S.J. Mohanbhai**, M.N. Sardoiwala, A. Sood, S. Karmakar, S.R Choudhury, Epigenetic Regulation of Bmi1 by Ubiquitination and Proteasomal Degradation Inhibit Bcl-2 in Acute Myeloid Leukemia, ACS Applied Materials & Interfaces, 12 (2020).
10. A. Dev, **S.J. Mohanbhai**, A.C. Kushwaha, A. Sood, M.N. Sardoiwala, S.R. Choudhury, S. Karmakar, κ -carrageenan-C-phycoyanin based smart injectable hydrogels for accelerated wound recovery and real-time monitoring, Acta Biomaterialia, 109 (2020) 121-131.
11. Kaundal, A. Srivastava, A. Dev, **S.J. Mohanbhai**, S. Karmakar, S. Roy Choudhury, Nanoformulation of EPZ011989 Attenuates EZH2–c-Myb Epigenetic Interaction by Proteasomal Degradation in Acute Myeloid Leukemia, Molecular Pharmaceutics, 17 (2020).
12. A. Sood, A. Dev, **S.J. Mohanbhai**, N. Shrimali, M. Kapasiya, A.C. Kushwaha, S. Roy Choudhury, P. Guchhait, S. Karmakar, Disulfide-Bridged Chitosan-Eudragit S-100 Nanoparticles for Colorectal Cancer, ACS Applied Nano Materials, 2 (2019) 6409-6417.
13. S. Singh, **S.J. Mohanbhai**, V. Tiwari, R. Chaturvedi, S. Khurana, S. Shukla, Axin-2 Knockdown Promote Mitochondrial Biogenesis and Dopaminergic Neurogenesis by regulating Wnt/ β -catenin Signaling in Rat Model of Parkinson's disease, Free Radical Biology and Medicine, 129 (2018).

List of abbreviations

- **5-ASA:** 5- Amino Salicylates
- **6-MP:** 6-Mercaptopurine
- **AB:** Alcian Blue
- **AD:** Anno Domini
- **ANOVA:** Analysis of variance
- **APC:** Allophycocyanin
- **bp:** Base pair
- **BSA:** Bovine Serum Albumin
- **CAF:** Central Animal facility
- **CCL2:** C-C motif chemokine ligand 2
- **CD:** Crohn's Disease
- **CDH1:** Cadherin 1
- **CLSM:** Confocal Laser Scanning Microscopy
- **CO2:** Carbon Dioxide
- **CPCSEA:** Committee for Purpose of Control and Supervision of Experiments on Animals
- **CSNPs:** Chitosan nanopartilces
- **CXCL8:** C-X-C motif chemokine ligand 8
- **CyD:** Cyclin D1
- **DAI:** Disease Activiyy Index
- **DAPI:** 4', 6- diamidino-2-phenylindole
- **DLS:** Dynamic Light scattering
- **DMEM:** Dulbecco's Modified Eagle Medium
- **DMPs:** Differentially Methylated Positions
- **DMSO:** Dimethyl Sulphoxide
- **DNA:** Deoxyribonucleic acid
- **DSS:** Dextran Sulfate Sodium,
- **ECL:** Enhanced Chemiluminescence
- **ECM:** Extracellular Matrix
- **EDTA:** Ethylenediaminetetraacetic acid
- **EUCSNPs:** Eudragit coated chitosan nanopartilces

- **EZH2:** Enhancer of Zeste Homolog 2
- **FBS:** Fetal bovine serum
- **FDA:** Food and Drug Administration
- **FESEM:** Scannine Electron Microscope
- **FITC:** Fluorescein Isothiocyanate
- **FT-IR:** Fourier transform infrared spectroscopy
- **GIT:** Gastrointestinal Tract
- **H&E:** Haematoxylin and Eosin
- **H2O2:** Hydrogen Peroxide
- **H3k27Me3:** Tri-Methyl-Histone H3 (Lys27)
- **HIOMT:** Hydroxyindole-O-methyltransferase
- **HLA:** Human Leukocyte Antigens
- **HRP:** Horseradish Peroxidase
- **IAEC:** Institutional Animal Ethic Committee
- **IBD:** Inflammatory Bowel Disease
- **ICAM-1:** Intercellular adhesion molecule
- **ICG:** Indocyanine Green
- **IFN:** Interferons
- **IgG1:** Immunoglobulin G 1
- **IL-1 β :** Interleukin 1- β
- **IL-13:** Interleukin-13
- **IL-23R:** Interleukin 23 Receptor
- **IL-4:** Interleukin-4
- **IL-5:** interleukin-5
- **IL-6:** Interleukin-6
- **IL-10:** Interleukin-10
- **ip:** Intraperitoneal
- **iv:** Intravenous
- **IVIS:** in vivo imaging system
- **KBr:** Potassium Bromide
- **kDa:** Kilo Dalton
- **LiCl:** Lithium Chloride

- **LPS:** Lipopolysaccharide
- **Mel-CSNPs:** Melatonin Loaded Chitosan nanopartilces
- **Mel-EUCSNPs:** Melatonin loaded Eudragit coated chitisan nanopartilces
- **MHC:** Major Histocompatibility Complex
- **mM:** Mili Molar
- **MMPs:** Matrix Metalloproteinase
- **MPO:** Myeloperoxidase
- **MT1:** Melatonin receptor-1
- **MTT:** 3-[4,5-dimethylthiazol-2-yl]-2,5-diphenyltetrazolium bromide
- **mV:** Millivolts
- **NaCl:** Sodium Choride
- **NF- κ B:** Nuclear factor kappa-light-chain-enhancer of activated B cells
- **NFR:** Nuclear Fast Red
- **nm:** Nano molar
- **NOD:** Nucleotide-binding oligomerization domain
- **NO:** Nitric Oxide
- **NOS2:** Nitric Oxide Synthase 2
- **NSAIDs:** on-steroidal anti-inflammatory drugs
- **OCT:** Optimal Cutting Temperature
- **OD:** Optical Density
- **PBMC:** Peripheral Blood Mononuclear Cell
- **PBS:** Phosphate Buffer Saline
- **PGE2:** Prostaglandin E2
- **PLA:** Polylactic acid
- **PLGA:** Poly(lactic-co-glycolic acid)
- **PMSF:** Phenylmethylsulfonyl fluoride
- **RO:** Reverse Osmosis
- **S.E.M:** Standard Error of Mean
- **Si RNA:** Silencing RNA
- **SNPs:** Single Nucleotide Polymorphisms
- **STPP:** Sodium tripolyphosphate
- **TB:** Toluidine Blue

- **TEM:** Transmission Electron Microscope
- **Th:** T-helper
- **TLR:** Toll Like receptor
- **TNF- α :** Tumor Necrosis Factor- α
- **TRAF6:** Tumor necrosis factor receptor associated factor 6
- **Treg:** T regulatory
- **TRITC:** Tetramethylrhodamine Isothiocyanate
- **UC:** Ulcerative colitis
- **μg :** Micro gram
- **μM :** Micro Molar
- **μM :** Micro molar
- **VCAM-1:** Vascular Cell Adhesion Molecule
- **XRD:** X-ray diffraction
- **$\beta 7$ I -tsNPs:** $\beta 7$ Integrin targeted liposomal nanoparticles

List of Figures

| Number | Name | Page Number |
|-------------------|----------------------------------------------------------------------------------------------------------------------------------------------------------------------------------------------------------------------------------------------------------------------------------------------------------------------------------------------------------------------------------------------------|-------------|
| Figure 1.1 | Schematic representation of components of inflammatory pathway: (i) inflammatory inducers (ii) sensors (iii) inflammatory mediators and, (iv) target tissues. | 9 |
| Figure 1.2 | Schematic representation of diseases linked to non-resolving inflammation. | 11 |
| Figure 1.3 | Schematic representation of pathophysiology of Ulcerative Colitis. : Disturbance of tight junction and mucus layer followed by immune cell activation and increase vascular permeability | 15 |
| Figure 3.1 | <i>In vitro</i> therapeutic effect of melatonin: (A) Nitrite estimation in LPS stimulated RAW 264.7 (B) Western blot analysis for determining effect of Melatonin and EPZ011989 on protein expression when challenged with LPS (C,D,E) Quantification for protein expression analysis of EZH2, NOS2 and H3K27me3. (*p≤0.05) | 51 |
| Figure 3.2 | EZH2-NOS2 crosstalk: (A) Immuno-precipitation analysis for protein interaction study in Raw 264.7 murine macrophages (B) Agarose gel electrophoresis of PCR products of ChIP assay (C) ChIP-Quantitative PCR result shows EZH2 binding on NOS2 promoter regions (PS1=Promoter Sequence 1 and PS2=Promoter Sequence 2) (D) Schematic representation of EZH2 binding to promoter sequence. (*p≤0.05) | 53 |
| Figure 3.3 | <i>In vivo</i> mice model and therapeutic effect of melatonin: (A) Percentage body weight change in BALB/c mouse, (B) Disease Activity Index for assessing severity of inflammation in mouse daily (C-D) Change in colon length analysis. (*p≤0.05) | 54 |

| | | |
|--------------------|--------------------------------------------------------------------------------------------------------------------------------------------------------------------------------------------------------------------------------------------------------------------------------------------------------------------------------|-----------|
| Figure 3.4 | Inflammatory gene expression analysis: (A) Myeloperoxidase activity study in colon tissue homogenate (B-D) Gene expression study of IL1 β , IL6 and NF κ B in colon tissue homogenates. (*p \leq 0.05) | 56 |
| Figure 3.5 | Protein expression analysis: (A) Western blot analysis in colon tissue homogenates (B-D) Quantification for protein expression analysis of EZH2, H3K27me3 and NOS2. (*p \leq 0.05) | 57 |
| Figure 3.6 | IHC analysis: Immuno-histochemical analysis of EZH2 (Red) expression in the colonic tissue section using DAPI (Blue) counterstained for nucleus. (*p \leq 0.05) (Scale: 10 μ m) | 58 |
| Figure 3.7 | NOS2 expression analysis: Immuno-histochemical analysis of NOS2 (Red) expression in the colonic tissue section using DAPI (Blue) counterstained for nucleus. (*p \leq 0.05) (Scale: 10 μ m) | 58 |
| Figure 3.8 | Colocalization analysis: Immuno-histochemical co-localisation study of EZH2 and NOS2 in a cross section of colon tissue (Red- EZH2, Green- NOS2 and Blue-Nucleus). | 59 |
| Figure 3.9 | Pathological demarcation study: Haematoxylin& Eosin staining for evaluation of colonic tissue section (5 μ M) for analysis of pathological alterations due inflammatory condition. (*p \leq 0.05) Scale: 200 μ m, 100 μ m, 50 μ m) (Arrow head shows immune cells infiltration and arrow shows crypt damage) | 60 |
| Figure 3.10 | Mast cells determination: Toluidine Blue stain examining localisation of mast cells (Violet) due inflammatory condition in colonic tissue section (5 μ M). | 60 |
| Figure 3.11 | Goblet cells examination: Alcian Blue and Nuclear Fast staining for evaluation of colonic tissue section (5 μ M) for analysis of pathological alterations due inflammatory condition on specifically Goblets cells responsible for mucous secretion. | 61 |

(*p≤0.05) (Scale: 200µm, 100µm, 50µm)

- Figure 4.1a** Characterization of nanoparticles (A) Dynamic Light scattering measurement of mean hydrodynamic size of chitosan nanoparticles (CSNPs) and Melatonin loaded chitosan nanoparticles (Mel-CSNPs) (B)-Surface zeta potential measurement of CSNPs ($+ 36 \pm 2\text{mV}$) and Mel-CSNPs ($+35 \pm 1\text{mV}$) and (C)TEM images of CSNPs and Mel-CSNPS shows nano-sized particles. **68**
- Figure 4.1b** Field emission scanning electron microscopy (FESEM) of CSNPS (A) and Mel-CSNPs (B). (Scale bar = 500nm) **68**
- Figure 4.2** (A)-FTIR spectra of CSNPs, Mel-CSNPs, Melatonin and Chitosan (B) - X-RD diffraction spectra of CSNPs, Mel-CSNPs, Melatonin and Chitosan. **70**
- Figure 4.3a** (A) *In-vitro* drug release indicates biphasic release, (B) MTT assay for biocompatibility of nanoformulation, (C) Nitrite estimation for anti-inflammatory activity assessment,(D) Confocal laser microscopy (CLSM) images show major cytoplasmic accumulation of nanoparticles.(*p≤0.05, **p≤0.001 and ***p≤0.0001)(Scale bar= 20 µm) **71**
- Figure 4.3b** *In-vitro* drug release indicating initial burst release followed by gradual release pattern at pH 4.5 **71**
- Figure 4.4** CLSM micrographs reflect anti-inflammatory action of Mel-CSNPs by showing reduction in nuclear translocation of NF-kB p65against LPS stimulation. **73**
- Figure 4.5** Haemolysis analysis (A) Percentage lysis of RBC upon treatment with nanoformulations (B) Images of blood sample after treatment with nanoformulations. **74**
- Figure 4.6** (A) In-vivo bio-distribution study of Indocyanine green (ICG)-tagged Mel-CSNPs and (B-C)–Ex-vivo bio-distribution of ICG- **75**

Mel-CSNPs, (a-stomach, b-deodenum, c-ileum+jejunum, d-colon, e- spleen, f- heart, g-kidney, h- brain and i-liver) show good bio-distribution and clearance path of nanoparticles

- Figure 4.7** (A)- Disease Activity Index, (B) Percentage change in body weight,(C-D) Colon length evaluation, (E) Myeloperoxidase (MPO) assay in colonic tissue homogenates and(F)Gene expression of analysis in colonic tissue sample of mice confirms anti-inflammatory potential of Mel-CSNPs. (* $p \leq 0.05$, ** $p \leq 0.001$, *** $p \leq 0.0001$ and ns: non-significant). **76**
- Figure 4.8** (A)- Haematoxylin and Eosin (H&E) staining of cross section of colon (7 μ m) indicates pathological demarcation. (B)- Alcian Blue and Nuclear Fast Red (AB-NR) staining of cross section of colon (7 μ m)for evaluating goblet cells (Blue) and epithelial cells (Red) (C) Histological score for H&E stained cross section of colon. (D) Goblet cell(s) count per crypt in cross section of colon. (* $p \leq 0.05$, ** $p \leq 0.001$, *** $p \leq 0.0001$ and ns: non-significant). **79**
- Figure 4.9** (A) Immuno-histochemical staining of Nitric Oxide synthase 2 (NOS2) indicates M1 macrophage infiltration due to inflammation (B) Quantification of the fluorescence intensity. (* $p \leq 0.05$, ** $p \leq 0.001$ and *** $p \leq 0.0001$) **81**
- Figure 4.10** (A) Immuno-histochemical stained CLSM images for Nitro-tyrosine represents inflammatory condition (B) Quantification of the fluorescence intensity. (* $p \leq 0.05$, ** $p \leq 0.001$ and *** $p \leq 0.0001$) **82**
- Figure 5.1** Scheme elucidates better targeting potential of Eudragi-S-100 coated colon targeted chitosan of nanoparticles. (red= CSNP, blue- Eudragit coat and orange-melatonin) **91**
- Figure 5.2** Size and morphology analysis: (A-B) Transmission Electron Micrograph of Chitosan nanoparticles (CSNP) (D-E) Eudragit- **92**

S-100 coated Chitosan nanoparticle (EU-CSNPs) (C) Mean hydrodynamic size of Chitosan nanoparticles (CSNPs) and Eudragit-S-100 coated Chitosan nanoparticle (Eu-CSNPs).

- Figure 5.3** Fourier transform infrared (FT-IR) analysis of Melatonin, Chitosan, CSNPs, Mel-CSNPs, Eudragit-S-100, EuCSNPs, Mel-EuCSNPs. **94**
- Figure 5.4** *In vitro* drug release : (4A) pH dependent release of Melatonin from Chitosan nanoparticle (Mel-CSNPs) (4B) pH dependent release of Melatonin from Eudragit-S-100 coated Chitosan **95**
- Figure 5.5** Nitric Oxide (NO) scavenging activity of Melatonin, Mel-CSNPs and Mel-EUCSNPs in LPS stimulated RAW 264.7 macrophages. **98**
- Figure 5.6** (A) *In-vivo* & (A') *ex-vivo* bio-distribution analysis of Indocyanine green-Chitosan nanoparticle (ICG-CSNPs); (B) & (B') *In-vivo* bio-distribution analysis of Indocyanine green-Eudragit-S-100 coated Chitosan nanoparticle (ICG-EU-CSNPs)(a=stomach, b=duodenum, c=jejunum, d= ileum, e=colon, f=spleen, g=heart, h=kidney, j=brain and k=liver). **99**
- Figure 5.7** (A) Percentage body weight change daily (B) Disease Activity Index analysis for assessing the inflammatory pathology. **101**
- Figure 5.8** Myeloperoxidase assay in colon tissue homogenates to determine degree of neutrophilic infiltration. **102**
- Figure 5.9** (A) Expression of Nitric oxide synthase 2 (NOS2) in colon tissue lysate (B) Densitometry analysis of Nitric oxide synthase 2 (NOS2) in colon tissue lysate Western Blot expression of Nitric oxide synthase 2 (NOS2). **103**
- Figure 5.10** (A) Haematoxylin & Eosin (H&E) stain of colon sections (B) Alcian blue stain for goblet cells stain (C) Histological score for determining degree of inflammation in H&E stained cross **104**

section (10µm) of colon (D) Goblet cell number per crypt in cross section (10µm) of colon.

Figure 5.11 Immuno-histochemical expression analysis of Interleukin 1-β (IL-1β) in cross section (10µm) of colon tissue. **106**

List of Tables

| Number | Name | Page number |
|----------------|-------------------------------------------|--------------------|
| Table 1 | Disease Activity Index scoring parameters | 40 |
| Table 2 | List of primer sequence | 42 |

Table of Contents

| | |
|-----------------------------------------------------------------|-------------|
| Abstract..... | 1-2 |
| Synopsis..... | 3-7 |
| Chapter 1: Introduction | 8-31 |
| 1.0 Introduction..... | 8 |
| 1.1 Spectrum of the inflammatory response | 9 |
| 1.2 Resolving inflammation and non-resolving inflammation | 10 |
| 1.3 Inflammatory Bowel Disease..... | 11 |
| 1.3.1 Epidemiology..... | 12 |
| 1.3.2 Pathophysiology | 12 |
| 1.3.2.1 Epithelial barrier | 12 |
| 1.3.2.2 Commensal microflora..... | 13 |
| 1.3.2.3 Antigen recognition | 13 |
| 1.3.2.4 Deregulation of immunological responses | 13 |
| 1.3.2.5 Leucocyte recruitment | 14 |
| 1.3.2.6 Genetic factors | 14 |
| 1.3.2.7 Epigenetic factors..... | 14 |
| 1.4 Diagnosis..... | 15 |
| 1.5 Management of UC..... | 16 |
| 1.5.1 5- Amino Salicylates | 16 |
| 1.5.2 Corticosteroids..... | 16 |
| 1.5.3 Thiopurines | 17 |
| 1.5.4 Anti-tumor necrosis factor antibodies | 17 |
| 1.5.5 Calcineurin inhibitors | 18 |
| 1.5.6 Anti-integrins..... | 18 |
| 1.5.7 Tofacitinib | 18 |
| 1.5.8 Surgical treatment..... | 18 |
| 1.6 Role of nanotechnology for management of UC | 19 |
| 1.6.1 Size mediated targeting | 20 |
| 1.6.2 pH-mediated targeting | 20 |
| 1.6.3 Charge mediated | 21 |
| 1.6.4 Ligand receptor-mediated targeting..... | 21 |

| | |
|----------------------------------------------------------------------------------------------------|--------------|
| 1.6.5 Degradation mediated targeting..... | 22 |
| 1.6.6 Microbiota-mediated targeting | 22 |
| 1.7 Role of melatonin in UC therapy | 22 |
| 1.8 References..... | 24 |
| Chapter 2: Materials and methods..... | 32-47 |
| 2.0 Materials | 32 |
| 2.1 Methods..... | 33 |
| 2.1.1 Synthesis of Chitosan nanoparticle and Eudragit-S-100 coated chitosan nanoparticle..... | 33 |
| 2.1.2 Drug loading Content..... | 34 |
| 2.1.3 Determination of size, zeta potential and morphology | 34 |
| 2.1.4 Fourier Transform infrared (FTIR) and X-Ray Diffraction (XRD) analysis..... | 34 |
| 2.1.5 <i>In-vitro</i> drug release study | 35 |
| 2.1.6 <i>In-vitro</i> cellular uptake study | 35 |
| 2.1.7 Biocompatibility of nanoparticles..... | 36 |
| 2.1.8 Nitrite estimation (NO)..... | 36 |
| 2.1.9 NF- κ B p65 nuclear translocation study | 36 |
| 2.1.10 Haemolysis assay | 37 |
| 2.1.11 Animals..... | 37 |
| 2.1.12 <i>In-vivo</i> therapeutics and model development | 37 |
| 2.1.12a Objective 1 | 38 |
| 2.1.12b Objective 2 | 38 |
| 2.1.12c Objective 3 | 38 |
| 2.1.13 <i>In-vivo</i> bio-distribution study..... | 39 |
| 2.1.14 Disease Activity Index (DAI), % Body weight Change and colon length measurement | 39 |
| 2.1.15 Western Blot, Immunoprecipitation (IP) and Chromatin Immunoprecipitation (ChIP) assay | 40 |
| 2.1.16 Quantitative polymerase chain reaction (qPCR) study..... | 42 |
| 2.1.17 Myeloperoxidase (MPO) assay..... | 43 |
| 2.1.18 Histology..... | 43 |
| 2.1.18a Haematoxylin and Eosin (H&E)..... | 43 |
| 2.1.18b Alcian Blue and Nuclear Fast Red..... | 44 |

| | |
|-----------------------------------------------------------------------------------------------------------------------------------------------------------------------------|--------------|
| 2.1.18c Toluidine blue staining..... | 44 |
| 2.1.18d Immunohistochemistry | 44 |
| 2.1.19 Statistical Analysis..... | 45 |
| 2.2 References..... | 46 |
| Chapter 3: Melatonin Mediated Inhibition of EZH2-NOS2 Crosstalk Attenuates Inflammatory Bowel Disease in Preclinical <i>In Vitro</i> and <i>In Vivo</i> Models | 48-65 |
| 3.0 Background..... | 48 |
| 3.1 Results and Discussion | 49 |
| 3.1.1 Melatonin scavenged Nitric Oxide (NO) production in LPS stimulated RAW264.7 cells..... | 49 |
| 3.1.2 Melatonin attenuated EZH2, H3k27me3 and NOS2 expression in RAW 264.7 cells..... | 50 |
| 3.1.3 Melatonin mechanistic action of epigenetic regulation revealed direct interaction of NOS2 and EZH2..... | 52 |
| 3. 1.4 Melatonin has regulatory effect on EZH2 binding at NOS2 promoter..... | 52 |
| 3. 1.5 Melatonin treatment reduced DSS induced ulcerative colitis symptoms in mice | 54 |
| 3. 1.6 Reduced MPO activity and inflammatory genes expression as restorative effect of melatonin in UC mice model..... | 55 |
| 3. 1.7 Melatonin inhibited EZH2 and NOS2 expressions to suppress UC symptoms in mice | 56 |
| 3. 1.8 Melatonin reversed pathological demarcation, restricted mast cells infiltration and restored goblet cells | 59 |
| 3.2 Conclusion | 62 |
| 3.3 References..... | 63 |
| Chapter 4: Melatonin-loaded chitosan nanoparticles endows nitric oxide synthase 2 mediated anti-inflammatory activity in inflammatory bowel disease model | 66-88 |
| 4.0 Background..... | 66 |
| 4.1 Results and discussion | 67 |
| 4.1.1 Size and morphological analysis of nanoparticles | 67 |
| 4.1.2 Fourier transform infrared spectroscopy (FT-IR) and X-ray diffraction (XRD) analysis..... | 68 |
| 4.1.3 <i>In-vitro</i> drug release study | 70 |

| | |
|------------------------------------------------------------------------------------------------------------------|----------------|
| 4.1.4 <i>In-vitro</i> cellular internalization of nanoparticles..... | 72 |
| 4.1.5 <i>In-vitro</i> anti-inflammation analysis..... | 72 |
| 4.1.6 Nuclear factor kappa-light-chain-enhancer of activated B (NF-kB) | |
| p65 - nuclear translocation study | 72 |
| 4.1.7 Haemolysis analysis..... | 74 |
| 4.1.8 <i>In-vivo</i> bio distribution study | 74 |
| 4.1.9 <i>In-vivo</i> therapeutic efficacy study | 75 |
| 4.1.10 Myeloperoxidase assay | 77 |
| 4.1.11 qPCR analysis – gene expression study | 77 |
| 4.1.12 Haematoxylin and Eosin staining | 78 |
| 4.1.13 Alcian Blue and Nuclear Fast Red staining | 78 |
| 4.1.14 Nitric Oxide Synthase 2 (NOS2) and Nitro-tyrosine | 80 |
| 4.2 Conclusion | 83 |
| 4.3 References..... | 85 |
| Chapter 5: Colon targeted chitosan-melatonin nanotherapy for preclinical Inflammatory Bowel Disease | 89-111 |
| 5.0 Background..... | 89 |
| 5.1 Results and Discussion | 91 |
| 5.1.1 Size and morphological examination of nanoparticles..... | 91 |
| 5.1.2 Fourier transform infrared spectroscopy (FT-IR)..... | 93 |
| 5.1.3 Drug loading and <i>In-vitro</i> drug release study | 95 |
| 5.1.4 Nitrite estimation | 97 |
| 5.1.5 Bio-distribution study | 98 |
| 5.1.6 <i>In-vivo</i> therapeutic | 100 |
| 5.1.7 Myeloperoxidase (MPO) Assay | 101 |
| 5.1.8 Western Blot | 102 |
| 5.1.9 Histology | 104 |
| 5.1.10 Immuno-histochemical analysis | 105 |
| 5.2 Conclusion | 106 |
| 5.3 References..... | 108 |
| Chapter 6: Summary and conclusion..... | 112-114 |

Abstract

The incidence of Inflammatory Bowel Disease (IBD), which was previously only seen in western nations, has recently grown considerably in India. Ulcerative Colitis (UC) and Crohn's Disease (CD) are the two pathological disorders that are part of the IBD. Individuals suffering from UC exhibit severe inflammatory changes which include intestinal inflammation, hematochezia, melena and accumulation of inflammatory immune cells that occur specifically in the colonic tissue. Inflammation often affects the whole gastrointestinal system in CD, but only the colon and rectum in UC. Intrinsic defense cells, particularly macrophages, in the epithelium of the colon, are activated by pathogen invasion and release pro-inflammatory cytokines that trigger the release of interleukin-1 β (IL-1 β), IL-6, IL-18, transforming growth factor (TGF), and tumor necrosis factor (TNF) when the intestinal epithelial cell barrier is breached. Despite substantial research in this field, the precise cause and treatment of this condition are still unclear. Traditional treatments for UC management include 5-aminosalicylates, immuno-suppressants, antibiotics, and corticosteroids, which merely treat symptoms and do not treat the underlying cause of the condition. Therefore, there is an urgent need for innovative pharmaceutical treatments that might induce remission and prevent illness relapse. The pathogenesis of IBD is linked to both inflammation and oxidative stress. Therefore, a potent anti-inflammatory and anti-oxidative agent that may inhibit these damages may aid in the treatment of IBD. Melatonin possesses anti-inflammatory and antioxidant properties which have been proven useful in numerous experimental and clinical trials, including those on IBD. Therefore, the current thesis concentrates on comprehending and investigating the molecular basis of epigenetic regulation as well as enhancing the treatment strategy to reduce inflammation in colitic mice using melatonin. Melatonin attenuates inflammatory signals and promotes healing in UC conditions through a variety of molecular mechanisms. In this study, we have investigated the regulation of the epigenetic molecular process by melatonin in lipopolysaccharide (LPS) activated murine macrophages (M1) RAW 264.7 cells and colitic mice (female BALB/C). The putative role and interactions of the epigenetic protein biomarker Enhancer Zeste Homolog 2 (EZH2) and Nitric Oxide Synthase were explored and investigated in this work. EZH2 is an essential component of the polycomb repressive complex 2 (PRC2), which is largely involved in gene silencing. Nitric oxide synthase (NOS2) produces nitric oxide (NO) which is essential for enhancing inflammatory signals. The therapeutic potential to suppress inflammation of melatonin is further hampered due to its low solubility and short plasma half-life ($t_{1/2}$).

Hence, we have developed a nano-therapeutic approach to overcome these limitations. In order to achieve the necessary anti-inflammatory activity, we have synthesized and characterized polymeric nanoparticles of chitosan. Optimized nanoparticles were administered in colitic mice intravenously for assessing its therapeutic potential in comparison to a bare melatonin. Chitosan nanoparticles considerably improved pathological markers and inhibited nuclear localization NF κ B in murine macrophages to increase the anti-inflammatory efficacy of melatonin compared to the bare drug in colitic mice. Although this approach increases the therapeutic potential of melatonin, there are several drawbacks, including sterility and issues with patient compliance with intravenous administration. Generally oral administration is preferred over intravenous administration. Hence, we have modified chitosan nanoparticles using pH-sensitive polymers for the development of a colon-targeted drug delivery system. Eudragit-S-100 has been coated on drug-loaded nanoparticles to target desired location based on the principle of pH difference in gastrointestinal tract (GIT). Moreover, using ICG-tagged nanoparticles in a bio-distribution study on mice, we were able to validate the targeted transport of the coated nanoparticles to the colon. Therapeutic efficacy of the colon targeted nanoparticles was evaluated against colitic mice. Colon targeted nanoparticles improved anti-inflammatory effect in terms of nitrite assay, Disease Activity Index (DAI), colon length, body weight improvement, myeloperoxidase assay, Nitric Oxide Synthase 2 and histoarchitecture evaluations in colonic tissues. Thus, the thesis concludes that melatonin regulates its anti-inflammatory action via epigenetic molecular mechanism involving EZH2-NOS2 interaction and the therapeutic efficacy of melatonin was enhanced by delivering through polymeric nanoparticles. Moreover, colon-targeted nanoparticles when loaded with melatonin as an anti-inflammatory therapeutic agent highlighted its significant potential as a therapy option for UC and also increased the therapeutic efficacy for the same compared to non-targeted nanoparticles.

Synopsis

Inflammation is a general physiological process related to our body's natural immune response to foreign objects or any other harmful tissue damage. It is marked by redness, swelling, heat, pain, and loss of function of the tissue [1, 2]. Inflammation typically subsides quickly after it begins, which is crucial for preserving the body's normal physiology. However, if it is not resolved and persists for a longer period because of the body's inability to remove pathogens or harmful waste, this can result in a severe inflammatory response and pathological conditions like Inflammatory Bowel Disease (IBD), rheumatoid arthritis, or even cancer [3]. The word “itis” is used as a suffix to present any kind of inflammatory disease i.e. inflammation of the colon-“colitis” [4]. Inflammatory bowel disease is a chronic inflammatory condition that can occur as sporadic – Ulcerative colitis or may be genetic - Crohn’s disease. Ulcerative colitis affects generally the adult population whereas Crohn’s disease majorly affects children. Pro-inflammatory cytokines, which trigger the inflammation cascade, are produced by an unchecked immune response, which leads to uncontrolled inflammation [4]. Pro-inflammatory cytokines like TNF- α , NF-kB, IL-6, histamine, etc. play a major in activating severe inflammatory responses. TNF- α , NF-kB, IL-6, histamine, and other pro-inflammatory cytokines have a significant role in triggering severe inflammatory reactions [5].

The prevalence of IBD has increased significantly in the last few decades in developing countries which raises an alarm for the health authorities as these countries do not have sufficient health infrastructure systems for the management of this disease. Because of their way of life and eating habits, western nations were formerly thought to be more susceptible to this disease [4]. For the treatment of mild to severe UC, medications such as 5-aminosalicylates (sulfasalazine and mesalazine), corticosteroids (budesonide and prednisolone), thiopurines (azathioprine and 6-mercaptopurine), anti-TNF- antibodies (infliximab, adalimumab, and golimumab), calcineurin inhibitors [6]. However, most of the drugs used for the management of UC at present have one or the other adverse effect leading to their compromised use in UC. They can also trigger relapse if stopped abruptly, whilst prolonged use is linked to serious toxicities. Therefore, in order to get over the aforementioned restrictions, we now urgently need innovative therapeutic medicines that can treat the illness and prevent its resurgence. A neurohormone with a well-established function in preserving circadian rhythm is melatonin [7]. Melatonin has powerful anti-inflammatory

properties as well, which can be investigated for the treatment of UC [8]. The use of melatonin as an adjuvant in UC therapy has demonstrated its protective impact in the treatment of UC. Melatonin has not yet been demonstrated to be a potent therapeutic alternative that can be used in the treatment of UC due to our limited understanding of the molecular mechanism underlying its activity as well as its limitations deriving from its physicochemical properties.

The current thesis investigates the molecular mechanism through which melatonin decreases inflammation in a mouse model of colitis. Particularly, the role of epigenetics in controlling inflammation in murine macrophages has been thoroughly studied. Additionally, a nanotherapeutic approach has been investigated for improving its anti-inflammatory efficacy in colitic mice in order to circumvent physicochemical limits since it offers a smaller size and greater targeting efficacy to precisely release medication at the diseased site. The following objectives were achieved to investigate and improve the therapeutic efficacy of melatonin in treating Inflammatory Bowel Disease preclinical models:

Objective 1 (Chapter 3): Role of melatonin in regulating EZH2, a master epigenetic regulator, and its beneficiary effect in case of IBD management.

Objective 2 (Chapter 4): Formulation, characterization, and anti-inflammatory efficacy evaluation of melatonin loaded chitosan nanoparticles in inflammatory models.

Objective 3 (Chapter 5): Formulation, characterization and anti-inflammatory efficacy evaluation of melatonin-loaded colon targeted chitosan nanoparticles in inflammatory models.

Chapter 1 of thesis deals with the introduction and review of literature on inflammation and the diseases associated with it. It mainly focuses on one of the major inflammatory disease i.e. Ulcerative Colitis- pathophysiology, epidemiology, current management system, and insight of melatonin as a potential newer anti-inflammatory candidate. It focuses deeply on current therapeutic agent used in the management of UC and their limitation in managing the disease. Also, it focuses on the role of inflammation in the normal physiological systems and diseases associated with unresolved inflammation. The role of epigenetics in UC and potential of inhibitors in managing UC have been discussed.

Chapter 2 of the thesis deals with various materials, methods, and techniques executed in the experiments. Protocols for synthesis and characterization of nanoparticles, methods for

developing inflammatory models *in vitro* and *in vivo*, etc. have been discussed in this chapter in detail.

Chapter 3 (Objective 1) of the thesis deals with the role of melatonin's anti-inflammatory effect against *in vitro* (RAW 264.7 murine macrophage) and *in vivo* (DSS-induced colitis in mice) model by administering intravenously (*i.v.*). Investigating the role of melatonin in regulating inflammation via enhancer of zeste homolog 2 (EZH2) in managing Ulcerative colitis has been explored. Exploring molecular interaction between EZH2 and nitric oxide synthase 2 (NOS2) has been carried out. In this chapter, melatonin anti-inflammatory activity has been evaluated by estimating nitrite level, gene expression, protein expression, gross pathological features and histological changes in colonic tissue, etc. Melatonin was used at a concentration up to 0, 1, 10, 100, 250 and 500 µg/ml against LPS stimulated RAW 264.7 murine macrophages. The expression of protein biomarkers like EZH2, NOS2, and H3k27me3 has been investigated. It focuses highly on the role of NOS2 in the inflammatory response in macrophages and colitic mice. Interlink between NOS2-EZH2 and their connection in the progression of inflammation leading to Ulcerative Colitis. Physical interaction between EZH2-NOS2 and the binding of EZH2 on promoter region of NOS2 has been explored in this chapter. Body weight loss, disease activity index, and colon length have been investigated. Hematoxylin and eosin, alcian blue-nucleus red, and toluidine blue staining have been performed for evaluating histoarchitecture alterations. Immunofluorescence staining of EZH2 and NOS2 has been performed for evaluating their expression.

Chapter 4 (Objective 2) of the thesis deals with the formulation of chitosan nanoparticles for the delivery of melatonin in an *in-vitro* and *in-vivo* (*i.v.*) colitic mice. Chitosan nanoparticles were prepared by ionic gelation method and loaded with an anti-inflammatory agent to evaluate their anti-inflammatory efficacy. Characterization of nanoparticles was carried out by dynamic light scattering measurement for estimating the mean hydrodynamic size of nanoparticles, zeta potential to confirm a charge on the surface of nanoparticles, and transmission electron microscopy for confirming their spherical morphology. *In-vitro* cumulative release, cell viability, nitrite level, and cellular uptake for nanoparticles have been discussed in this chapter. Nuclear translocation of NF-κB has been also performed to check its migration from cytosol to nucleus. Moreover, a bio-distribution study of chitosan nanoparticle has been discussed. Gross pathological changes like disease activity index, weight loss, colon length, gene expression, myeloperoxidase assay, and histological studies

have been discussed for the same. An immunofluorescence study for evaluating the expression of NOS2 and nitro-tyrosine in the colon has been explored in this chapter.

Chapter 5(Objective 3) of the thesis deals with the formulation colon targeted chitosan nanoparticles for specific colon delivery of melatonin in colitic mice. As oral drug delivery is preferred over intravenous (*i.v*) due to issues related to sterility and patient compliance. Simple chitosan nanoparticles are strongly mucoadhesive, which limits their ability to reach the appropriate colonic region when administered orally and reduces their therapeutic efficacy. Hence, we have modified chitosan nanoparticles by coating them with pH sensitive polymer (Eudragit-S-100). Ionic gelation process was used to create chitosan nanoparticles as described earlier, which were then coated with an enteric coating polymer, Eudragit-S-100. Dynamic light scattering was used to determine the mean hydrodynamic size of nanoparticles, transmission electron microscopy to verify their spherical form and enteric coating on their surface, and FTIR to verify any changes in their chemical composition. *In vitro* drug release studies at various physiological pH and their best-fitted models have been discussed. To validate the specific targeting of the colon, biodistribution studies was performed. Gross pathological alterations have been explored for this, including disease activity index, weight loss, colon length, myeloperoxidase assay, and histological study. This chapter has examined an immunofluorescence investigation to assess IL-1 expression and an immunoblot for NOS2 in the colon.

The thesis therefore concludes that melatonin controls its anti-inflammatory effect via an epigenetic molecular mechanism involving an interaction between EZH2 and NOS2, and that melatonin's therapeutic efficacy was increased by delivery through polymeric nanoparticles. Additionally, colon-targeted nanoparticles that were loaded with the anti-inflammatory therapeutic agent, melatonin showed its substantial promise as a treatment alternative for UC and improved the therapeutic efficacy of the same in comparison to non-targeted nanoparticles.

References:

- [1] R. Medzhitov, Cell, 140 (2010) 771-776.
 - [2] L. Chen, H. Deng, H. Cui, J. Fang, Z. Zuo, J. Deng, Y. Li, X. Wang, L. Zhao, Oncotarget, 9 (2018) 7204-7218.
 - [3] C. Nathan, A. Ding, Cell, 140 (2010) 871-882.
 - [4] W.D. Lynch, R. Hsu, Ulcerative Colitis, StatPearls, StatPearls Publishing
- Copyright © 2022, StatPearls Publishing LLC., Treasure Island (FL), 2022.
- [5] G. Arango Duque, A. Descoteaux, Front Immunol, 5 (2014) 491.
 - [6] J.M. Fell, R. Muhammed, C. Spray, K. Crook, R.K. Russell, B.I.w. group, Arch Dis Child, 101 (2016) 469-474.
 - [7] K. Doghramji, Journal of clinical sleep medicine : JCSM : official publication of the American Academy of Sleep Medicine, 3 (2007) S17-23.
 - [8] G. Tahan, R. Gramignoli, F. Marongiu, S. Aktolga, A. Cetinkaya, V. Tahan, K. Dorko, Dig Dis Sci, 56 (2011) 715-720.

Chapter 1:

Introduction

1.0 Introduction

Inflammation is a normal physiological response evoked by the body when it senses any harmful stimulus from pathogens, toxic compounds or damaged cellular products [1, 2]. It is a defensive mechanism to clear toxicants and pathogens from the body via immunological response to maintain homeostasis [3]. Aulus Cornelius Celsus, a Roman physician, established the four primary signs of inflammation in the first century. They are redness and swelling with heat and pain (“*rubor et tumor cum calore et dolore*”) in his treatise called *De Medicinia* [4]. Later, Augustus Waller (1846 AD) and Julius Cohnheim (1867 AD) revealed leucocyte migration from blood vessels and other morphological alterations including vasculature enlargement, revealing the physiological significance of the aforementioned four cardinal symptoms. By observing under a microscope Cohnheim noted vasodilation, plasma leakage, and migration of leucocytes into tissues from blood vessels [5]. Rudolph Virchow later included the fifth cardinal symptom, disturbance of function (*functio laesa*), of inflammation in his book *Cellularpathologie* [4]. Consequently, we can characterize inflammation as a necessary immune response that supports the body during an infection or damage and preserves tissue homeostasis under a variety of adverse conditions [2].

The discovery of phagocytosis in 1892 AD by Elie Metchnikoff, who formulated the theory of cellular immunity and refuted the notion that only soluble chemicals in the blood had a role in inflammation, was one of the key turning points in the field of inflammation research (antibodies). He proposed the idea that not only antibodies but cells also actively participate in destroying foreign invading substances. Despite the discovery of cellular immunity, the theory of humoral immunity was only considered widely until the 1940 AD. Cellular immunity theory was considered only after scientists began to reexamine the role of cellular immunity. After the invention of serum therapy against diphtheria and tetanus toxins by Emil von Behring and Shibasaburo Kitasato in 1890 AD, Paul Ehrlich narrowed his focus to the function of humoral immunity. Thus, a modern theory of immunity was developed which considered the role of both i.e. cellular and humoral immunity. Hence, the role of macrophages and microphages were established and their significance in maintaining immunological response was addressed. The process of the inflammatory response consists of series of events which work in a specific manner to regulate immune response and maintain physiological balance.

1.1 Spectrum of the inflammatory response

Inflammation is a normal physiological response which consists of series of events and components which are essential for it. Each inflammatory component has several different manifestations, and its organized function might be connected to various inflammatory pathways. Inflammatory stimuli that activate specific pathways, such as bacterial infections, are recognized by Toll-like receptors (TLRs), which are found on tissue resident macrophages. These receptors stimulate the production of inflammatory cytokines (such as Tumor Necrosis Factor- (TNF-), Interleukin 1- (IL-1) and Interleukin-6 (IL-6) as well as chemokines (such as C-C motif chemokine ligand 2 (CCL2) and C-X-C motif chemokine ligand 8 (CXCL8).

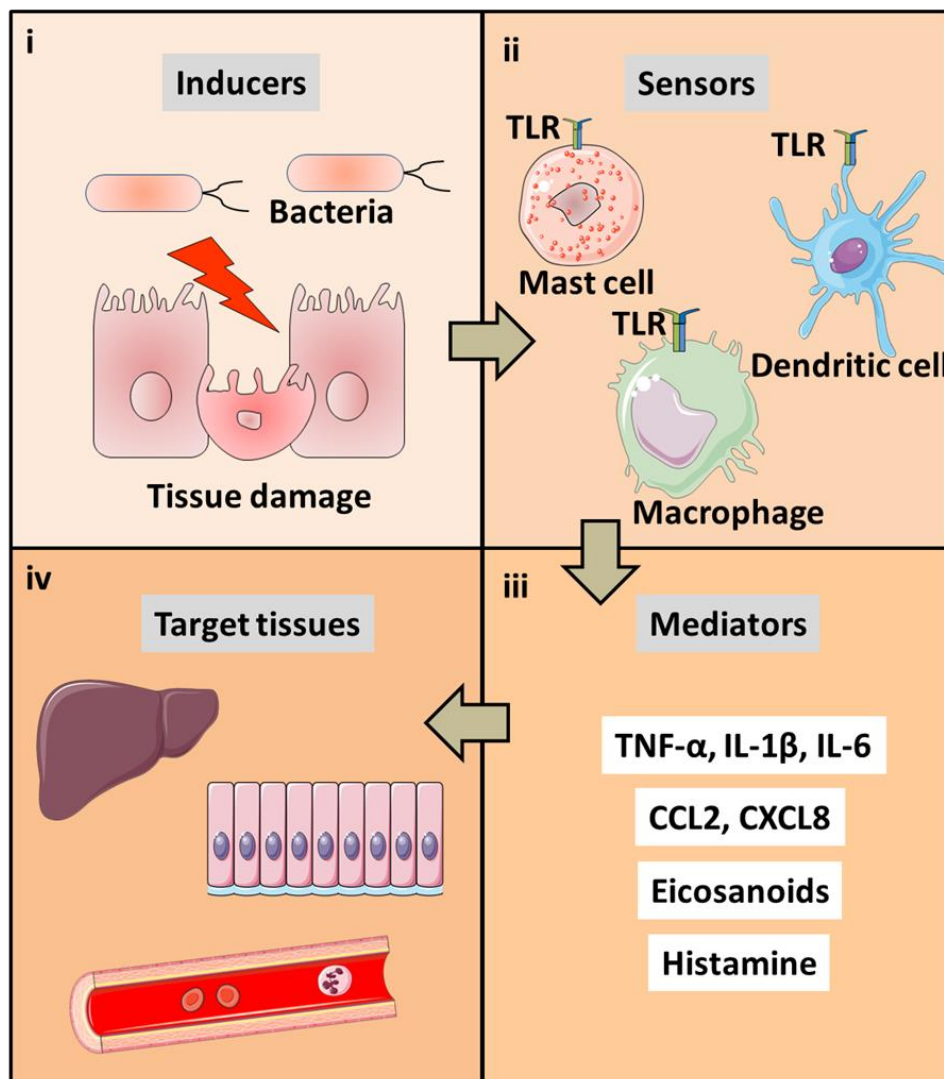


Figure 1.1: Schematic representation of components of inflammatory pathway: (i) inflammatory inducers (ii) sensors (iii) inflammatory mediators and, (iv) target tissues.

These inflammatory mediators exert their effect on target tissues by inducing vasodilation, infiltration of microphages (neutrophils), macrophages localized in tissue and mast cells to clear the invading pathogens [2]. Apart from the above response inflammatory process is aided by plasma components which include antibodies and compliment system. $TNF-\alpha$, and IL-6 causes the release of C-reactive proteins from hepatocytes thereby showing its systemic effect. Prostaglandins like PGE2 can cause stimulate particular neurons in the central nervous system to promote fever, fatigue, anorexia and depression [6]. The component of inflammatory response consists of (i) inflammatory inducers (ii) sensors (iii) inflammatory mediators and,(iv) target tissues.

Cytotoxic lymphocytes are activated when a viral infection causes the synthesis of type 1 interferon (IFN) by the infected cells. Mast cells and basophils produce histamine, interleukin-4 (IL-4), interleukin-5 (IL-5), and interleukin-13 (IL-13) in response to a parasite infection [7, 8].

1.2 Resolving inflammation and non-resolving inflammation

Once the initiating insult is no longer present and has been eliminated from the body, the acute inflammation often comes to an end. Resolution of inflammation refers to the cessation of inflammation and return to the normal homeostatic condition. Lipoxins and other factors have been discovered to be important in this process [9].

Resolution of the inflammation may not be reached if the inflammation-causing chemical is not eliminated from the body or remains in the system for some reason, which could result in a chronic condition of inflammation. Chronic infections, inadequate tissue repair, undigested foreign objects, or endogenous compounds like monosodium urate can all cause this disease. [10]. Inflammatory Bowel Disease, atherosclerosis, obesity, cancer, and neurological illness may not all be caused primarily by persistent inflammation, but it considerably speeds up their etiology. [3]. One of the major diseases brought on by persistent, unresolving inflammation is ulcerative colitis, which is described in more detail below

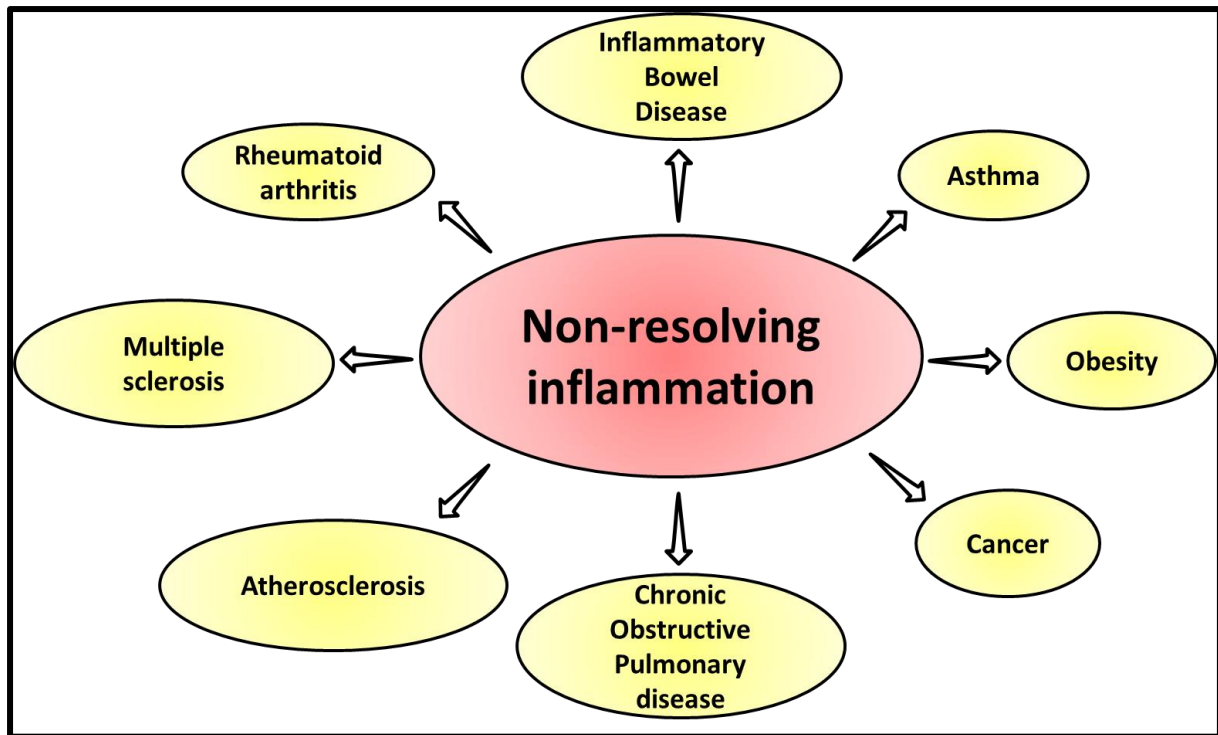


Figure 1.2: Schematic representation of diseases linked to non-resolving inflammation.

1.3 Inflammatory Bowel Disease

Inflammatory Bowel Disease consists of two major pathological conditions which predominantly affect the gastrointestinal tract causing stomach pain, hematochezia, and weight loss leading to compromised lifestyle and increased financial burden on IBD patients [11]. Idiopathic IBDs, such as Crohn's disease and ulcerative colitis, affect clinically immune-competent patients and are characterized by severe (but noninfectious) cytokine-driven intestinal inflammation [12]. Excessive IL-12/IL-23 and IFN- γ /IL-17 production has been associated to Crohn's disease, which affects the small intestine and colon and causes discontinuous ulceration and full thickness intestinal wall inflammation with granulomas. Along with systemic symptoms including weight loss, fever, and exhaustion, patients often report having gastrointestinal symptoms such stomach pain, diarrhoea, and rectal bleeding. Patients suffering with Crohn's disease may also develop obstructive intestinal strictures as well as inflammatory attachments (fistulae) between bowel segments or between the gut and the skin and other organs. Ulcerative colitis, on the other hand, is associated with increased IL-13 production and mostly affects the colon [13]. A persistent mucosal inflammation almost invariably involves the rectum and extends proximally. Despite the absence of fistula formation, the symptoms are comparable to those of Crohn's disease. Although ulcerative

colitis may be treated by surgically removing the colon, both illnesses are often chronic and recurring [14].

Ulcerative colitis is an idiopathic condition, leading to chronic inflammation of the colonic mucosal layer, originating in the rectum and may extend throughout the entire colonic region. The main signs and symptoms of UC are hematochezia, melena, intestinal inflammation, and colonic immune cell infiltration [15]. Current thesis deals specifically with UC hence we have focused on it in detail.

1.3.1 Epidemiology

The highest incidence rates of the Inflammatory Bowel Disease worldwide were found in northern Europe and North America. Since the western way of life and eating habits are intimately related to this condition. There are 9–20 instances of UC per year. 1 lakh people per year, compared to 156 to 291 cases per lakh people per year for its prevalence [16].

The main onset peak of UC is between the ages of 15 and 30; the second, less severe peak of incidence is between the ages of 50 and 70. This suggests that the incidence pattern of UC is bimodal [16]. The shift of this disease has occurred from developed to developing countries like India which is a major concern for health authorities worldwide. Khosla et al., reported prevalence of 42.8 per 1 lakh in 1986 in Haryana [17]. Sood et al., reported 44.3 cases per 1 lakh in Punjab in 2003 [18]. A survey carried out in 2012 reported an equal prevalence of UC in northern and southern states of India [19].

1.3.2 Pathophysiology

1.3.2.1 Epithelial barrier

Figure 1.3 describes the pathophysiology of UC in detail. The mucous-covered epithelial layer barrier, which isolates the host immune system from the luminal gut microbiota, serves as the first line of defense. Colonic mucin (mucin 2) production and modification are reduced in UC [20]. Damage to the epithelial barrier causes an increase in permeability, which leads in faulty tight junction integrity [21]. Additionally, the host defense system is strengthened by the epithelial barrier, which produces anti-microbial peptides that prevent the entrance of dangerous bacteria [22].

1.3.2.2 Commensal microflora

Maintaining balance between dietary antigens and commensal gut microbiota tolerance is the job of the intestinal immune system. The commensal gut microbiota colonizes the transgenic models, causing inflammatory symptoms to emerge, but these symptoms do not appear in the germ-free condition [23, 24]. Clinical research on humans indicates a substantial role for enteric gut bacteria in the etiology and severity of intestinal inflammation [25]. As a result, we might surmise that the gut microbiota, host mucosal immunity, and an imbalance in homeostasis may all contribute to the etiology of UC.

1.3.2.3 Antigen Recognition

Antigen recognition plays an important role in innate immunity through its interaction with macrophages and dendritic cells. Dendritic cells can sample and recognize antigens from the lumen using its dendrite [26]. Macrophage and dendritic cells reside in the lamina propria that presents antigen to B cells and T cells. In UC condition the number of activated and mature dendritic cells is increased highly. Dendritic cells express microbial pattern recognition receptors, including Toll-like receptors (TLR), and Nucleotide-binding oligomerization domain (NOD)-like receptors which play an essential role in providing protection from injury, intestinal homeostasis and epithelial barrier integrity. In the lamina propria of UC patients, TLR4 receptor expression is significantly increased [27]. The activation of the transcription factor nuclear factor-kB (NF-kB) and other molecules involved in the inflammatory signaling cascade may occur as a result of TLR stimulation, which might cause an innate immune response [28]. NF-kB regulates cell survival and pro-inflammatory signaling in macrophages and T-cells [29]. NF-kB shows a protective effect in case of intestinal epithelial cells [30] which creates confusion about whether it has a beneficiary or harmful effects in the case of UC condition.

1.3.2.4 Deregulation of immunological responses

T-regulator and effector T-cell homeostasis are out of balance (eg. Th-1, Th-2, and Th-17). The report suggests that UC is linked with an atypical Th2 response mediated by natural killer T cells producing interleukin 5 and 13. Interleukin 13 exhibits a cytotoxic effect on intestinal epithelial cells [21]. Natural killer T-cells, which play a crucial role in the pathophysiology of UC, can be positively influenced by interleukin 13 [31]. Additionally, the

absence of anti-inflammatory signaling is associated with severe ulcerative colitis and interleukin 10 receptor-1 or interleukin 10 receptor deficiencies [32]. Tumor necrosis factor (TNF)- α level is increased in blood, stool, and mucosa of UC patients [33, 34]. This discovery has aided in the development of numerous therapeutic medicines for treating UC in patients.

1.3.2.5 Leucocyte recruitment

Due to the release of chemoattractants like CXCL8, which is significantly up-regulated in the case of UC, leucocytes are drawn to the location of inflamed mucosa [35]. Mucosal addressin cellular adhesion molecule-1 (MAdCAM-1), which promotes leucocyte adherence and extravasation into tissue, is one example of a cell adhesion molecule whose expression is increased by proinflammatory cytokines [36].

1.3.2.6 Genetic factors

Genome-wide association studies have identified several UC-vulnerable genes, advancing our understanding of the condition. A paper showed a connection between UC and the MHC area, where associated single nucleotide polymorphisms (SNPs) were correlated with changes in HLA Class II expression and IL-23R with UC. Additionally, the strongest connection is found in the MHC Class-2 area, close to HLA-DRA [37]. The loss of a protein required for epithelial cell adhesion might result in impaired barrier function, which may worsen the pathophysiology of UC. This protein is encoded by genes including hepatocyte nuclear factor - 4a, CDH1, and laminin-1 [38]. Mutation in a protein called E-cadherin was the first genetic correlation found between UC and colorectal cancer [39].

In summary, we can conclude that inflammation in UC begins with an exaggerated T-cell (Th2) response that causes mucosal hyper responsiveness to commensal gut microbiota in genetically prone individuals.

1.3.2.7 Epigenetic factors

Epigenetics deal with heritable features that involve transcriptional regulation without altering any nucleotide sequences [40]. Hallmark feature of epigenetics is DNA methylation of cytosine which is followed by guanine (CpG). When DNA methylation occurs in a gene's promoter region, it silences the gene by blocking transcription proteins from attaching to the

area [41, 42]. In the case of IBD, there is a considerable change in the DNA methylation of peripheral blood mononuclear cells. A study [40] found an overlap of 45 % between UC and CD differentially methylated positions (DMPs). The promoter region of TRIM 39-RPP2, one of the key IBD-associated PBMC differentially methylation areas, was discovered to be hypomethylated in the colonic mucosa of young UC patients. Additionally, PBMCs from IBD patients were shown to have TRAF6 hypermethylation [40].

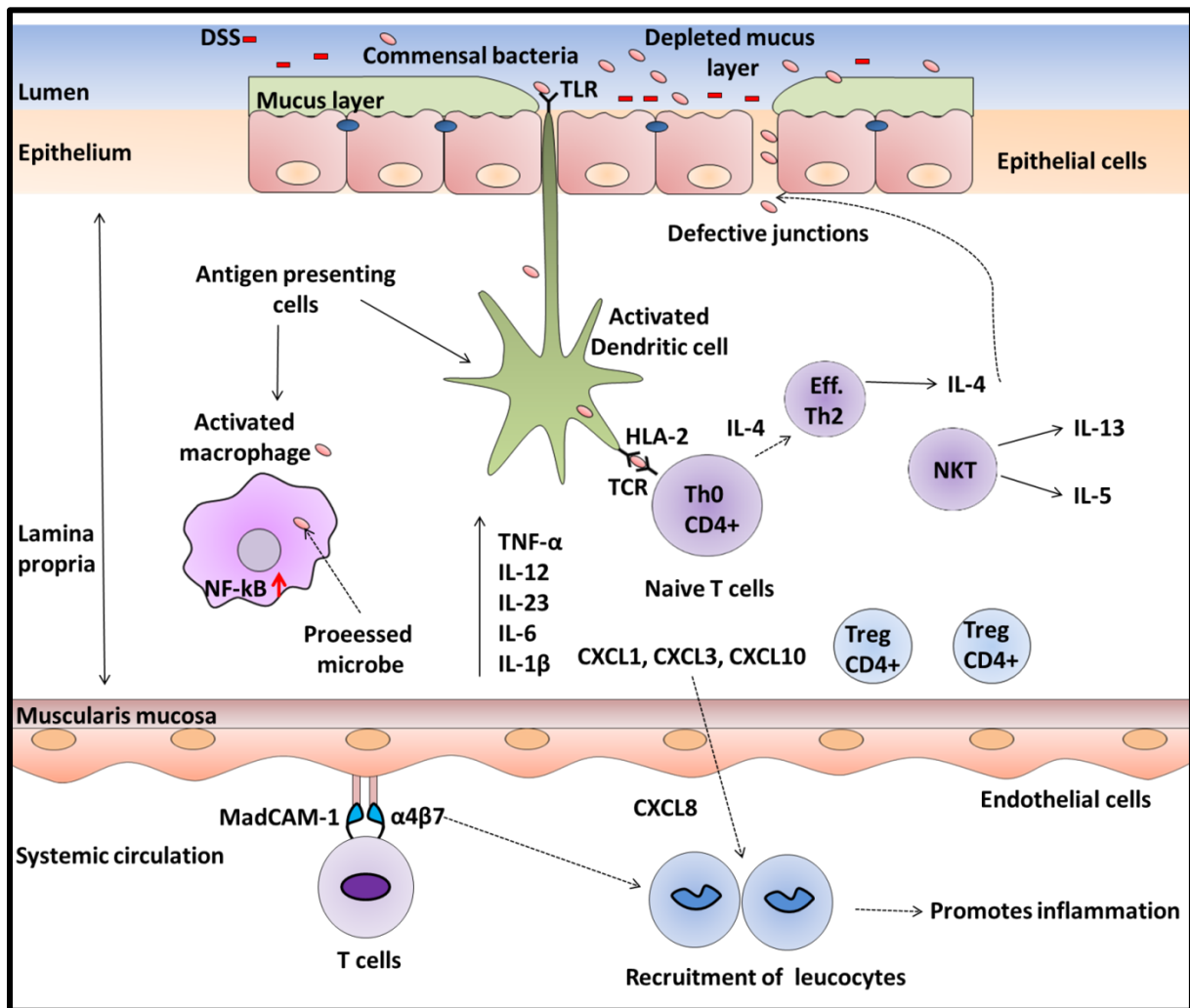


Figure 1.3: Schematic representation of pathophysiology of Ulcerative Colitis. : Disturbance of tight junction and mucus layer followed by immune cell activation and increase vascular permeability

1.4 Diagnosis

Hematochezia, melena, tenesmus, and stomach pain are among the specific distinctive symptoms that the majority of UC patients exhibit. Significant deviations from healthy persons can be seen in the total blood count, liver function test, erythrocyte sedimentation

rate (ESR), and other measurements [43]. The level of calprotectin is increased in the fecal matter of IBD patients which can be used as a diagnostic marker for IBD [44]. Endoscopy of colonic region can be done to confirm disease if required [43]. Differentiating between UC and CD can be done using magnetic resonance enterography. Extraintestinal manifestations like arthritis [45], liver sclerosing cholangitis [46], and uveitis (iritis) [47] can also occur in UC patients.

In conclusion, a thorough history, physical exam, lab tests, esophagogastroduodenoscopy (EGD), and ileocolonoscopy are essential for making an accurate diagnosis of IBD. Histology is also very important. Additionally, imaging of the small bowel is required.

1.5 Management of UC

The treatment of UC is given following the guidelines of regulatory authorities of the healthcare system. The treatment regime may consist of drugs like 1- 5-ASA agents, corticosteroids, thiopurines, anti-tumor necrosis factor antibodies, antibiotics/probiotics, and newer agents.

1.5.1 5- Amino Salicylates

Sulfasalazine and mesalazine (5-ASA) are currently the two main treatments options for UC. These agents can persuade and maintain reduction of UC in the individuals having mild to the moderate conditions of UC [48]. Sulphasalazine has common side effects like nausea, vomiting, abdominal pain, indigestion and headache. Consequently, the scientist created 5-ASA medications to overcome the aforementioned restriction. In order to treat UC Mesalazine is administered in divided dosages, although a single dose is also just as effective for keeping UC quiescent [49]. Maintaining remission of UC can be accomplished using topical preparations of 5-ASA similar to suppositories or enema. Orally 5-ASA is given 4.8 g/day for inducing remission of UC which can be reduced to 2.4 g/day but not lower than that [50-52]. Failure to achieve this goal after 2-4 weeks is a sign that corticosteroids should be used as the next treatment.

1.5.2 Corticosteroids

Corticosteroid therapy is given to a patient with moderate to severe UC condition. It is not advised for a patient to take for an extended period of time due to its unfavourable toxicities. Patients should get an intravenous dose of a corticosteroid like methylprednisone that ranges from 40 to 60 mg (20 mg every 8 hours) on a daily basis [53]. If the medication dosage is lowered or stopped after three to four months, there is a chance that the illness will return. If prednisone doesn't work to treat the problem, oral beclomethasone dipropionate may be advised [54].

1.5.3 Thiopurines

Treatment for UC involves the use of purine analogues such as azathioprine and 6-mercaptopurine. The length of the disease's remission is greater and could last 10–14 weeks. Azathioprine 2.5 mg/kg and 1-1.5 mg/kg are the suggested doses (6-MP). Typically, this treatment began with a maximal dose [55]. The risk of lymphoma may rise with thiopurine use. It is vital to routinely monitor blood parameters and do liver function tests because thiopurine methyltransferase activity may result in myelosuppression [56].

1.5.4 Anti-tumor necrosis factor antibodies

Anti-tumor necrosis factor- α antibodies like infliximab [57], adalimumab [58], and golimumab [59] are available therapy for induction and maintenance of remission of UC. Typically, these medications are used with corticosteroids. Only infliximab is utilized for paediatric patients. An IgG1 monoclonal antibody called infliximab, which is chimeric (human and murine), has an affinity for TNF- and blocks its effects [60]. Adalimumab and golimumab are monoclonal antibodies of human origin. Infliximab can be used for steroid-refractory UC condition in patients. The results obtained by a study done using infliximab with thiopurine show improvement in the therapy of UC patients [61]. Among all anti-TNF- α agents infliximab has the highest efficacy and is the choice of drug for UC.

One of the most frequent adverse effects of anti-TNF medications is infection, which can include sinusitis, otitis media, and the common cold. It is advised that the patient undergo tests to rule out latent tuberculosis and chronic hepatitis B infection before beginning treatment with an anti-TNF medication because they may become active due to an immunocompromised state [62].

1.5.5 Calcineurin inhibitors

Calcineurin inhibitors are immunosuppressants generally used for the management of the autoimmune disease. Cyclosporine can be used for induction of remission in case of severe-to-fulminant steroid-refractory colitis. Cyclosporine is used at limited places for IBD treatment but does not have any effect in chronic therapy for IBD. Infusion of cyclosporine is given at a dose of 2-4 mg/kg/day [63, 64]. Therapeutic drug monitoring should be done every alternate day to check the range between 200 and 400 ng/ml at a dose of 2 to 4 mg/kg respectively. Although there is evidence available about the use of tacrolimus for UC therapy, it is not advised for use [65].

1.5.6 Anti-integrins

Leucocyte migration in the intestines is significantly influenced by the type of protein known as integrins. Vedolizumab binds to $\alpha 4$ - $\beta 7$ integrin and inhibits the relocation of leucocytes to the intestines. For the induction of remission in moderate to severe UC, vedolizumab has demonstrated therapeutic efficacy and been licensed [66, 67]. Vedolizumab was the first anti-integrin authorized for the treatment of UC. Because of its positive effects on the gut, it is the safest biological now in use, with little side effects such as intestinal infection [68].

1.5.7 Tofacitinib

A Janus kinase inhibitor called tofacitinib is prescribed for use in UC. Adults with moderate to severe forms of UC are eligible to receive therapy with it [69]. It is the first oral formulation of a small molecule which is two times a day at a dose of 5 and 10 mg. If desired therapeutic effect is not achieved within 16 weeks its usage shall be discontinued for the same. For people with hepatic impairment, it is not advised. Its side effects are comparable to those of anti-TNF agents, which include opportunistic infections and infections brought on by bacteria, viruses, or invasive fungi [69]. It is recommended to get tested for latent TB before starting this treatment because it could make it active.

1.5.8 Surgical treatment

Surgery for UC may be necessary and classified as elective, urgent, or emergency care. In cases of life-threatening conditions, emergent surgical surgery is advised if patients do not respond to any medications. Patients with UC who have been admitted to the hospital and

who are not responding to medication therapy may need urgent surgical surgery. Due to uncontrolled inflammation that otherwise could have been fatal to life, the primary goal of surgically removing a severely inflamed colon on an emergency or urgent basis is to restore the patient's health.

1.6 Role of nanotechnology in management of UC

To improve the therapeutic efficacy of pharmacological agents various novel technologies are employed which increase their efficacy many folds and thereby reduces the dose and also the toxicity associated with that concentration. Nanotechnology based drug delivery system has gained major attention recently due to their higher efficiency in improving drug delivery system compared to conventional systems. Conventional methods for ameliorating colonic diseases include parenteral, rectal, and oral routes of administration. The rectal route has advantage for delivering drug to the distal colonic region[70] but is not suitable if the disease is in ascending colon [71]. Moreover, this route of administration causes patient non-compliance which makes it difficult for application in the management of UC. The most preferred route of drug administration is oral, which is widely accepted and does not cause any uneasiness to the patient, and reaches the colon [72].

For oral drug delivery of drugs, conventional therapy includes approaches like pH-sensitive coating which can assist the delivery of drug specific to the colon by overcoming physiological barriers. Conventional colon-specific drug delivery system despite having targeted delivery exhibits patient limited specificity for healthy versus diseased colon [73]. Due to the size of conventional drug delivery systems, which prevents them from penetrating through the mucus layer and prevents them from helping UC patients repair their damaged epithelial layer. Due to their smaller size and capacity to quickly be phagocytosed by inflammatory cells due to their increased permeability, nanoparticle systems can easily penetrate the mucus layer at the site of inflammation [74, 75]. As a result, the management of UC in individuals with active disease may benefit greatly from the use of nano-drug delivery systems for the treatment of colitis.

For designing colon-specific nano-drug delivery system, many physical, chemical, and physiological barriers need to be considered while synthesis. A targeted drug delivery system has the great potential to exacerbate UC by improving the therapeutic efficacy of the drug delivery system. The nanoparticle system present in the human body initiates an

immunological response via recognition by the mononuclear phagocytic system. The size, shape, and charge of nanoparticles contribute to their interaction with mononuclear phagocytic system which is responsible for the fate of nanoparticles like internalization, bio distribution, and clearance from body. Approaches for nanoparticles targeting IBD are as follows:

1.6.1 Size mediated targeting

Due to severe inflammation, vascular permeability and epithelial permeability are highly increased in UC [76]. A study conducted by Lamprecht et al., demonstrated the effect of size on the accumulation of nanoparticles in the inflamed tissues where they administered polystyrene particles of various sizes (100 μm , 1 μm , and 100 nm) orally by gavage. 100 nm particles revealed the highest retention in an inflamed colon region compared to others suggesting the role of size in targeting IBD [77]. Another study also suggested localization of budesonide loaded nanoparticles (200 nm) was found in an inflamed colonic tissue of colitic mice [78]. Nanoparticles owing to the advantage of smaller can easily penetrate the mucus barrier and reach up to serosa in an inflamed colon. Another study compared microparticles (3 μm) with nanoparticles (250 nm) of PLGA exhibited a higher accumulation of microparticles in ulcers whereas nanoparticles penetrated deep and were found in the serosal layer [79].

1.6.2 pH-mediated targeting

The strategy of pH-dependent targeting is based on the difference in pH of the entire gastrointestinal tract (GIT). The pH of the last region of the ileum and colon is higher compared to the upper region of GIT [80, 81]. Hence, a researcher can exploit this difference in pH for developing pH-dependent nano-delivery system for targeting drugs to the specific desired location and releasing the drug. The best approach is to coat the nanocarrier with pH-sensitive polymers (Eudragit-S-100) [82]. The enteric coating offers a wide range of protection in terms of degradation of pharmaceutically active agents from harsh environment of GIT e.g. gastric acid, bile juice and microbial enzymes. Methacrylic acid copolymers (Eudragit®) are widely used for this purpose and approved by FDA for the same. Eudragit® polymers are available in wide ranges based on the pH at which it degrades. Eudragit L 100 and Eudragit-S-100 are the most widely used polymers for colon targeting as it degrades in pH range of 6 to 7 [83]. Eudragit-S-100 coated chitosan nanoparticles have shown colon

targeting and attenuated inflammatory conditions in colitic mice [84]. Nanocapsules of prednisolone coated with Eudragit-S-100 exhibited pH-dependent release in an *in vitro* condition with higher loading of lipophilic [85] agents suggesting its advancement in therapeutic improvement for application in IBD. Also, budesonide loaded PLGA nanoparticles when coated with Eudragit-S-100 alleviated inflammation colitic mice by significantly down-regulating the expression of proinflammatory cytokines [86]. Hence, based on the above results and observation we can speculate on the efficacy of enteric coating polymer in alleviating IBD in patients.

1.6.3 Charge mediated

In UC condition the mucus layers deplete resulting in the reduction of mucus and thereby *in situ* aggregation of positively charged proteins which leads to a higher positive charge at the site of inflammation. Hence, researchers can exploit this to develop charge-based nanocarriers for efficient drug delivery to ameliorate UC. A study conducted by Jubeh et al., revealed that negatively charged nanocarriers have a higher binding affinity on inflamed colonic explants compared to healthy [87]. Anionic liposomes adhered to inflamed colonic mucosal explant (twice) compared to neutral and cationic liposomes. Negatively charged particles were easily engulfed by monocytes, which caused their apoptosis and thereby improving disease condition in case of inflammatory disease. Negatively charged microfibers of ascorbyl palmitate were investigated in UC mice models for their efficacy in improving the anti-inflammatory action of dexamethasone via rectal route using enema [88].

1.6.4 Ligand receptor-mediated targeting

Severe chronic inflammation causes an increase in expression of certain protein biomarkers on cell surface i.e. ligands or receptors which can be used for specific targeting of nanocarriers for alleviating disease e.g. leucocyte migration to the inflamed tissues via leucocyte-endothelial interaction which increased upon inflammation [89]. Endothelial cell overexpresses adhesion molecules like vascular cell adhesion molecule (VCAM)-1, P-selectin, and intercellular adhesion molecule (ICAM-1) on their luminal surface whereas ligands (P-selectin glycoprotein ligand-1) which participate in leucocyte adhesion are overexpressed. Integrin like $\alpha_4\beta_7$, $\alpha_4\beta_1$, $\alpha_L\beta_2$, and $\alpha_M\beta_2$ are over expressed which helps in cell adhesion on the endothelial cell surface [89]. Recently, Sakhalkar et al., developed PEGylated PLA nanoparticles conjugated with recombinant PSGL-1 mimicking leucocyte-

endothelial adhesion biochemistry which exhibited a significant rolling and adhesion in the inflamed tissues [90]. β_7 integrin targeted liposomal nanoparticles (β_7 I -tsNPs) loaded CyD1-Si RNA having the ability to target a specific subset of leucocytes and treat colitic mice through silencing Cyclin D1 (CyD1) which is abruptly unregulated in immune cells and endothelial cells in UC [91]. The CyD1-Si RNA loaded nanoparticle exhibited remarkable improvement in the leucocyte infiltration in the colonic region, reversed body weight loss, and hematocrit decrease.

1.6.5 Degradation mediated targeting

Enzymes or specific molecules occur in extracellular matrix (ECM) or microbiota present in an inflamed colon which can digest nanodelivery systems and can be exploited to deliver therapeutic agents to exacerbate IBD. Chronic inflammation causes overproduction of reactive oxygen species (ROS) in a mucosal layer which can be exploited for the degradation of nanoparticles and deliver drugs [92]. Thioketal nanoparticles developed by Wilson et al., degraded in response to ROS at the site of inflammation to deliver TNF- α Si-RNA in colitic mice [93]. Proteolytic enzymes like matrix metalloproteinase (MMPs) are highly up-regulated in the inflamed extracellular matrix. MMP-sensitive nanodelivery system could be used delivery of biologics and drugs to the site of inflammation [94].

1.6.6 Microbiota-mediated targeting

Immunological response due to host bacteria is crucial in IBD and proves to be harmful leading to uncontrolled severe inflammation. Prebiotics show beneficiary effect by increasing the growth of probiotics and beneficial microbes [95]. Probiotic bacteria have been developed using genetic engineering which resides in a specific niche in the colon where they can release biologically active proteins to get desired beneficial effect. IL-10 has been delivered using *Lactococcus Lactis* as an anti-inflammatory therapy in IBD [96]. *Lactococcus lactis* secreting LCrV protein and trefoil factors decreased inflammation in the intestines of colitic mice [97, 98].

1.7 Role of melatonin and its limitation in UC therapy

When individuals do not react to treatment with topical, oral, or 5-aminosalicylates, the condition is known as refractory UC [99]. As a result, there is a demand for more advanced

therapeutics that could be employed to more effectively treat this disease. Melatonin was given as an anti-inflammatory and antioxidant, which can enhance the therapeutic regimen [100]. In 1958, Aron Lerner and colleagues for the first time extracted and purified melatonin (N-acetyl-5-methoxy tyryptamine) from the cow pineal gland [101]. Later, it was revealed that it was also made in tissues such as the gastrointestinal (GI) tract, where it was 400–500 times higher than in the pineal gland, but that it changed under the influence of disease [102]. Because its physiological function is not well understood, we are unsure of its precise function in the gut, where enterochromaffin cells produce it [103]. Additionally, GI illnesses may be linked to its imbalance in the gut. Locally acting as an antioxidant in the gut, melatonin can aid in managing increasing oxidative stress. Melatonin regulates sympathetic and parasympathetic nerves by decreasing the release of hydrochloric acid, triggering an immunological response, aiding in tissue healing, and improving microcirculation. This indirect action occurs through the central nervous system [104]. Improvements in clinical symptoms, a decrease in faecal calprotectin, and improved quality of life were reported with melatonin administered as adjuvant therapy (3 mg) in UC [105]. The concentration of melatonin in the gut of UC patients [106] is debatable its concentration in gut is increased but decreased in plasma [107]. According to a study by Cezary et al., colonic mucosa may have higher amounts of melatonin synthesizing hormone due to a higher need for antioxidants brought on by disease-induced stress [106]. UC is a chronic inflammatory condition that alters the level of various pro-inflammatory cytokines and oxidative stress. Elevated inflammatory condition and oxidative stress lead to up-regulation in proinflammatory cytokine NF-kB [108] and assist in the progression of UC. NF-kB increases the severity of UC by elevating the level of inflammatory cytokines TNF- α , IL-6 and IL-1 β [109]. Melatonin has an inhibitory effect on the expression of NF-kB and thereby attenuating inflammatory cytokine which is beneficial to UC therapy [110-112]. Due to its limitations in terms of water solubility, poor absorption, and short plasma half-life in the body, although having substantial anti-inflammatory activity, its significance in alleviating IBD has not been thoroughly proven. Because of their ability to improve the aforementioned melatonin constraint, nanotechnology thus provides us with a clear understanding of how strong a position they can hold in treating IBD. As part of this thesis, we investigate the role of melatonin via epigenetic mechanisms involved in the regulation of inflammation in macrophages, as well as nanotechnology to overcome the physicochemical limitations that limit its efficacy.

1.8 References

- [1] L. Chen, H. Deng, H. Cui, J. Fang, Z. Zuo, J. Deng, Y. Li, X. Wang, L. Zhao, *Oncotarget*, 9 (2018) 7204-7218.
- [2] R. Medzhitov, *Cell*, 140 (2010) 771-776.
- [3] C. Nathan, A. Ding, *Cell*, 140 (2010) 871-882.
- [4] G. Majno, *The healing hand : man and wound in the ancient world*, Harvard University Press, Cambridge, Mass., 1975.
- [5] G.J.I. Majno, (2004).
- [6] E. Pecchi, M. Dallaporta, A. Jean, S. Thirion, J.D. Troadec, *Physiology & behavior*, 97 (2009) 279-292.
- [7] J.J. McLeod, B. Baker, J.J. Ryan, *Cytokine*, 75 (2015) 57-61.
- [8] E. Mitre, T.B. Nutman, *Chemical immunology and allergy*, 90 (2006) 141-156.
- [9] J.A. Chandrasekharan, N. Sharma-Walia, *J Inflamm Res*, 8 (2015) 181-192.
- [10] I. Damjanov, 23 (2005) 482-483.
- [11] A. Kaser, S. Zeissig, R.S. Blumberg, 28 (2010) 573-621.
- [12] D.K. Podolsky, *N Engl J Med*, 347 (2002) 417-429.
- [13] I.J. Fuss, F. Heller, M. Boirivant, F. Leon, M. Yoshida, S. Fichtner-Feigl, Z. Yang, M. Exley, A. Kitani, R.S. Blumberg, P. Mannon, W. Strober, *The Journal of clinical investigation*, 113 (2004) 1490-1497.
- [14] R.S. McLeod, *Dig Dis*, 21 (2003) 168-179.
- [15] C. Nigg, U.K. Naumann, L. Käser, W. Vetter, *Praxis*, 97 (2008) 167-173; quiz 174-165.
- [16] W.D. Lynch, R. Hsu, *Ulcerative Colitis*, StatPearls, StatPearls Publishing
- Copyright © 2022, StatPearls Publishing LLC., Treasure Island (FL), 2022.
- [17] S.N. Khosla, N.K. Girdhar, S. Lal, D.S. Mishra, *The Journal of the Association of Physicians of India*, 34 (1986) 405-407.
- [18] A. Sood, V. Midha, N. Sood, A.S. Bhatia, G. Avasthi, *Gut*, 52 (2003) 1587-1590.
- [19] G.K. Makharia, B.S. Ramakrishna, P. Abraham, G. Choudhuri, S.P. Misra, V. Ahuja, S.J. Bhatia, D.K. Bhasin, S. Dadhich, G.K. Dhali, D.C. Desai, U.C. Ghoshal, B.D. Goswami, S.K. Issar, A.K. Jain, V. Jayanthi, G. Loganathan, C.G. Pai, A.S. Puri, S.S. Rana, G. Ray, S.P. Singh, A. Sood, *Indian J Gastroenterol*, 31 (2012) 299-306.

- [20] B.J. Van Klinken, J.W. Van der Wal, A.W. Einerhand, H.A. Büller, J. Dekker, *Gut*, 44 (1999) 387-393.
- [21] F. Heller, P. Florian, C. Bojarski, J. Richter, M. Christ, B. Hillenbrand, J. Mankertz, A.H. Gitter, N. Bürgel, M. Fromm, M. Zeitz, I. Fuss, W. Strober, J.D. Schulzke, *Gastroenterology*, 129 (2005) 550-564.
- [22] A. Rahman, A. Fahlgren, B. Sitohy, V. Baranov, A. Zirakzadeh, S. Hammarström, A. Danielsson, M.L. Hammarström, *Inflammatory bowel diseases*, 13 (2007) 847-855.
- [23] J.D. Taurog, J.A. Richardson, J.T. Croft, W.A. Simmons, M. Zhou, J.L. Fernández-Sueiro, E. Balish, R.E. Hammer, *The Journal of experimental medicine*, 180 (1994) 2359-2364.
- [24] K. Isaacs, *Gastroenterology*, 127 (2004) 1272–1273.
- [25] *Biochem Biophys Res Commun*, 598 (2022) 139.
- [26] J.H. Niess, S. Brand, X. Gu, L. Landsman, S. Jung, B.A. McCormick, J.M. Vyas, M. Boes, H.L. Ploegh, J.G. Fox, D.R. Littman, H.C. Reinecker, *Science (New York, N.Y.)*, 307 (2005) 254-258.
- [27] A.S. Vamadevan, M. Fukata, E.T. Arnold, L.S. Thomas, D. Hsu, M.T. Abreu, *Innate immunity*, 16 (2010) 93-103.
- [28] F.X. Zhang, C.J. Kirschning, R. Mancinelli, X.P. Xu, Y. Jin, E. Faure, A. Mantovani, M. Rothe, M. Muzio, M. Arditi, *The Journal of biological chemistry*, 274 (1999) 7611-7614.
- [29] G. Rogler, K. Brand, D. Vogl, S. Page, R. Hofmeister, T. Andus, R. Knuechel, P.A. Baeuerle, J. Schölmerich, V. Gross, *Gastroenterology*, 115 (1998) 357-369.
- [30] L. Eckmann, T. Nebelsiek, A.A. Fingerle, S.M. Dann, J. Mages, R. Lang, S. Robine, M.F. Kagnoff, R.M. Schmid, M. Karin, M.C. Arkan, F.R. Greten, *Proc Natl Acad Sci U S A*, 105 (2008) 15058-15063.
- [31] F. Heller, I.J. Fuss, E.E. Nieuwenhuis, R.S. Blumberg, W. Strober, *Immunity*, 17 (2002) 629-638.
- [32] E.O. Glocker, D. Kotlarz, K. Boztug, E.M. Gertz, A.A. Schäffer, F. Noyan, M. Perro, J. Diestelhorst, A. Allroth, D. Murugan, N. Hätscher, D. Pfeifer, K.W. Sykora, M. Sauer, H. Kreipe, M. Lacher, R. Nustede, C. Woellner, U. Baumann, U. Salzer, S. Koletzko, N. Shah, A.W. Segal, A. Sauerbrey, S. Buderus, S.B. Snapper, B. Grimbacher, C. Klein, *N Engl J Med*, 361 (2009) 2033-2045.
- [33] S.H. Murch, V.A. Lamkin, M.O. Savage, J.A. Walker-Smith, T.T. MacDonald, *Gut*, 32 (1991) 913-917.

- [34] C.P. Braegger, S. Nicholls, S.H. Murch, S. Stephens, T.T. MacDonald, *Lancet*, 339 (1992) 89-91.
- [35] R. Matsuda, T. Koide, C. Tokoro, T. Yamamoto, T. Godai, T. Morohashi, Y. Fujita, D. Takahashi, I. Kawana, S. Suzuki, S. Umemura, *Inflammatory bowel diseases*, 15 (2009) 328-334.
- [36] M. Briskin, D. Winsor-Hines, A. Shyjan, N. Cochran, S. Bloom, J. Wilson, L.M. McEvoy, E.C. Butcher, N. Kassam, C.R. Mackay, W. Newman, D.J. Ringler, *The American journal of pathology*, 151 (1997) 97-110.
- [37] M.S. Silverberg, J.H. Cho, J.D. Rioux, D.P. McGovern, J. Wu, V. Annese, J.P. Achkar, P. Goyette, R. Scott, W. Xu, M.M. Barmada, L. Klei, M.J. Daly, C. Abraham, T.M. Bayless, F. Bossa, A.M. Griffiths, A.F. Ippoliti, R.G. Lahaie, A. Latiano, P. Paré, D.D. Proctor, M.D. Regueiro, A.H. Steinhardt, S.R. Targan, L.P. Schumm, E.O. Kistner, A.T. Lee, P.K. Gregersen, J.I. Rotter, S.R. Brant, K.D. Taylor, K. Roeder, R.H. Duerr, *Nature genetics*, 41 (2009) 216-220.
- [38] J.C. Barrett, J.C. Lee, C.W. Lees, N.J. Prescott, C.A. Anderson, A. Phillips, E. Wesley, K. Parnell, H. Zhang, H. Drummond, E.R. Nimmo, D. Massey, K. Blaszczuk, T. Elliott, L. Cotterill, H. Dallal, A.J. Lobo, C. Mowat, J.D. Sanderson, D.P. Jewell, W.G. Newman, C. Edwards, T. Ahmad, J.C. Mansfield, J. Satsangi, M. Parkes, C.G. Mathew, P. Donnelly, L. Peltonen, J.M. Blackwell, E. Bramon, M.A. Brown, J.P. Casas, A. Corvin, N. Craddock, P. Deloukas, A. Duncanson, J. Jankowski, H.S. Markus, C.G. Mathew, M.I. McCarthy, C.N. Palmer, R. Plomin, A. Rautanen, S.J. Sawcer, N. Samani, R.C. Trembath, A.C. Viswanathan, N. Wood, C.C. Spencer, J.C. Barrett, C. Bellenguez, D. Davison, C. Freeman, A. Strange, P. Donnelly, C. Langford, S.E. Hunt, S. Edkins, R. Gwilliam, H. Blackburn, S.J. Bumpstead, S. Dronov, M. Gillman, E. Gray, N. Hammond, A. Jayakumar, O.T. McCann, J. Liddle, M.L. Perez, S.C. Potter, R. Ravindrarajah, M. Ricketts, M. Waller, P. Weston, S. Widaa, P. Whittaker, P. Deloukas, L. Peltonen, C.G. Mathew, J.M. Blackwell, M.A. Brown, A. Corvin, M.I. McCarthy, C.C. Spencer, A.P. Attwood, J. Stephens, J. Sambrook, W.H. Ouwehand, W.L. McArdle, S.M. Ring, D.P. Strachan, *Nature genetics*, 41 (2009) 1330-1334.
- [39] J.M. Wheeler, H.C. Kim, J.A. Efstathiou, M. Ilyas, N.J. Mortensen, W.F. Bodmer, *Gut*, 48 (2001) 367-371.
- [40] M. de Krijger, I.L. Hageman, A.Y.F. Li Yim, J. Verhoeff, J.J. Garcia Vallejo, P.H.P. van Hamersveld, E. Levin, T.B.M. Hakvoort, M.E. Wildenberg, P. Henneman, C.Y. Ponsioen, W.J. de Jonge, *Front Immunol*, 13 (2022) 840935.

- [41] A. Razin, H. Cedar, *Microbiological reviews*, 55 (1991) 451-458.
- [42] A.M. Deaton, A. Bird, *Genes & development*, 25 (2011) 1010-1022.
- [43] A. Levine, S. Koletzko, D. Turner, J.C. Escher, S. Cucchiara, L. de Ridder, K.L. Kolho, G. Veres, R.K. Russell, A. Paerregaard, S. Buderus, M.L. Greer, J.A. Dias, G. Veereman-Wauters, P. Lionetti, M. Sladek, J. Martin de Carpi, A. Staiano, F.M. Ruemmele, D.C. Wilson, *J Pediatr Gastroenterol Nutr*, 58 (2014) 795-806.
- [44] M.A. Quail, R.K. Russell, J.E. Van Limbergen, P. Rogers, H.E. Drummond, D.C. Wilson, P.M. Gillett, *Inflammatory bowel diseases*, 15 (2009) 756-759.
- [45] F.A. Jose, E.A. Garnett, E. Vittinghoff, G.D. Ferry, H.S. Winter, R.N. Baldassano, B.S. Kirschner, S.A. Cohen, B.D. Gold, O. Abramson, M.B. Heyman, *Inflammatory bowel diseases*, 15 (2009) 63-68.
- [46] U. Navaneethan, P.G. Venkatesh, B.A. Lashner, B. Shen, R.P. Kiran, *Aliment Pharmacol Ther*, 35 (2012) 1045-1053.
- [47] L.L. Troncoso, A.L. Biancardi, H.V. de Moraes, Jr., C. Zaltman, *World journal of gastroenterology*, 23 (2017) 5836-5848.
- [48] B.G. Feagan, J.K. Macdonald, *Cochrane Database Syst Rev*, 10 (2012) Cd000543.
- [49] A.C. Ford, K.J. Khan, W.J. Sandborn, S.V. Kane, P. Moayyedi, *Am J Gastroenterol*, 106 (2011) 2070-2077; quiz 2078.
- [50] G.R. Lichtenstein, D. Ramsey, D.T. Rubin, *Aliment Pharmacol Ther*, 33 (2011) 672-678.
- [51] P. Marteau, J. Crand, M. Foucault, J.C. Rambaud, *Gut*, 42 (1998) 195-199.
- [52] M. Safdi, M. DeMicco, C. Sninsky, P. Banks, L. Wruble, J. Deren, G. Koval, T. Nichols, S. Targan, C. Fleishman, B. Wiita, *Am J Gastroenterol*, 92 (1997) 1867-1871.
- [53] D. Turner, C.M. Walsh, A.H. Steinhart, A.M. Griffiths, *Clin Gastroenterol Hepatol*, 5 (2007) 103-110.
- [54] C. Romano, A. Famiani, D. Comito, P. Rossi, V. Raffa, W. Fries, *J Pediatr Gastroenterol Nutr*, 50 (2010) 385-389.
- [55] D. Turner, A. Levine, J.C. Escher, A.M. Griffiths, R.K. Russell, A. Dignass, J.A. Dias, J. Bronsky, C.P. Braegger, S. Cucchiara, L. de Ridder, U.L. Fagerberg, S. Hussey, J.P. Hugot, S. Kolacek, K.L. Kolho, P. Lionetti, A. Paerregaard, A. Potapov, R. Rintala, D.E. Serban, A. Staiano, B. Sweeny, G. Veerman, G. Veres, D.C. Wilson, F.M. Ruemmele, *J Pediatr Gastroenterol Nutr*, 55 (2012) 340-361.

- [56] E. Stourmaras, W. Qian, A. Pappas, Y.Y. Hong, R. Shawky, U.I.B. Investigators, T. Raine, M. Parkes, U.I.B. Investigators, *Gut*, 70 (2021) 677-686.
- [57] P. Rutgeerts, W.J. Sandborn, B.G. Feagan, W. Reinisch, A. Olson, J. Johanns, S. Travers, D. Rachmilewitz, S.B. Hanauer, G.R. Lichtenstein, W.J. de Villiers, D. Present, B.E. Sands, J.F. Colombel, *N Engl J Med*, 353 (2005) 2462-2476.
- [58] W.J. Sandborn, G. van Assche, W. Reinisch, J.F. Colombel, G. D'Haens, D.C. Wolf, M. Kron, M.B. Tighe, A. Lazar, R.B. Thakkar, *Gastroenterology*, 142 (2012) 257-265.e251-253.
- [59] W.J. Sandborn, B.G. Feagan, C. Marano, H. Zhang, R. Strauss, J. Johanns, O.J. Adedokun, C. Guzzo, J.F. Colombel, W. Reinisch, P.R. Gibson, J. Collins, G. Järnerot, P. Rutgeerts, *Gastroenterology*, 146 (2014) 96-109.e101.
- [60] D.M. Knight, H. Trinh, J. Le, S. Siegel, D. Shealy, M. McDonough, B. Scallon, M.A. Moore, J. Vilcek, P. Daddona, et al., *Mol Immunol*, 30 (1993) 1443-1453.
- [61] R. Panaccione, S. Ghosh, S. Middleton, J.R. Márquez, B.B. Scott, L. Flint, H.J. van Hoogstraten, A.C. Chen, H. Zheng, S. Danese, P. Rutgeerts, *Gastroenterology*, 146 (2014) 392-400.e393.
- [62] O.H. Nielsen, M.A. Ainsworth, *N Engl J Med*, 369 (2013) 754-762.
- [63] C.K. Rayner, G. McCormack, A.V. Emmanuel, M.A. Kamm, *Aliment Pharmacol Ther*, 18 (2003) 303-308.
- [64] G. Van Assche, G. D'Haens, M. Noman, S. Vermeire, M. Hiele, K. Asnong, J. Arts, A. D'Hoore, F. Penninckx, P. Rutgeerts, *Gastroenterology*, 125 (2003) 1025-1031.
- [65] H. Ogata, T. Matsui, M. Nakamura, M. Iida, M. Takazoe, Y. Suzuki, T. Hibi, *Gut*, 55 (2006) 1255-1262.
- [66] B.G. Feagan, G.R. Greenberg, G. Wild, R.N. Fedorak, P. Paré, J.W. McDonald, R. Dubé, A. Cohen, A.H. Steinhardt, S. Landau, R.A. Aguzzi, I.H. Fox, M.K. Vandervoort, *N Engl J Med*, 352 (2005) 2499-2507.
- [67] S.J. Bickston, B.W. Behm, D.J. Tsoulis, J. Cheng, J.K. MacDonald, R. Khanna, B.G. Feagan, *Cochrane Database Syst Rev*, (2014) Cd007571.
- [68] J.F. Colombel, B.E. Sands, P. Rutgeerts, W. Sandborn, S. Danese, G. D'Haens, R. Panaccione, E.V. Loftus, Jr., S. Sankoh, I. Fox, A. Parikh, C. Milch, B. Abhyankar, B.G. Feagan, *Gut*, 66 (2017) 839-851.

- [69] W.J. Sandborn, C. Su, B.E. Sands, G.R. D'Haens, S. Vermeire, S. Schreiber, S. Danese, B.G. Feagan, W. Reinisch, W. Niezychowski, G. Friedman, N. Lawendy, D. Yu, D. Woodworth, A. Mukherjee, H. Zhang, P. Healey, J. Panés, *N Engl J Med*, 376 (2017) 1723-1736.
- [70] U. Klotz, M. Schwab, *Advanced drug delivery reviews*, 57 (2005) 267-279.
- [71] E.M. Collnot, H. Ali, C.M. Lehr, *J Control Release*, 161 (2012) 235-246.
- [72] B. Homayun, A. Kumar, P.T.H. Nascimento, H.J. Choi, *Archives of pharmacal research*, 41 (2018) 848-860.
- [73] R. Malayandi, P.K. Kondamudi, P.K. Ruby, D. Aggarwal, *Drug delivery and translational research*, 4 (2014) 187-202.
- [74] B. Xiao, D. Merlin, *Expert opinion on drug delivery*, 9 (2012) 1393-1407.
- [75] A. Lamprecht, H. Yamamoto, H. Takeuchi, Y. Kawashima, *Journal of Pharmacology and Experimental Therapeutics*, 315 (2005) 196.
- [76] G. Tolstanova, X. Deng, S.W. French, W. Lungo, B. Paunovic, T. Khomenko, A. Ahluwalia, T. Kaplan, M. Dacosta-Iyer, A. Tarnawski, S. Szabo, Z. Sandor, *Laboratory Investigation*, 92 (2012) 9-21.
- [77] A. Lamprecht, U. Schäfer, C.-M. Lehr, *Pharmaceutical Research*, 18 (2001) 788-793.
- [78] H. Ali, B. Weigmann, E.M. Collnot, S.A. Khan, M. Windbergs, C.M. Lehr, *Pharm Res*, 33 (2016) 1085-1092.
- [79] C. Schmidt, C. Lautenschlaeger, E.M. Collnot, M. Schumann, C. Bojarski, J.D. Schulzke, C.M. Lehr, A. Stallmach, *J Control Release*, 165 (2013) 139-145.
- [80] J. Fallingborg, L.A. Christensen, B.A. Jacobsen, S.N. Rasmussen, *Dig Dis Sci*, 38 (1993) 1989-1993.
- [81] J. Bratten, M.P. Jones, *Dig Dis*, 24 (2006) 252-259.
- [82] M. Ashford, J.T. Fell, D. Attwood, H. Sharma, P.J. Woodhead, *International Journal of Pharmaceutics*, 95 (1993) 193-199.
- [83] L.F. Asghar, S. Chandran, *Journal of pharmacy & pharmaceutical sciences : a publication of the Canadian Society for Pharmaceutical Sciences, Societe canadienne des sciences pharmaceutiques*, 9 (2006) 327-338.
- [84] S.J. Mohanbhai, M.N. Sardoiwala, S. Gupta, N. Shrimali, S.R. Choudhury, S.S. Sharma, P. Guchhait, S. Karmakar, *Biomaterials Advances*, 136 (2022) 212796.
- [85] P. Legrand, G. Barratt, V. Mosqueira, H. Fessi, J.P.J.S.P.S. Devissaguet, 9 (1999) 411-418.

- [86] H. Ali, B. Weigmann, M.F. Neurath, E.M. Collnot, M. Windbergs, C.M. Lehr, *Journal of Controlled Release*, 183 (2014) 167-177.
- [87] T.T. Jubeh, Y. Barenholz, A. Rubinstein, *Pharmaceutical Research*, 21 (2004) 447-453.
- [88] S. Zhang, J. Ermann, M.D. Succi, A. Zhou, M.J. Hamilton, B. Cao, J.R. Korzenik, J.N. Glickman, P.K. Vemula, L.H. Glimcher, G. Traverso, R. Langer, J.M. Karp, *Science translational medicine*, 7 (2015) 300ra128.
- [89] E. Kim, O. Schueller, P.M. Sweetnam, *Lab on a chip*, 12 (2012) 2255-2264.
- [90] H.S. Sakhalkar, M.K. Dalal, A.K. Salem, R. Ansari, J. Fu, M.F. Kiani, D.T. Kurjiaka, J. Hanes, K.M. Shakesheff, D.J. Goetz, *Proc Natl Acad Sci U S A*, 100 (2003) 15895-15900.
- [91] D. Peer, E.J. Park, Y. Morishita, C.V. Carman, M. Shimaoka, *Science (New York, N.Y.)*, 319 (2008) 627-630.
- [92] H. Zhu, Y.R. Li, *Exp Biol Med (Maywood)*, 237 (2012) 474-480.
- [93] D.S. Wilson, G. Dalmaso, L. Wang, S.V. Sitaraman, D. Merlin, N. Murthy, *Nature Materials*, 9 (2010) 923-928.
- [94] H. Järveläinen, A. Sainio, M. Koulu, T.N. Wight, R. Penttinen, *Pharmacological reviews*, 61 (2009) 198-223.
- [95] G.A. Preidis, J. Versalovic, *Gastroenterology*, 136 (2009) 2015-2031.
- [96] L. Steidler, W. Hans, L. Schotte, S. Neiryneck, F. Obermeier, W. Falk, W. Fiers, E. Remaut, *Science (New York, N.Y.)*, 289 (2000) 1352-1355.
- [97] B. Foligne, R. Dessein, M. Marceau, S. Poiret, M. Chamailard, B. Pot, M. Simonet, C. Daniel, *Gastroenterology*, 133 (2007) 862-874.
- [98] K. Vandenbroucke, W. Hans, J. Van Huysse, S. Neiryneck, P. Demetter, E. Remaut, P. Rottiers, L. Steidler, *Gastroenterology*, 127 (2004) 502-513.
- [99] G. Pineton de Chambrun, B. Tassy, L. Kollen, G. Dufour, J.C. Valats, M. Bismuth, N. Funakoshi, F. Panaro, P. Blanc, *Best practice & research. Clinical gastroenterology*, 32-33 (2018) 49-57.
- [100] C. Chojnacki, M. Wisniewska-Jarosinska, E. Walecka-Kapica, G. Klupinska, J. Jaworek, J. Chojnacki, *J Physiol Pharmacol*, 62 (2011) 327-334.
- [101] I. Chowdhury, A. Sengupta, S.K. Maitra, *Indian journal of biochemistry & biophysics*, 45 (2008) 289-304.
- [102] K. Stebelová, I. Herichová, M. Zeman, *Neuro Endocrinol Lett*, 28 (2007) 159-165.

- [103] C. Chojnacki, M. Wisniewska-Jarosinska, G. Kulig, I. Majsterek, R.J. Reiter, J. Chojnacki, *World J Gastroenterol*, 19 (2013) 3602-3607.
- [104] G.A. Bubenik, *Dig Dis Sci*, 47 (2002) 2336-2348.
- [105] S. Shahrokh, R. Qobadighadikolaei, M. Abbasinazari, M. Haghazali, H. Asadzadeh Aghdaei, S. Abdi, H. Balaii, N. Khanzadeh-Moghaddam, M.R. Zali, *Iran J Pharm Res*, 20 (2021) 197-205.
- [106] C. Chojnacki, J. Blasiak, J. Fichna, J. Chojnacki, T. Poplawski, *Molecules*, 23 (2018).
- [107] M. Chen, Q. Mei, J. Xu, C. Lu, H. Fang, X. Liu, *Clin Chim Acta*, 413 (2012) 30-33.
- [108] Z.J. Zhao, J.Y. Xiang, L. Liu, X.L. Huang, H.T. Gan, *Int Immunopharmacol*, 12 (2012) 169-174.
- [109] M. Lappas, M. Permezel, H.M. Georgiou, G.E. Rice, *Biology of reproduction*, 67 (2002) 668-673.
- [110] J.H. Li, J.P. Yu, H.G. Yu, X.M. Xu, L.L. Yu, J. Liu, H.S. Luo, *Mediators Inflamm*, 2005 (2005) 185-193.
- [111] J.H. Li, W. Zhou, K. Liu, H.X. Li, L. Wang, *Saudi Med J*, 29 (2008) 1088-1094.
- [112] H.G. Sayyed, R.J. Jaumdally, N.K. Idriss, D.A. El Sers, A. Blann, *Dig Dis Sci*, 58 (2013) 3156-3164.

Chapter 2:

Materials and methods

2.0 Materials

Melatonin ($\geq 98\%$, M5250, SIGMA), Dulbecco's Modified Eagle Medium (DMEM) (AT186, Himedia), lipopolysaccharide (L4391, Sigma), Fetal bovine serum (RM9954, Himedia), Antibiotic and antimycotic 100x (A002, Himedia), sulphanimide (65404, sisco research lab), N-(1-naphthyl) ethylenediamine dihydrochloride (61166, sisco research lab), Dextran sulfate sodium salt, colitis grade (36,000 - 50,000) (9011-18-1, MP Biomedicals), QuantiPro™ BCA Assay Kit (QPBCA, Sigma), Protein A/G PLUS-Agarose (sc-2003, SCBT), Sodium dodecyl sulphate (L3771, Sigma), 2x Laemmli Sample Buffer (1610737EDU, BIO RAD), Bio-Rad Vertical Filter Paper (1703932, BIO RAD), Bovine serum albumin (RM3135, Himedia), Tris (hydroxymethyl) aminomethane (TC072, Himedia), Polysorbate 20 (Tween 20) (65296, sisco research lab), Triton™ X-100 (11332481001, Sigma), Anti-ENX-1 Antibody (D-8) (sc-137255, SCBT), Tri-Methyl-Histone H3 (Lys27) Rabbit mAb (9733, CST), iNOS Antibody (AF0199, Affinity Biosciences), Anti- β -Actin Antibody (C4) (sc-47778, SCBT), IL1- β Rabbit pAb (A11370, Abclonal), goat anti-mouse IgG-HRP (sc-2005, SCBT), goat anti-rabbit IgG-HRP (sc-2004, SCBT), TRITC-conjugated secondary antimouse (T5393, SCBT), FITC-conjugated secondary antimouse (F9887, Sigma), Clarity™ Western ECL Substrate (1705060, BIO RAD), Acrylamide (79-06-1, Sigma), N,N'-Methylenebisacrylamide (110-26-9, Sigma), Lithium Chloride (39692, sisco research lab), Sodium Chloride extrapure (41721, Sisco research lab), EDTA Dipotassium Salt extrapure (62196, Sisco research lab), Proteinase K (TC687, Himedia), RNase A (MB087, Himedia), RNA – Xpress™ Reagent (MB601, Himedia), Cryomatrix Gel (Thermo Scientific), Paraformaldehyde (158127, Sigma), o-Dianisidine Dihydrochloride extrapure (13261, Sisco research lab), Haematoxylin (S058, Himedia), Eosin (S007, Himedia), Alcian blue (48261, Sisco research lab), Nuclear Fast Red (68547, Sisco research lab), Toluidine Blue O (22134, Sisco research lab), Low molecular weight chitosan (5–20 mPa), Sodium tripolyphosphate (STPP) (238503, Sigma, 3-[4,5-dimethylthiazol-2-yl]-2,5-diphenyltetrazolium bromide (MTT) (RM113, Himedia), Indocyanine green (I0535, TCI), cDNA reverse transcription kit (Thermo), SYBR-green (Biorad), Eudragit-S-100 (E 1672, Otto chemie), Laemmli sample buffer (Bio-Rad, CAS number 1610737EDU), 4', 6- diamidino-2-phenylindole (DAPI) (10236276001, Sigma)

2.1 Methods

2.1.1 Synthesis of Chitosan nanoparticle and Eudragit-S-100 coated chitosan nanoparticles

Chitosan nanoparticles were synthesized using our previously published method with slight modification [1-4]. Briefly chitosan was dissolved in 1% acetic acid at concentration of 1.5 mg/ml. pH was adjusted to 4.5 using sodium hydroxide and filtered to remove insoluble materials. Sodium tripolyphosphate (STPP) was dissolved in Type-1 water at concentration of 3 mg/ml. Nanoparticles were formed using ionic gelation by gradually adding STPP in the chitosan solution till colloidal turbidity appears. Chitosan nanoparticles (CSNPs) were centrifuged at 15000 rpm and washed 3 times to purify. The ratio of Chitosan and STPP was optimised to 3:2 for nanoparticle synthesis for oral drug delivery and 2:1 for intravenous drug delivery. Similarly, melatonin was dissolved in chitosan solution and allowed to interact for 1 hour, melatonin loaded chitosan nanoparticles (Mel-CSNPs) were formed by adding STPP gradually. We have obtained optimum drug loading at melatonin and chitosan ratio of 1:2 by following our previous work [1]. For Eudragit-S-100 coated chitosan nanoparticles, ethanolic solution of Eudragit-S-100 (2 mg/ml) was gradually added to prepared chitosan nanoparticles with Chitosan: Eudragit-S-100 ratio of 6:1 and stirred at 850 rpm for 12 hours till the ethanol is completely evaporated [5]. The formulations were purified, lyophilised and stored for further application.

For preparation of Fluorescein Isothiocyanate (FITC) labelled chitosan nanoparticles, chitosan (100 mg) was dissolved in 1% acetic acid and 1 mg of FITC was allowed to react for 12 hours. The reacted chitosan and FITC was then dialysed against deionised water for 72 hours for removal of unreacted part. This fluorescent conjugated chitosan was then used to prepare FITC-CSNPs using ionotropic gelation method using STPP or lyophilized for future applications [6].

For the preparation of ICG-CSNPs, 2 mL of aqueous CSNP suspension (20 mg/ml) was combined with 1 mL of ICG aqueous solution (0.5 mg/mL). The resulting colloidal system was stirred on a rotary shaker for two hours at a speed of 300-400 rpm for two hours. The colloidal system was centrifuged and the product was washed three times. In order to disperse the pellet, it was reconstituted in saline and ultrasonically dispersed. ICG-CSNP samples were freshly prepared before administration [7].

2.1.2 Drug loading Content

For drug loading analysis, lyophilised Mel-CSNPs and Mel-EUCSNPs were weighed and re-suspended in methanol at concentration 1 mg/ml. The extraction was assisted by mild agitation for 24 hours followed by ultra-sonication. Methanolic extract was collected and used to determine drug loading in polymeric nanoparticle system. The analysis was carried out using UV-Visible spectrophotometer at 278 nm in 1 ml quartz cuvette. Drug loading was calculated using following equations:

$$\text{Drug Loading Content \%} = (\text{Weight of melatonin in nanoparticles}) / (\text{Weight of nanoparticles}) \times 100\%$$

2.1.3 Determination of size, zeta potential and morphology

Dynamic Light Scattering (DLS) was used to determine mean hydrodynamic diameter, zeta potential and PDI by Malvern zetasizer (Nano ZS, Malvern Instruments, UK). For DLS analysis we have used 1.2 mg/ ml nanoparticles. Morphological evaluation of CSNPs, Mel-CSNPs, EUCSNPs and Mel-EUCSNPs were performed using Transmission Electron Microscope (TEM) (JEOL 2100) by drop-casting on carbon coated copper grids. Phosphotungstic acid was used as negative stain. Field emission scanning electron microscopy (FESEM) (Quanta FEG 250) was performed by drop casting sample on silicon wafer for morphological analysis.

2.1.4 Fourier Transform infrared (FTIR) and X-Ray Diffraction (XRD) analysis

FTIR analysis of chitosan, melatonin, CSNPs, Mel-CSNPs, EUCSNPs and Mel-EUCSNPs were performed for functional group characterisation. Briefly, 2 mg of powdered sample were mixed potassium bromide (KBr) and pellet was formed using hydraulic pressure. The pellets were scanned for analysis and spectra were recorded 4000-400cm⁻¹ for each sample. The changes in crystallinity of melatonin were evaluated using X-ray diffraction (XRD) analysis after formation of nanoparticles and compared with chitosan and chitosan nanoparticles.

2.1.5 *In-vitro* drug release study

Objective 2

In-vitro drug release of Mel-CSNPs was performed using dialysis bag method[8]. Briefly, 5 mg melatonin loaded CSNPs was filled in dialysis bag and placed in sink condition, 0.1% tween 20 containing PBS pH 7.4 and acetate buffer pH 4.5. The system was stirred at 30 rpm and 1ml of samples was taken at predefined time intervals (0, 0.5, 1, 3, 6, 12 and 24 hour) refilled with fresh buffer of equal volume to maintain sink condition. The samples were analysed using multimode plate reader (Tecan Inc.) at 278 nm for evaluating the drug release profile of Mel-CSNPs.

Objective 3

Melatonin release from Mel-CSNPs and Mel-EUCSNPs in a varying pH range from 1.2, 6.8 and 7.4 was analysed using the dialysis membrane (12 kDa molecular weight cut off) method mentioned in our earlier report with slight modification without adding any solubilizing agent [1]. The sink volume was set to be 25 ml for drug release study and 1 ml of sample was withdrawn for analysis at a definite time interval. 1 ml blank release media was added to maintain sink condition after removal of sample. The samples were analysed by taking absorbance at 278 nm using infinite ®200 Pro multimode plate reader (Tecan Austria GmbH). For better understanding release kinetics from nano-formulation we have used DDSolver software which is an add-in programme highly useful to study dissolution models based on built-in libraries. The software is freely available and widely used for studying drug dissolution profile [9].

2.1.6 *In-vitro* cellular uptake study

In-vitro cellular uptake study was performed for FITC-tagged CSNP to determine the uptake of nanoparticles in RAW 264.7 murine macrophages procured from National Centre of Cell Science (NCCS), Pune. The cells were maintained in Dulbecco Minimum Essential Medium (DMEM, Himedia Lab) supplemented with 10% heat inactivated foetal bovine serum (FBS) (Gibco), 100Uml⁻¹penicillin and 100 µgmL⁻¹ streptomycin. Cell line was maintained at 37°C and 5% CO₂ in humidified incubator. Cells were harvested and 5x10⁵ cells were seeded on sterile poly-L-lysine coated coverslips. Briefly, cells were treated with FITC-tagged nanoparticles for 1 hour [6] and thereafter, coverslips were washed with chilled 10 mM phosphate buffer saline (PBS) pH 7.4 and fixed with 4% paraformaldehyde solution. Nucleus

of cells was counter stained using DAPI (4', 6-diamidino-2-phenylindole) before mounting on glass slide. These cells were observed in a confocal laser scanning microscope (CLSM) (LSM880, Zeiss) to analyse the cellular localisation of FITC-tagged chitosan nanoparticles.

2.1.7 Biocompatibility of nanoparticles

In order to investigate the cytotoxicity of Melatonin, CSNPs, EUCSNPs, Mel-CSNPs and Mel-EUCSNPs 3-[4, 5-dimethylthiazol-2-yl]-2, 5-diphenyltetrazolium bromide (MTT) assay was performed. RAW 264.7 cells were seeded in 96-wells plate. Nanoparticles were dispersed in PBS pH 7.4 and cells were treated with different concentration of nanoparticles for 24 hour. 10 μ L of 5 mg/mL 3-[4,5-dimethylthiazol-2-yl]-2,5-diphenyltetrazolium bromide (MTT) solution was added to each well and incubated for 2 hours at 37°C. Culture medium was removed and formazan crystals were dissolved using 100 μ L Dimethyl Sulphoxide (DMSO). Absorbance of dissolved formazan crystals was recorded at 570 nm and percentage cell viability was determined in comparison with control.

2.1.8 Nitrite estimation (NO)

To estimate anti-inflammatory potential of nanoformulation *in-vitro* model of inflammation induced using LPS (1 μ g/mL) was followed. The cells were pre-treated with various concentrations of melatonin for 1 hour before addition of lipopolysaccharide (LPS, 1 μ g/ml) based on the earlier published work [1, 10]. After treatment, the nitrite estimation was done as described previously with slight modification [11]. The nitrite estimation was performed using Griess method for NO detection. Briefly, 100 μ L of cell supernatant is mixed with 100 μ L of Griess Reagent (1% sulphanilamide and 0.1% naphthylethelenediaminedihydrochloride), incubated at room temperature 10 min in the dark. The absorbance was recorded at 540 nm [12].

2.1.9 NF-kB p65 nuclear translocation study

NF-kB p65 nuclear translocation were performed using Raw 264.7 cell line[13] The cells were seeded on poly-l-lysine coated coverslips placed in 6 wells plate at density of 5×10^5 cells per well and incubated for 24 hours in complete DMEM media. On next day, cells were washed with 1X PBS and pre-treated with melatonin and Mel-CSNPs for 1 hour before LPS (1 μ g/mL) mediated stimulation for 30 minutes. After completion of treatment, the cells were washed with PBS pH 7.4 and fixed with chilled paraformaldehyde 4% in PBS for 20 minutes and washed three times with 1X PBS. The cells were permeabilised with cold ethanol at -

20°C for 30 minutes followed by blocking in 1% bovine serum albumin (BSA) in 1XPBS pH 7.4. The cells were incubated with NF-κB p65 primary antibody (SCBT) overnight at 4°C. After overnight incubation with primary antibody cells were washed three times with 1XPBS and further incubated Tetramethylrhodamine Isothiocyanate (TRITC)-tagged anti-mouse secondary antibody. Nuclei were stained using 6-diamidino-2-phenylindole (DAPI) and image was captured using confocal laser scanning microscope (LSM 880, Zeiss). The translocation of NF-κB was evaluated in the same manner as reported in with a few minor modifications. For each cell, the mean fluorescence signal of NF-κB located in the nucleus region (located with DAPI fluorescence) was calculated using ImageJ software. As a brief summary, fluorescent images of nuclei were taken at the focal layer (positioned with DAPI) of cells.

2.1.10 Haemolysis assay

The blood was collected in 3.8% sodium citrate was centrifuged to collect Red Blood Cell (RBC) for haemolysis test of the nanoparticles by following methodology of our previous study [14]. Briefly, 10 time dilution of 1 mL of RBC was prepared using PBS pH 7.4. 900 μL of diluted RBC was added to 100 μL nanoparticles and melatonin loaded suspensions. 0.1% Triton-X 100 and saline were used as positive and negative control, respectively. Finally, 2 mL microcentrifuge tubes were incubated at 37° C and centrifuged at 3500 rpm for 10 minutes. The collected supernatant was utilized to estimate OD values at 540 nm to determine the % haemolysis using the following equations.

Haemolysis % = (OD of the samples – OD of the negative control)/ (OD of the positive control – OD of the negative control)

2.1.11 Animals

All the animals used in the experiment were approved by the Institutional animal ethical committee (IAEC of NIPER and RCB) following guidelines provided by Committee for Purpose of Control and Supervision of Experiments on Animals (CPCSEA). Balb/C mice, 6-8 weeks were housed under 12 hours light and dark cycle under controlled environmental conditions at standard temperature 25 ± 2 °C with 50 ± 10 % humidity.

2.1.12 *In-vivo* therapeutics and model development

Female BALB/c mice (6-8 weeks) were procured and housed in the Central Animal facility (CAF) and were subjected to 12/12 hours light and dark cycles. DSS (36-50 k Da) was given at 5 % w/v in drinking water for five days for induction of ulcerative colitis. For developing Dextran Sodium Sulphate (DSS) induced Inflammatory Bowel Disease (Ulcerative Colitis) in mouse model, DSS (36-50 k Da) was administered orally by dissolving in autoclaved drinking water (5% w/v) for 5 days.

2.1.12a Objective 1

Animals were randomly divided in 3 groups (n=6): (Group-1) Control- received autoclaved RO water (Group-2) received 5 % w/v Dextran Sodium Sulphate (DSS) in autoclaved drinking water and (Group- 3) received 5 % DSS in autoclaved drinking water + Melatonin (4 mg/kg, *i.v.*) for 7 days. DSS is widely used to establish Ulcerative colitis in mice as it damages epithelial layer [15]. Melatonin showed its pharmacological effect between 2 to 8 mg/Kg. Hence we have selected 4mg/kg to get its optimum therapeutic effect in colitic mice following our earlier published report [1]. For an intravenous injection of melatonin, the mouse was placed in a restrainer and its tail wiped the rubbing alcohol to clean and make it sterile. Melatonin (4mg/kg *i.v.*) was administered by a 27 gauge sterile needle and 1 ml syringe. The needle is placed parallel to the lateral vein and inserted into it. The access of the lateral tail vein was confirmed and drug was injected gradually (not more than 100 µL) in saline.

2.1.12b Objective 2

Animals were randomly divided in 3 groups (n=6): Female Balb/C mice were randomly divided in 5 groups (n=6). Treatment with drug and nanformulations were given simultaneously for their anti-inflammatory *in-vivo* efficacy study. The animals were divided in 5 groups: group 1- Control (RO water), group 2- DSS, group 3- DSS+CSNPs, and group 4- DSS + Melatonin (4 mg/kg, *i.v.*) and group 5-DSS + Mel-CSNPs (4 mg/kg, *i.v.*).

2.1.12c Objective 3

Animals were randomly divided into 4 groups (n=6). Dextran Sodium Sulphate (DSS, 36-50kDa) was dissolved in 200 ml drinking water (5%w/v) for 5 days to induce to each group except control mice[16]. The animals were dosed orally once in a day Mel-CSNPs (4 mg/Kg/day, p.o.) and Mel-EUCSNPs (4 mg/kg/day, p.o.) daily for 7 days. The Control group

received only water. Animals were grouped as: Group 1-Control, Group-2 DSS5%, Group 3-DSS5%+ Mel-CSNPs (4 mg/kg, *p.o.*) and Group 4- DSS5% + Mel-EUCSNPs (4 mg/kg, *p.o.*).

2.1.13 *In-vivo* bio-distribution study

Animals were acclimatised for three days prior commencement of the experimental study. The fur of mouse was removed from thoracic and abdominal region using hair remover cream. Indocyanine green (ICG) tagged Mel-CSNP (4mg/mL, *i.v.*) was dispersed in sterile saline solution and administered intravenously. Similarly ICG tagged Mel-EUCSNPs was administered orally via oral feeding gavage in mice. Indocyanine green is a fluorescent dye generally used as medical diagnostics agent used for evaluating cardiac output, hepatic function, liver and gastric blood flow which makes it highly suitable agent for determining bio-distribution of Mel-CSNPs and Mel-EUCSNPs. ICG has spectral absorbance at about 800 nm. The imaging was performed using whole body imaging system for animal (IVIS, Perkin Elmer) at different time points for bio-distribution analysis of ICG-tagged Mel-CSNPs and Mel-EUCSNPs. At the end of experiment, mice were sacrificed using CO₂ asphyxiation method and vital organs were collected and imaged using IVIS for tissue distribution study analysis.

2.1.14 Disease Activity Index (DAI), % Body weight Change and colon length measurement

Disease Activity Index (DAI) was calculated considering parameters like stool consistency, bleeding, and loss of body weight, scored based on criteria mentioned in **Table:1** [17]. To assess the severity of disease in mice model we have measured colon length post sacrifice of mice. Shortening of colon occurs due to severe inflammatory condition in colon [18]. Daily change in a body weight of animals was recorded to assess health status of mice and effect of treatment to determine its efficacy.

| Score | Weight Loss | Stool Consistency | Bleeding |
|-------|---------------|-------------------|-----------------|
| 0 | None | Normal | No bleeding |
| 1 | 1-5 % | | |
| 2 | 5-10% | Loose stools | Slight Bleeding |
| 3 | 10-15% | | |
| 4 | More than 15% | Watery Diarrhea | Gross bleeding |

Table 1: Disease Activity Index scoring parameters

2.1.15 Western Blot, Immunoprecipitation (IP) and Chromatin Immunoprecipitation (ChIP) assay

In order to study the molecular mechanism behind the protective effect of melatonin we have performed various molecular techniques. Immunoblotting was performed to study expression analysis of target proteins. Cells and tissues were treated with melatonin and LPS or DSS as described in previous experimental sections. To study effect of pharmacological inhibition of EZH2 we have used EPZ011989 at 10 μ M and 25 μ M. Then, proteins were collected, immunoblot and IP analysis have been performed by following protocol of previous study[19]. Colon tissues or RAW 264.7 macrophages were lysed in a cold tissue lysis buffer (RIPA+ 0.5 mM phenylmethylsulphonylfluoride (PMSF), protease inhibitor cocktail). Isolated protein was quantified using the BCA protein quantification kit (Sigma-Aldrich, USA). Immunoprecipitation was performed to study interaction of target protein like EZH2 and NOS2. For immunoprecipitation protein A/G beads (SCBT) were used to isolate EZH2 using its primary antibody. The samples for western blot were prepared using Laemmli sample buffer and resolved using sodium dodecyl sulphate-polyacrylamide gel electrophoresis (SDS-PAGE) followed by transfer on PVDF membrane using Trans blot turbo system (Bio-Rad, USA). The blots were blocked for 1 hour at room temperature using 5% BSA in Tris-base Saline-Tween 20 (TBST) pH 7.4 followed by overnight incubation with primary antibodies of EZH2 (1:1000, SCBT), H3k27me3 (1:1000, SCBT), β -actin (1:1000, SCBT) and NOS2(1:1000, SCBT) at 4°C. After incubation with primary antibodies, blots were washed three times using 1X TBST solution and incubated with respective HRP tagged secondary antibodies. The blots were developed using ECL clarity western substrate (Bio-Rad) and images were captured in the LAS500 chemiluminescence system (GE). The results

were quantified using Image J software and represented as relative protein expression with respect to β -actin for NOS2, EZH2 and H3K27me3.

Chromatin immunoprecipitation study was performed for revealing the interaction of protein for its target gene. For immunoprecipitation study protein samples (100 μ g) were incubated with primary NOS2 antibody (2 μ l, 1 mg/ml) was incubated for 1 hour at 4 °C. Thereafter 20 μ l of A/G and agarose beads were allowed to incubate for 12 hours. The beads were centrifuged and washed with 1 x PBS thrice. The washed pellets were then resuspended in 40 μ l of 2x SDS gel loading buffer and ran on SDS-PAGE and western blotting was performed to check interaction. Only IgG was used as control for each sample.

The cells were cross linked using formaldehyde 37% (w/v) directly into culture media at the end of treatment and shake for 15 minutes at room temperature. After the crosslinking was over it was stopped using glycine to final concentration of 0.125-0.150 M and shake for 5 minutes at room temperature. After this, washing was done with PBS. By adding chilled PBS + PMSF (1mM) and scraping the cells in a 15 ml falcon. The cells were centrifuged at 4000 rpm for 5 minutes at 4°C. Then cells were incubated with lysis buffer with PMSF 1mM having protease inhibitor for 10 minutes on ice at the density of 2×10^6 cells/ml. The cells were sonicated to get DNA fragments 250 to 1000 bp (we have sonicated using probe-sonicator 10 Amplitude, at 2 seconds pulse rate for 4 times). We have used 200 μ l lysate per condition and 20 μ l was saved for use as INPUT at further stages. These lysates were then diluted 10 times using a dilution buffer. 20 μ l of protein A/G beads were used to pre-clear the samples by incubating it for 1 hour at 4°C with samples. Samples were centrifuged at 4000 rpm and supernatant were collected for further study. EZH2 primary antibody was added 4 μ g to each sample and incubated on rotating platform overnight at 4°C.

After the incubation is over protein A/G beads 20 μ l was added and incubated at 4°C for 1 hour on a rotating platform. To collect bound fragments with protein A/G beads, samples were centrifuged at 4000 rpm. Supernatant was saved as an unbound fraction and collected protein A/G beads were washed with a low salt buffer, high salt buffer, LiCl (Lithium Chloride) immune complex wash buffer and finally by TE (Tris-EDTA) buffer. Immune complex attached to protein A/G beads was eluted by an elution buffer by vortexing slowly at room temperature for 15 minutes. Supernatant was collected by centrifuging at 4000 rpm to get immune complex. Immune complex was reverse cross linked using 5M NaCl and incubated at 65°C for 4 hours. After this 1 μ l 0.5M EDTA, 20 μ l 1M Tris-HCl pH 6.5, 2 μ l RNase (10 μ g/ μ l), 2 μ l (20 μ g/ μ l) of proteinase K were added and incubated for one hour at 45°C to remove RNA and proteins. DNA was recovered by phenol/chloroform extraction

method followed by ethanol precipitation and finally the sample was diluted in the TE buffer. qPCR analysis was carried out using NOS2 promoter specific primer sequence 1 (Forward primer 5'-CCACTATTCTGCCCAAGCTGACT-3' and reverse primer 5'-ATGGTGCCAATATTCCAACACGCC-3') and primer sequence 2 (Forward primer 5'-AGGAGTGTCTTCCTGCTTGGGAAA-3' and reverse primer 5'-TGGGTGTGCTTCTTACACCTTCCA-3') from the earlier published report [20].

2.1.16 Quantitative polymerase chain reaction (qPCR) study

The quantitative gene expression has been analysed by following protocol of previous study [19]. For *in vitro* study RAW 264.7 cells were used and for *in vivo* study samples were obtained from colon region of mice. Singlex qPCR analysis for gene expression profile of interleukin-1 β (IL-1 β), interleukin-6 (IL-6) and Nuclear Factor of kappa light polypeptide Gene Enhancer in B-Cells (NF- κ B) has been studied. For each gene expression analysis about 100-500 ng/mL reaction cDNA template, 10 μ L of SYBR-green (Bio-Rad), 250 nM primers and nuclease free water up to 20 μ L for each reaction was prepared. The data was analysed using Quant Studio 3 software (Thermo Scientific, Version 1.4.3). GAPDH has been considered as endogenous control. The list of primers is described in **Table-2** the annealing temperature was fixed at 52°C for IL-1 β , NF- κ B and 48°C for IL-6.

| Gene | Forward primer sequence (5'-3') | Reverse primer sequence (5'-3') | Melting Temperature (T _m) |
|----------------|----------------------------------|------------------------------------------|---------------------------------------|
| IL-1 β | AAT CTG TAC TCC TGC CTG TT | TGG GTA ATT TTT GGG ATC TAC ACT CT | For=58.4 °C Rev=55.9°C |
| IL-6 | CCA GCT ATG AAC TCC TTC TC | GCT TGT TCC TCA CAT CTC TC | For=52.2°C Rev=52.9°C |
| NF- κ B | CCC CAC GAG CTT GTA GGA AAG | CCA GGT TCT GGA AAC TGT GGA T | For=57.7 °C Rev=57°C |
| GAPDH | GAC TCA TGA CCA CAG TCC ATG C | AGA GGC AGG GAT GAT GTT CTG | For=57.9 °C Rev=56.7°C |
| NOS2 (1) | ATGGTGCCAATATT CCAACACGCC | ATGGTGCCAATAT TCCAACACGCC | For=59°C Rev=60.3°C |
| NOS2 (2) | AGGAGTGTCTTCCT GCTTGGGAAA | TGGGTGTGCTTCTT ACACCTTCCA | For=60.2°C Rev=60.4°C |

Table 2: List of primer sequence

2.1.17 Myeloperoxidase (MPO) assay

Tissue samples of colon from mice were collected, cleaned with forceps to remove faecal matter, weighed and placed in 1.5 ml sterile micro centrifuge tubes. Tissue samples were placed on ice all time during this process. Tissues were homogenised using hand homogeniser in appropriate amount of hexadecyltrimethylammonium bromide (HTAB) buffer according to their weight (50 mg/ml). After complete homogenisation of tissues, clear supernatants were collected by centrifuging for 6 minutes (13400 x g, 4 °C). Supernatants were collected were used for MPO assay and unused sample were stored in – 80 °C.

For MPO assay, o-dianisidine solution (100 ml) prepared by mixing 16.7 mg o-dianisidinedihydrochloride in 90 mL of Type-1 water and 10 ml potassium phosphate buffer. The solution should be freshly prepared for every assay. 7 µL of tissue supernatants were placed in 96 well plate. 50 mL of 3% H₂O₂ was added to each well to o-dianisidine mixture. 200 µL H₂O₂ containing o-dianisidine was added to each well. Absorbance at 450 nm was recorded using spectrophotometer (Tecan Inc.). Triple readings were recorded at 30 seconds interval. MPO activity was calculated to assess the therapeutic efficacy of nanoformulations.[21]

2.1.18 Histology

2.1.18a Haematoxylin and Eosin (H&E)

Histological study for evaluations of pathological alterations during DSS induced inflammatory conditions in colonic tissue sections were carried out using H&E staining. After sacrificing animals, colon tissue were collected and in formalin solution for 1 week. Briefly, the tissues were frozen in optimal cutting temperature (OCT) media and sectioned in 7 µm thickness using Cryo-microtome (Thermo scientific, USA). The sections were stained and microscopically examined for evaluation of pathological changes. The sections were mounted on poly-L-lysine coated slide and stained using standard staining protocol. Briefly, slides were washed in distilled water for 3 times (5 minutes) followed by 10 minutes staining in Haematoxylin solution (Himedia lab). Followed by a single dip in ammonia water (bluing agent) and washed with DI water. After which the slides were stained with Eosin solution (Himedia lab) for 30 seconds, followed by dehydration using gradient alcohol method and finally dipped in xylene for complete dehydration. Finally slides were mounted using permanent mounting medium DPX and allowed to dry for 24 hours. These stained slides were observed and imaged using optical microscope (EVOS, Thermo).For Histological

scoring; H&E stained sections were scored blindly scored using published system for the assessment disease severity. Crypt architecture (normal-1, severely distorted with loss of entire crypt-3), muscle thickness (base of the crypts sits on the muscularis mucosae-0, marked muscle thickening present-3), degree of inflammatory cell infiltration (normal-0, dense inflammatory infiltrate-3), goblet cell depletion (absent-0, present-1) and crypt abscess (absent-0, present-1) [21].

2.1.18b Alcian Blue and Nuclear Fast Red

Colonic tissue section slides were washed and hydrated with deionised water. The slides were placed in Alcian Blue (AB) (SRL lab) staining solution for 30 minutes followed by washing in running tap water for 2 minutes. The slides were rinsed with deionised water, counterstained using Nuclear Fast Red (SRL lab) for 5 minutes and washed in running tap water for 1 minute. Slides were dehydrated using alcohol gradient and cleared with xylene. Finally, it was mounted with resinous mounting medium DPX (Himedia lab). Alcian Blue stains goblets cells in blue colour whereas Nuclear Fast Red is used as counter stain for staining nuclei of epithelial cells [22]. Loss of goblet cells observed per crypt can be used as parameter for assessing the intensity of disease [23, 24].

2.1.18c Toluidine blue staining

Toluidine Blue (TB) stain was performed for detection of mast cell infiltration in colonic tissue using previously reported protocol [25].

2.1.18d Immunohistochemistry

To study expression of protein in colonic tissue cross section, we performed immunohistochemical expression study. For immuno-histochemical analysis, colonic tissue cross sections (5 μ m) were hydrated and washed with PBS pH 7.4 and incubated in blocking buffer (2.5 % BSA/1XPBS pH 7.4) for 1 hour at RT. After blocking, samples were incubated with IL1- β (1:100), EZH2 (1:100) and Inducible Nitric oxide synthase 2 (NOS2) (1:100) primary Nitro-tyrosine (1:250) antibody overnight at 4°C followed by allophycocyanin (APC) or fluorescein isothiocyanate (FITC) tagged secondary antibody for 1 hour at RT. Finally sections were washed, counterstained with 4', 6-diamidino-2-phenylindole (DAPI) and mounted using mounting media. Fixed slides were imaged and observed using fluorescent confocal laser microscopy (Zeiss, LSM 880). The fluorescence intensity of samples were calculated using Image J software using and plotted for comparison (n=6).

2.1.19 Statistical Analysis

All data were calculated as \pm S.E.M of each experiment, for *in-vitro* (n = 3) and *in-vivo* (n=6). Significance was determined using analysis of variance (ANOVA) followed by Tukey's post-test using GraphPad Prism6. For significance (* $p \leq 0.05$, ** $p \leq 0.001$ and *** $p \leq 0.0001$)

2.2 References

- [1] J.M. Soni, M.N. Sardoiwala, S.R. Choudhury, S.S. Sharma, S. Karmakar, *Mater Sci Eng C Mater Biol Appl*, 124 (2021) 112038.
- [2] P. Calvo, C. Remunan-Lopez, J.L. Vila-Jato, M.J.J.o.A.P.S. Alonso, 63 (1997) 125-132.
- [3] S. Kumar Yadav, A. Kumar Srivastava, A. Dev, B. Kaundal, S. Roy Choudhury, S. Karmakar, *Nanotechnology*, 28 (2017) 365102.
- [4] M.N. Sardoiwala, S. Karmakar, S.R. Choudhury, *Carbohydr Polym*, 254 (2021) 117435.
- [5] S. Chen, F. Guo, T. Deng, S. Zhu, W. Liu, H. Zhong, H. Yu, R. Luo, Z. Deng, *AAPS PharmSciTech*, 18 (2017) 1277-1287.
- [6] L.Q. Jiang, T.Y. Wang, T.J. Webster, H.-J. Duan, J.Y. Qiu, Z.M. Zhao, X.X. Yin, C.L. Zheng, *International journal of nanomedicine*, 12 (2017) 6383-6398.
- [7] D. Sonin, E. Pochkaeva, S. Zhuravskii, V. Postnov, D. Korolev, L. Vasina, D. Kostina, D. Mukhametdinova, I. Zelinskaya, Y. Skorik, E. Naumysheva, A. Malashicheva, P. Somov, M. Istomina, N. Rubanova, I. Aleksandrov, M. Vasyutina, M. Galagudza, *Nanomaterials (Basel, Switzerland)*, 10 (2020).
- [8] S. Mao, J. Chen, Z. Wei, H. Liu, D. Bi, *International Journal of Pharmaceutics*, 272 (2004) 37-43.
- [9] Y. Zhang, M. Huo, J. Zhou, A. Zou, W. Li, C. Yao, S. Xie, *AAPS J*, 12 (2010) 263-271.
- [10] J. Hambleton, S.L. Weinstein, L. Lem, A.L. DeFranco, *Proc Natl Acad Sci U S A*, 93 (1996) 2774-2778.
- [11] W.J. Yoon, S.S. Kim, T.H. Oh, N.H. Lee, C.G. Hyun, *Lipids*, 44 (2009) 471-476.
- [12] J. Benevides Bahiense, F.M. Marques, M.M. Figureueueira, T.S. Vargas, T.P. Kondratyuk, D.C. Endringer, R. Scherer, M. Fronza, *Pharmaceutical biology*, 55 (2017) 991-997.
- [13] A.V. Bagaev, A.Y. Garaeva, E.S. Lebedeva, A.V. Pichugin, R.I. Ataulakhanov, F.I. Ataulakhanov, *Scientific reports*, 2019, pp. 4563.
- [14] A. Dev, S.J. Mohanbhai, A.C. Kushwaha, A. Sood, M.N. Sardoiwala, S.R. Choudhury, S. Karmakar, *Acta Biomaterialia*, 109 (2020) 121-131.
- [15] P.M. Munyaka, M.F. Rabbi, E. Khafipour, J.E. Ghia, *J Basic Microbiol*, 56 (2016) 986-998.
- [16] J.J. Kim, M.S. Shajib, M.M. Manocha, W.I. Khan, *J Vis Exp*, (2012).

- [17] S. Gancarcikova, S. Lauko, G. Hrczkova, Z. Andrejcakova, V. Hajduckova, M. Madar, L. Kolesar Fecskeova, D. Mudronova, K. Mravcova, G. Strkolcova, R. Nemcova, J. Kacirova, A. Staskova, S. Vilcek, A. Bomba, *Cells*, 9 (2020).
- [18] B.R. Jin, K.S. Chung, S.Y. Cheon, M. Lee, S. Hwang, S. Noh Hwang, K.J. Rhee, H.J. An, *Sci Rep*, 7 (2017) 46252.
- [19] M.N. Sardoiwala, A.C. Kushwaha, A. Dev, N. Shrimali, P. Guchhait, S. Karmakar, S. Roy Choudhury, *ACS Biomaterials Science & Engineering*, 6 (2020) 3139-3153.
- [20] T.J. Gross, K. Kremens, L.S. Powers, B. Brink, T. Knutson, F.E. Domann, R.A. Philibert, M.M. Milhem, M.M. Monick, *J Immunol*, 192 (2014) 2326-2338.
- [21] J.J. Kim, M.S. Shajib, M.M. Manocha, W.I. Khan, *J Vis Exp*, (2012) 3678.
- [22] A. Arbab, G. Yocum, M. Rad, A. Khakoo, V. Fellowes, E. Read, J. Frank, *NMR in biomedicine*, 18 (2005) 553-559.
- [23] X. Wang, X. Kong, Y. Qin, X. Zhu, W. Liu, J. Han, *Food Funct*, 10 (2019) 4608-4619.
- [24] W. Chen, M. Zhuo, X. Lu, X. Xia, Y. Zhao, Z. Huang, J. Xu, W. Li, C. Yu, *Int J Biol Sci*, 14 (2018) 2051-2064.
- [25] P. Pittoni, C. Tripodo, S. Piconese, G. Mauri, M. Parenza, A. Rigoni, S. Sangaletti, M.P. Colombo, *Cancer Res*, 71 (2011) 5987-5997.

Chapter 3:

Melatonin mediated inhibition of EZH2-NOS2 crosstalk attenuates Inflammatory Bowel Disease in preclinical in vitro and in vivo models

3.0 Background

Inflammatory Bowel Disease (IBD), which includes Crohn's Disease and Ulcerative Colitis, has been a major health concern for decades. Infiltration of immune cells and elevation of inflammatory markers in IBD progression and pathogenesis have been proven in research [1, 2]. Several epigenetic alterations and environmental variables have been identified as contributing factors to IBD [3, 4]. Many anti-inflammatory drugs have been implicated in the treatment of IBD. Melatonin has been extensively researched and may be one of the promising anti-inflammatory choices for IBD treatment.

Melatonin (N-acetyl-5-methoxytryptamine), a wonder molecule, is the predominant secretory product of the pineal gland in the brain, and it aids in the maintenance of mammals' circadian and photoperiodic rhythms [5]. Melatonin is well-known as a potent anti-inflammatory agent used to treat a number of inflammatory diseases, including IBD. Melatonin's anti-inflammatory activity is attributed to its ability to scavenge free radicals and suppress inflammatory markers such as nitric oxide synthase (NOS) [6-11]. Melatonin is also known to inhibit immune cell invasion by acting on the melatonin receptor-1 (MT1), which causes vasoconstriction and so decreases immune cell vascular permeability [12]. Melatonin has recently been discovered to play a function in epigenetic regulation and the management of several diseases such as ageing, neurological disorders, and breast cancer [13, 14]. Recent research has identified Enhancer of Zeste Homolog 2 (EZH2), a master regulator and part of the polycomb repressor complex 2 (PRC2), as a critical molecule in the maintenance of macrophage/microglial activity and autoimmune inflammation [15]. EZH2 depletion has been demonstrated to inhibit toll-like receptor activation and cytokine signaling 3 expression, paving the door for IBD therapy. In the treatment of IBD, reduction of EZH2 histone methyltransferase activity has recently been proven as a therapeutic target to diminish induction of inflammatory markers interleukin 6 (IL-6) and interleukin-1 (IL-1) [16]. However, no studies have been conducted to investigate the influence of melatonin on EZH2 expression and its downstream regulation in IBD patients.

Nitric oxide (NO) is a free radical that is an essential signaling molecule that plays a significant function in exacerbating inflammation in disease conditions. NOS activity was reported to be eight times higher in ulcerative colitis mucosa than in healthy individuals [17]. NO and its toxic derivatives worsen the severity of IBD pathology. In the case of IBD, pharmacological EZH2 suppression was favourable. M1 macrophages express iNOS, which can be utilised to identify these cells. M1 macrophages play a vital part in host

defense systems during pathological infection induced by microorganisms in a variety of inflammatory disorders. However, uncontrolled macrophage activation can lead to serious autoimmune inflammatory diseases [18].

As a result, we studied melatonin's effects on EZH2 expression and activity in *in vitro* and *in vivo* IBD models. In addition, we investigated the role of EZH2-NOS2 crosstalk in the evolution and pathophysiology of ulcerative colitis. Melatonin was found to have a recuperative effect on EZH2, NOS2, and Histone 3 lysine 27 trimethyl (H3K27me3) expression in a DSS-induced IBD model.

3.1 Results and discussion

The recent upsurge in IBD incidence globally could enhance the risk of colorectal cancer in the long term. For severe pathophysiological conditions, the involvement and linkage of epigenetic regulators in IBD is vital. The major epigenetic alterations, such as histone and DNA methylation, render them excellent targets for IBD therapeutic intervention [19]. EZH2 is an important epigenetic regulator and a member of the polycomb repressive complex 2 [20], however its role in inflammation and IBD is still unknown. Recent research provides a clear picture of the role of EZH2 in the genesis of IBDs. It reveals that EZH2 depletion or suppression slows colitis progression and pathogenesis by limiting cytokine signaling, IL6 and IL1 expression [15, 16]. Due to the adverse reactions of existing IBD medication, such as nonsteroidal anti-inflammatory medicines (NSAIDs) presenting a modest response and anti-TNF- α therapy revealing inadequate intervention due to secondary infections, a new therapeutic candidate is desired [21]. Furthermore, melatonin has emerged as a strong anti-inflammatory molecule having negligible side effects and has been investigated as a therapeutic agent for a variety of inflammatory disorders, including IBD. Melatonin has been explored as a radical scavenger and anti-inflammatory medication for the treatment of IBD [6-10]. The effect of melatonin on EZH2 expression in IBD therapy, however, has not yet been explored. According to our knowledge, we are the first to look into the effect of melatonin on EZH2 expression in order to better comprehend the EZH2-mediated epigenetic regulatory role of melatonin in IBD treatment.

3.1.1 Melatonin scavenged Nitric Oxide (NO) production in LPS stimulated RAW264.7 cells

Melatonin's effect on NO generation was studied in murine macrophages RAW264.7 cells treated with LPS (1 $\mu\text{g/ml}$). To assess NO scavenging capacity, different doses of melatonin (0-500 $\mu\text{g/mL}$) were studied. LPS has demonstrated 225 % of overall NO production as an inflammatory hallmark. Melatonin has been shown to have a dose-dependent effect in NO

scavenging. Melatonin at 1g/mL had no effect on NO levels, 10 µg/mL lowered NO production to 145-150% from 225%, and 100-500 µg/mL had an anti-inflammatory effect, lowering NO levels by 100% from 225%. Melatonin displayed dose dependent NO scavenging effect at lower doses ranging from 1-100 µg/mL, but at higher doses ranging from 100-500 µg/mL, melatonin exhibited dose dependently significant alterations in NO scavenging action against LPS driven stresses (**Figure 3.1-A**).

Increased NO production is a well-known characteristic in inflammatory diseases including such UC [22]. Melatonin is also intensively explored as a NO scavenger to reduce inflammatory diseases [6, 23]. We have also verified melatonin's NO scavenging activity, which suppressed half of the NO levels caused by LPS exposure.

3.1.2 Melatonin attenuated EZH2, H3k27me3 and NOS2 expression in RAW 264.7 cells

Melatonin's effect on the epigenetic biomarkers EZH2 and H3k27me3 was studied by assessing its protein expression profile in response to LPS-induced inflammatory conditions. LPS triggered conditions resulted in considerable upregulation of EZH2, H3k27me3, and NOS2. Melatonin, on the other hand, inhibited EZH2 and H3k27me3, as well as diminished NOS2 expression levels as compared to LPS-induced damages. (**Figure 3.1-B**) The quantitative protein expression of EZH2, NOS2 and H3k27me3 has been depicted in **Figure 3.1- C, D and E**. Melatonin has been shown to inhibit EZH2 expression. As a result, we used a potent inhibitor of EZH2 (EPZ011989) to demonstrate that EZH2 has a direct association with inflammatory regulation. We observed that EPZ011989 treatment inhibited EZH2 and H3k27me3 (10µM and 25µM). Interestingly, the decline of NOS2 has also been witnessed with inhibition of EZH2 expression (**Figure 1-B**). The protein expression has been measured and demonstrated in **Figure 1-D**.

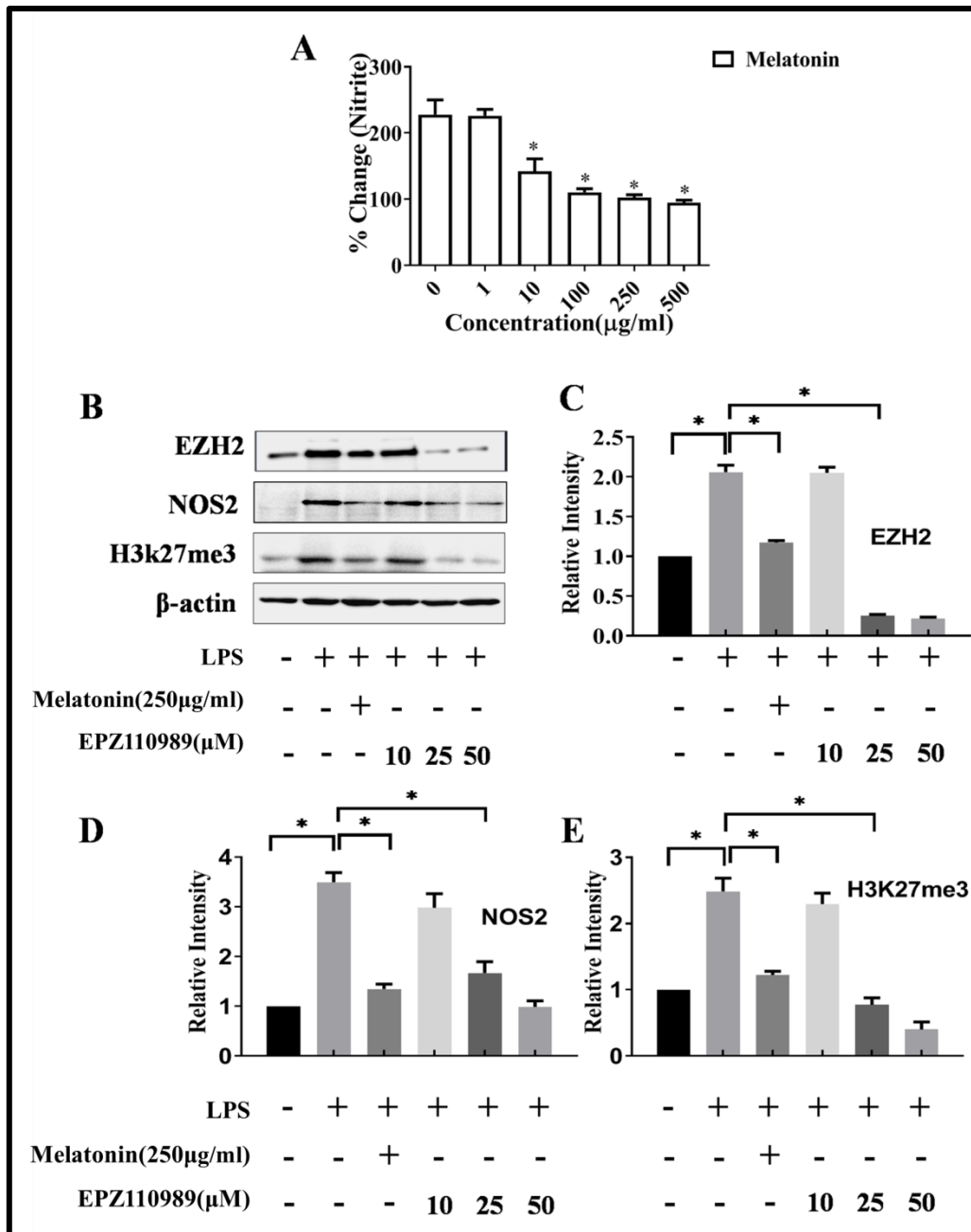


Figure 3.1: *In vitro* therapeutic effect of melatonin: (A) Nitrite estimation in LPS stimulated RAW 264.7 (B) Western blot analysis for determining effect of Melatonin and EPZ011989 on protein expression when challenged with LPS (C,D,E) Quantification for protein expression analysis of EZH2, NOS2 and H3K27me3. (* $p \leq 0.05$)

Furthermore, the protein expression of UC, NOS2, and IBD-associated epigenetic marker, EZH2, was taken into account in the study to reveal a relationship between these therapeutic targets. Several investigations have found that NOS2 is modulated during IBD conditions [24, 25]. The role melatonin in attenuating expression of NOS2 has been frequently documented [26, 27], which supports our current work, that likewise indicated an

inhibitory impact of melatonin on NOS2. Similarly, EZH2 has been identified as an IBD-associated epigenetic marker, and inhibition has been shown to be a viable treatment option [15, 16]. Melatonin inhibited EZH2 expression in the present research, which validates the outcomes of the described report. As a result, the reduction in NO concentrations, NOS2 expression, and EZH2 expression suggests that melatonin has therapeutic potential in the treatment of UC. EPZ011989 pharmacological inhibition of EZH2 established linkage between two potent therapeutic targets, NOS2 and EZH2. NOS2 inhibition has been connected to EZH2 suppression.

3.1.3 Melatonin mechanistic action of epigenetic regulation revealed direct interaction of NOS2 and EZH2

The outcomes of pharmacological inhibition of EZH2 have shown hopeful correlation between EZH2 and NOS2 expression. As a result, an immunoprecipitation study was carried out to validate the relationship between EZH2 and NOS2. The result uncovered direct physical interaction of both target proteins **Figure 3.2-A**. In this study, we found that NOS2 and EZH2 interaction was more evident in LPS-induced environments. On the other hand, reduced interaction of these proteins has been discovered as a result of melatonin treatment, implying its regulatory mechanism in inflammation mitigation. Melatonin's anti-inflammatory impact decreases EZH2 expression, resulting in a smaller pool of EZH2 for promoter binding and stimulation of NOS2 expression. Melatonin inhibits EZH2 binding to the NOS2 promoter region via decreasing EZH2 availability at the NOS2 promoter site.

To confirm the novel finding, an immune-precipitation study was performed, which established a direct physical connection between NOS2 and EZH2. Melatonin seems to have an inhibitory effect on NOS2 and EZH2 interaction, which protects against UC repercussions. As a result, EZH2 plays an essential role in anti-inflammatory activity in macrophages, and the severity of the inflammatory response can be lowered by directly targeting it with melatonin [15]. Furthermore, an earlier published report reveals that EZH2 has a direct connection with NOS2 because it binds to the promoter site and modulates its expression [28]. This divulges that EZH2 may have a modulatory effect on NOS2 expression, concluding in an inflammation management.

3.1.4 Melatonin has regulatory effect on EZH2 binding at NOS2 promoter

We explored EZH2 binding to the NOS2 gene promoter sequence region to see if melatonin's anti-inflammatory mechanism works through epigenetic regulation. We conducted a ChIP-qPCR test to determine whether the EZH2-NOS2 relationship has any consequence on NOS2 transcription regulation. In the LPS-stimulated group, the findings confirmed strong EZH2

binding to the NOS2 promoter sequence region. Our findings corroborate with an earlier study that suggested H3K27me3 binding to a specific area of the NOS2 promoter in an inflammatory situation [28, 29]. In **Figure 3.2-C**, with LPS stimulation, there is a considerable increase in EZH2 binding to the NOS2 promoter area, and melatonin has an inhibitory effect on EZH2 binding to the NOS2 promoter site. The outcome of agarose gel electrophoresis has also depicted the amplicon products of ChIP-qPCR in **Figure 3.2-B**. As a result, the findings suggest that melatonin's anti-inflammatory activity is epigenetically regulated by lowering EZH2 expression.

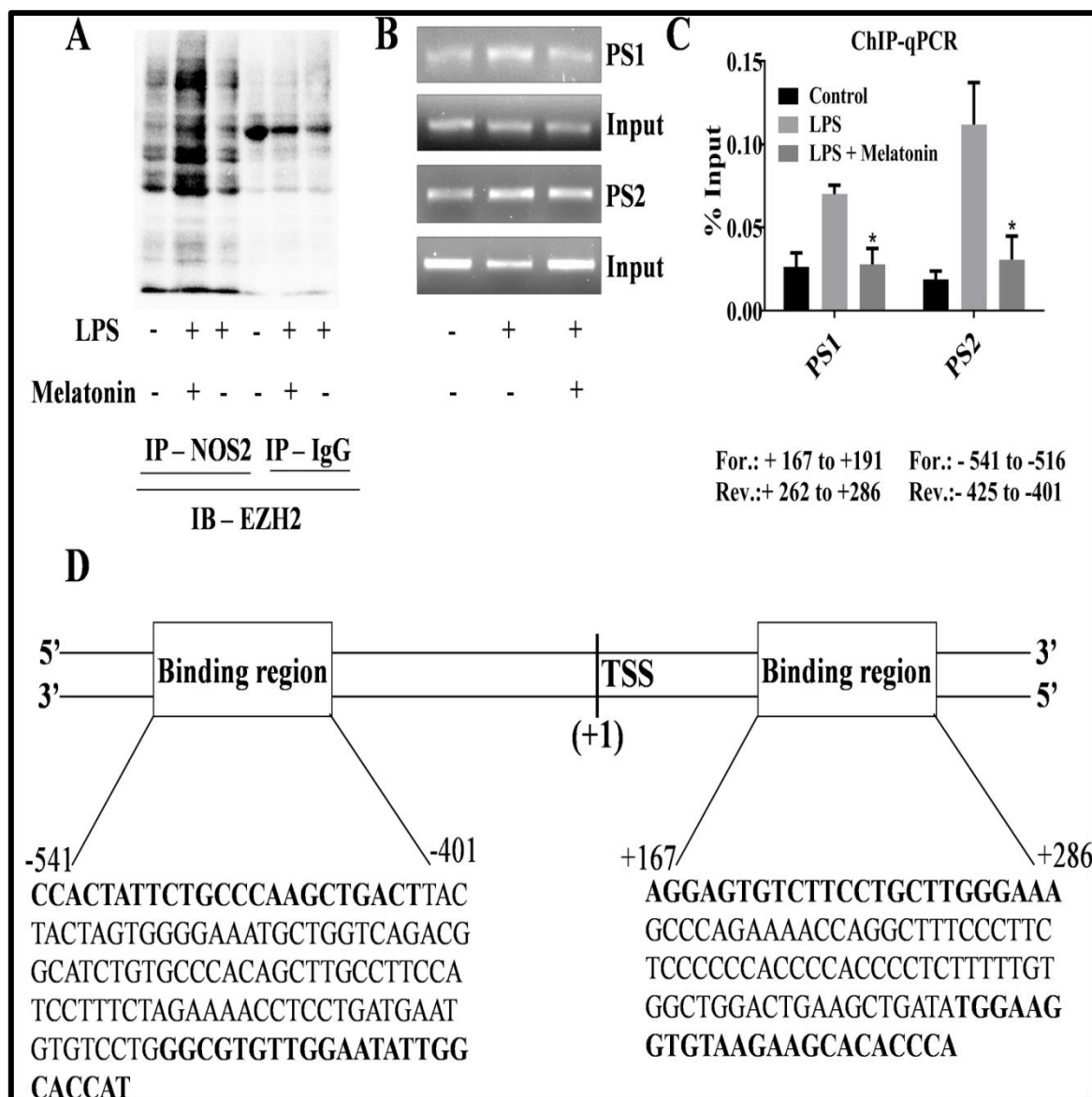


Figure 3.2: EZH2-NOS2 crosstalk: (A) Immuno-precipitation analysis for protein interaction study in Raw 264.7 murine macrophages (B) Agarose gel electrophoresis of PCR products of ChIP assay (C) ChIP-Quantitative PCR result shows EZH2 binding on NOS2 promoter

regions (PS1=Promoter Sequence 1 and PS2= Promoter Sequence 2) (D) Schematic representation of EZH2 binding to promoter sequence. (* $p \leq 0.05$)

3.1.5 Melatonin treatment reduced DSS induced ulcerative colitis symptoms in mice

Melatonin's effect on UC was studied; mice were fed a daily dose of 5% (w/v) DSS for five days in drinking water. During the experiment, the mice were treated with a daily intravenous (*i.v.*) dose of 4mg/kg melatonin. Melatonin therapy significantly reduces the percentage bodyweight loss induced by DSS, as per our findings (**Figure 3.3-A**). DSS causes a 20% decrease in bodyweight percentage, which is reversed by melatonin, which results in a 10% recovery in bodyweight percentage. Interestingly, the disease activity index (DAI) was dropped by four index numbers in the melatonin-treated group as compared to the DSS-induced colitis condition (**Figure 3.3-B**). Colonic inflammation was found in DSS-induced conditions by a 5 cm reduction in colon length when compared to the control group. Melatonin reduced DSS-induced symptoms by restoring 2 cm colon length (**Figure 3.3-C and 3.3-D**).

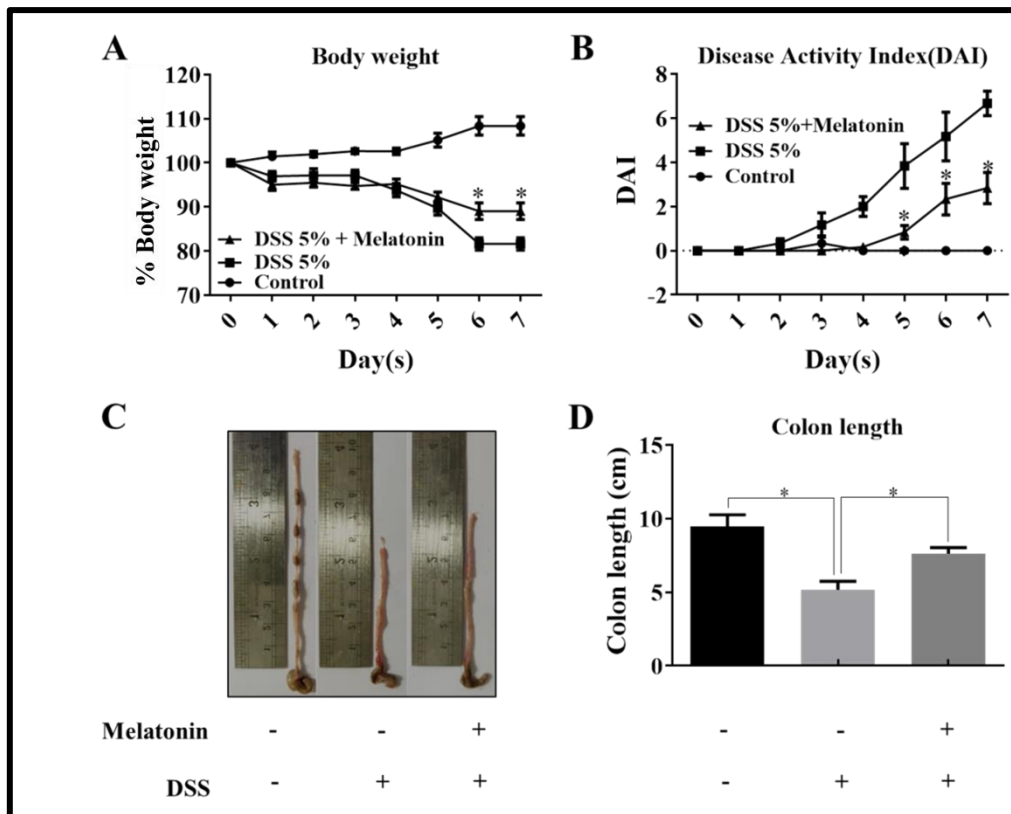


Figure 3.3: *In vivo* mice model and therapeutic effect of melatonin: (A) Percentage body weight change in BALB/c mouse, (B) Disease Activity Index for assessing severity of inflammation in mouse daily (C-D) Change in colon length analysis. (* $p \leq 0.05$)

Melatonin's therapeutic efficacy in an *in vivo* UC mouse models and effects on EZH2 expression were also explored after *in vitro* investigations to further understand its efficacy. DSS is a commonly used chemical agent that causes intestinal inflammation in mice, mimicking the immunological and histological aspects of human IBD [30]. Melatonin has been proven in studies to have therapeutic promise in the reduction of inflammation in chemically induced IBD models [7-10]. We have shown that melatonin can restore body weight and colon length with the DAI index. The current study's findings also support the concept that melatonin dosing lowers the onset and clinical signs of DSS-induced UC in mice models.

3.1.6 Reduced MPO activity and inflammatory genes expression as restorative effect of melatonin in UC mice model

To validate melatonin's anti-inflammatory effect, the enzyme myeloperoxidase (MPO) was assessed in colonic tissues. MPO levels in DSS-induced colonic tissues varied by 6 U/mg when compared to controls, and melatonin treatment mitigated DSS-induced injuries (**Figure 3.4-A**). Furthermore, the gene expression of inflammatory markers IL1, IL6, and NFB has been investigated to comprehend melatonin's anti-inflammatory action. There was an approximate 1.5 fold increase in the expression of the investigated inflammatory markers in the DSS-induced inflammation compared to control group. Melatonin significantly restored IL1 β , IL6, and NFB expression to normal levels as an effective intervention to alleviate DSS-induced inflammatory symptoms (**Figure 3.4- B, C and D**).

Melatonin also altered the inflammatory process by decreasing gene expression in colonic tissue that produces inflammatory indicators such as IL1 β , NF κ β and IL-6. Existing data support our findings of reduced inflammatory gene expression by melatonin, implying anti-inflammatory efficacy in IBD management [31, 32]. In addition, the Myeloperoxidase (MPO) enzyme levels were examined to validate the restriction of immune cell invasion. MPO is found in neutrophils and acts as an indicator of neutrophilic infiltration as a consequence of an inflammatory response; melatonin restores its level [8, 33]

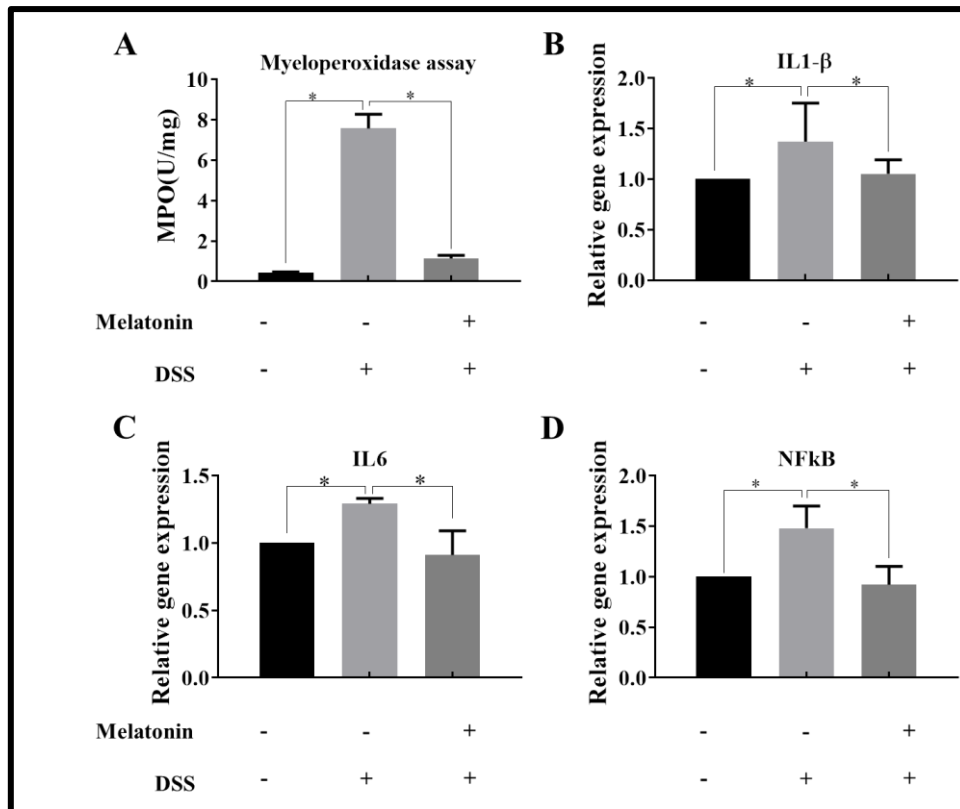


Figure 3.4: Inflammatory gene expression analysis: (A) Myeloperoxidase activity study in colon tissue homogenate (B-D) Gene expression study of IL1 β , IL6 and NF κ B in colon tissue homogenates. (* $p \leq 0.05$)

3.1.7 Melatonin inhibited EZH2 and NOS2 expressions to suppress UC symptoms in mice

To explore the effect of melatonin *in vivo*, the protein expression of EZH2 and NOS2 was also addressed. The findings are consistent with those of an *in vitro* UC model, which indicated that melatonin had a greater therapeutic efficacy *in vivo* with a ~50-fold suppression of NOS2 against DSS-induced changes. Similarly, ~3 fold reduction of EZH2 (**Figure 3.5-B**) and ~3 fold reduction in H3k27me3 (**Figure 3.5-C**) has been found due to therapeutic effect of melatonin in UC prevention. The immunohistochemical examination was carried out to determine the protein expression of EZH2 and NOS2. Overexpression of EZH2 (**Figure 3.6**) and NOS2 (**Figure 3.7**) have been observed with the DSS treated group and decline of expression level of both protein targets have been found by melatonin treatment. In addition, as shown in **Figure 3.8**, we undertook a co-localisation experiment to confirm if EZH2 is selectively up regulated in colon associated macrophages. Up regulation of co-localized NOS2 and EZH2 in the intestinal area indicates DSS-induced inflammation.

Melatonin, on the other hand, has been demonstrated to effectively suppress NOS2-EZH2 signaling.

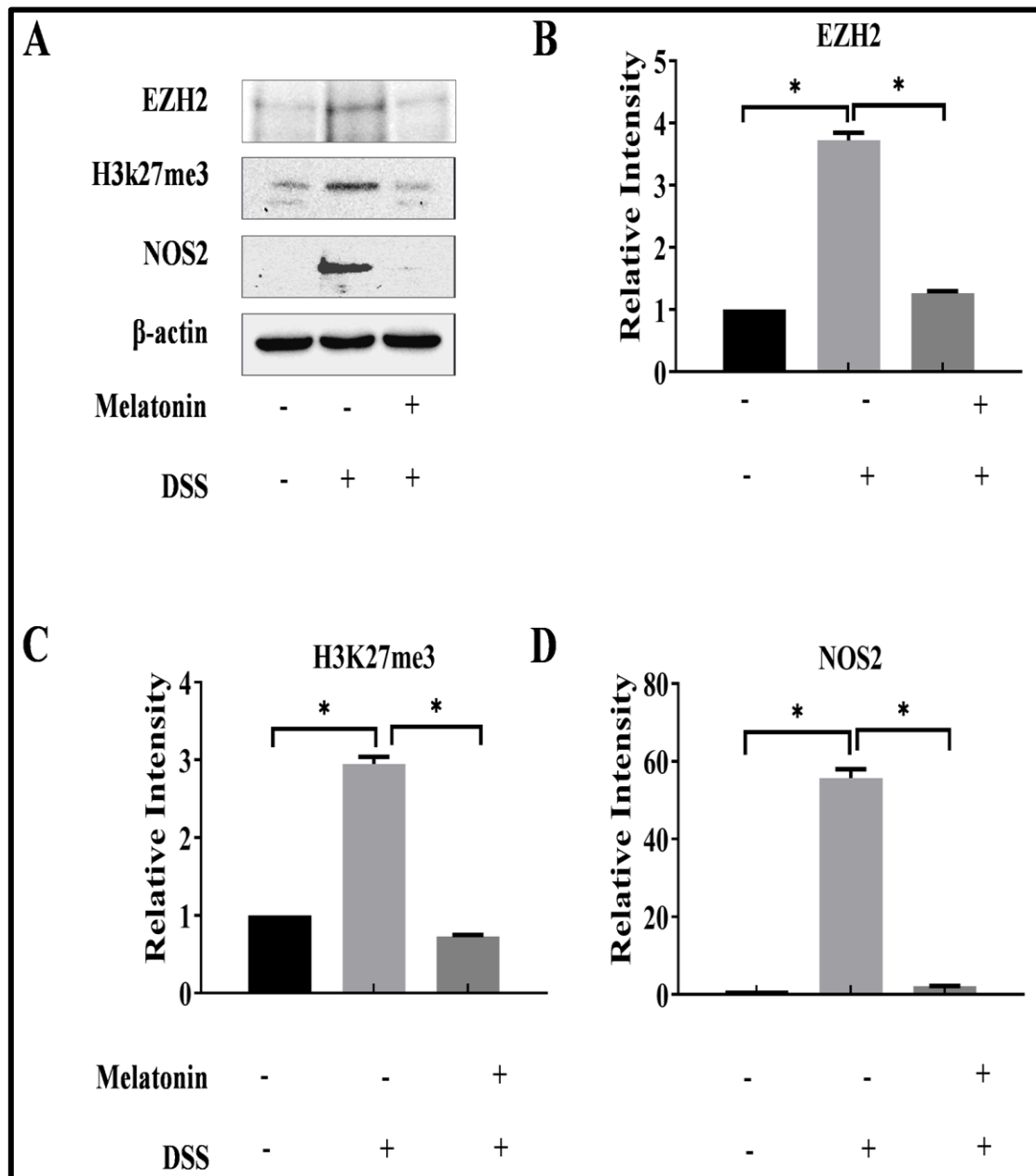


Figure 3.5: Protein expression analysis: (A) Western blot analysis in colon tissue homogenates (B-D) Quantification for protein expression analysis of EZH2, H3K27me3 and NOS2. (* $p \leq 0.05$)

Interestingly, EZH2 is responsible for regulating macrophage numbers at the site of inflammation [34], and a decline in EZH2 expression may be responsible for such a fall in macrophage numbers at the site of inflammation. Furthermore, melatonin's curative impact in an *in vivo* animal has been verified by a declined protein expression profile of NOS2, EZH2,

and H3k27me3 [34], the reduction in EZH2 expression might be responsible for such reduction in macrophages population at the inflammation site (colon). Further, down regulated protein expression profile of NOS2, EZH2 and H3k27me3 has confirmed the restorative effect of melatonin in *in vivo* models.

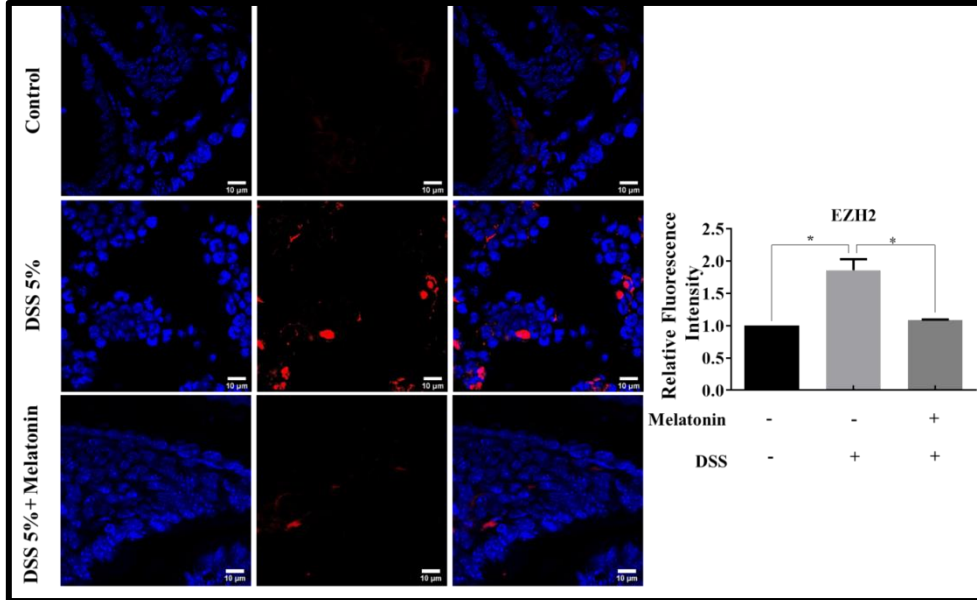


Figure 3.6: IHC analysis: Immuno-histochemical analysis of EZH2 (Red) expression in the colonic tissue section using DAPI (Blue) counterstained for nucleus. (* $p \leq 0.05$) (Scale: 10 μ m)

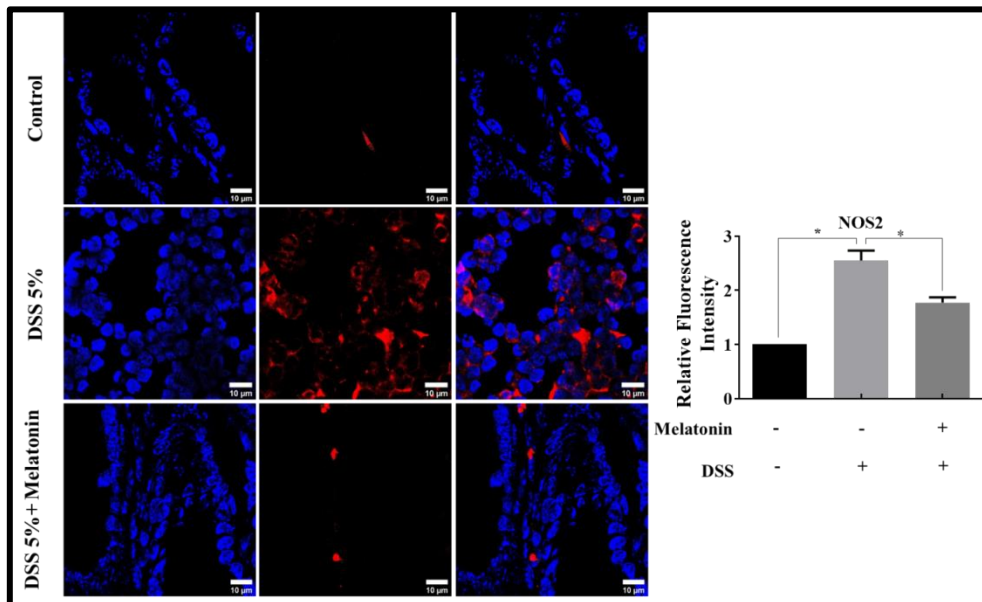


Figure 3.7: NOS2 expression analysis: Immuno-histochemical analysis of NOS2 (Red) expression in the colonic tissue section using DAPI (Blue) counterstained for nucleus. (* $p \leq 0.05$) (Scale: 10 μ m)

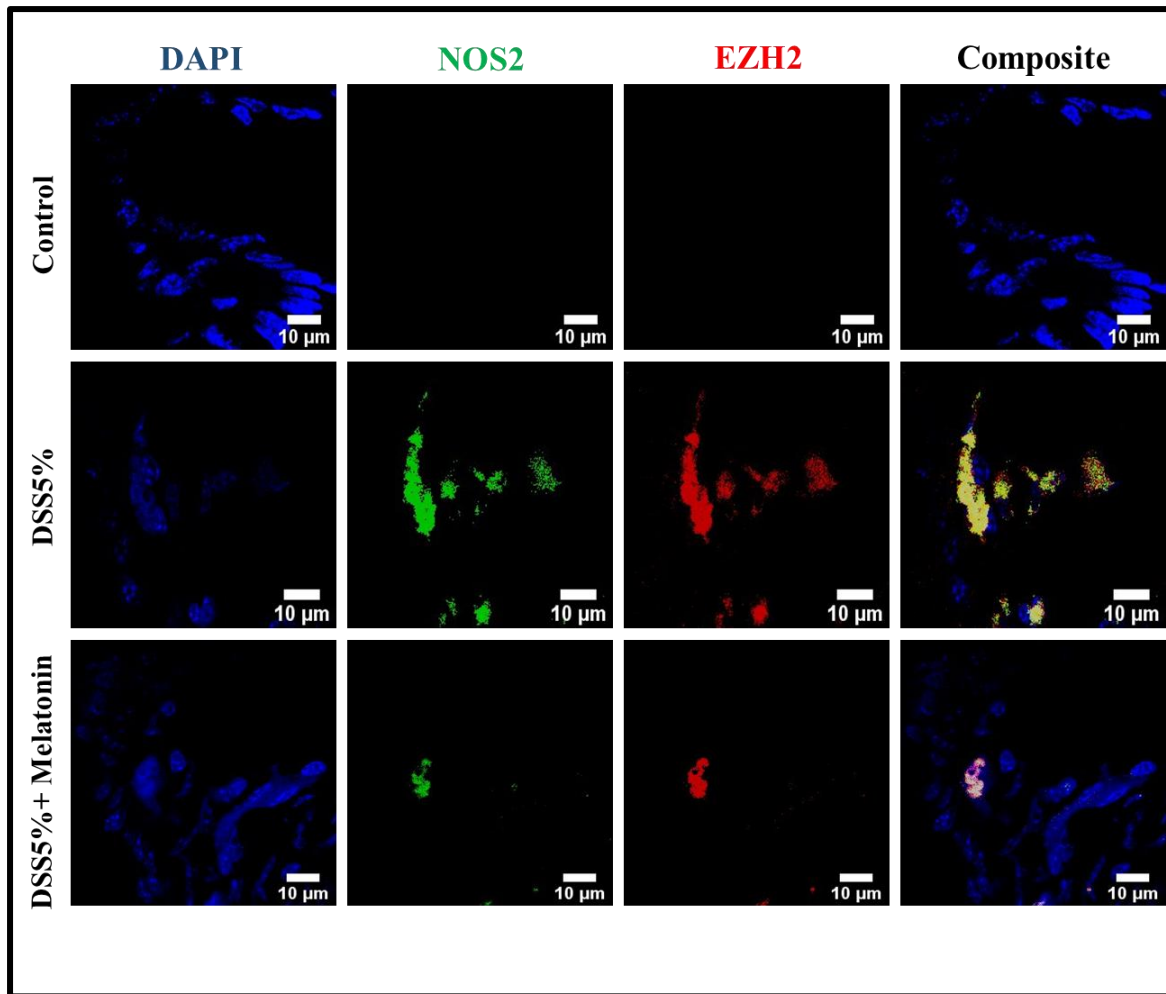


Figure 3.8: Colocalization analysis: Immuno-histochemical co-localisation study of EZH2 and NOS2 in a cross section of colon tissue (Red- EZH2, Green- NOS2 and Blue-Nucleus).

3.1.8 Melatonin reversed pathological demarcation, restricted mast cells infiltration and restored goblet cells

An H&E staining investigation has revealed pathological demarcation as a consequence of DSS-induced inflammatory symptoms. With DSS detrimental impact, altered crypt architecture with profound immune cell infiltration was noted, and melatonin restored crypt structure with recovery in pathological symptoms (**Figure 3.9**). The assessment of histopathological score demonstrated that melatonin has an anti-inflammatory function, reducing the score against DSS-induced abnormalities by 5 times. In **Figure 3.10** shows Toluidine Blue stained microscope images used to distinguish mast cells with inflammatory properties. Mast cells were observed penetrated in DSS-induced colonic tissues. Melatonin therapy, on the other hand, inhibited mast cell invasion. In **Figure 3.11**, the microscope photographs reveal that melatonin has therapeutic effects on goblet cells/crypt in DSS

impaired colon tissues. The quantification of goblet cells/crypt indicated a 5 fold restoration of goblet cells, confirming that melatonin has the ability to treat inflammatory illnesses such as IBD.

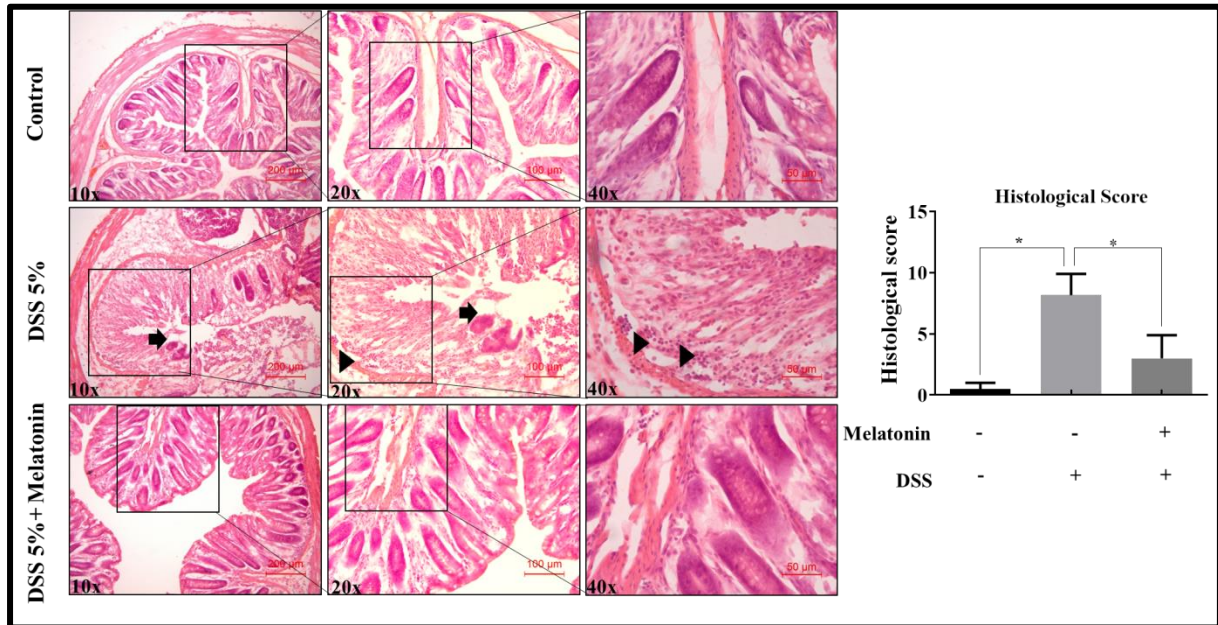


Figure 3.9: Pathological demarcation study: Haematoxylin& Eosin staining for evaluation of colonic tissue section (5µM) for analysis of pathological alterations due inflammatory condition. (* $p \leq 0.05$) Scale: 200µm, 100µm, 50µm) (Arrow head shows immune cells infiltration and arrow shows crypt damage)

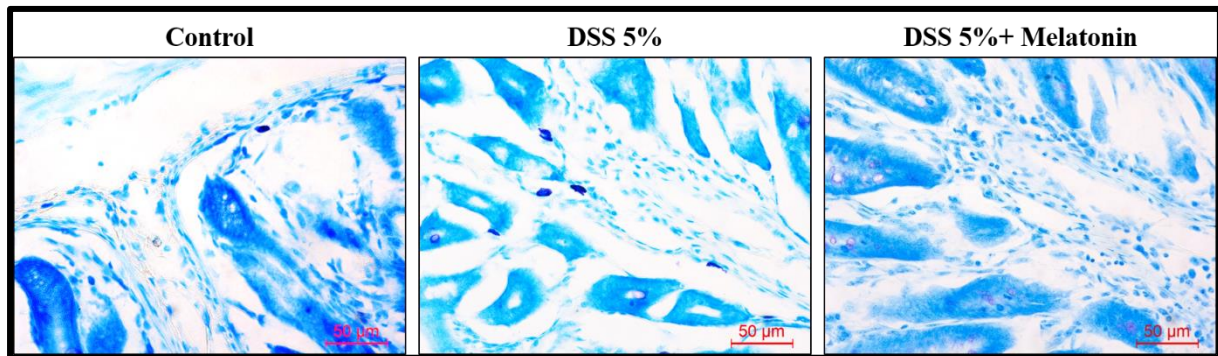


Figure 3.10: Mast cells determination: Toluidine Blue stain examining localisation of mast cells (Violet) due inflammatory condition in colonic tissue section (5µM).

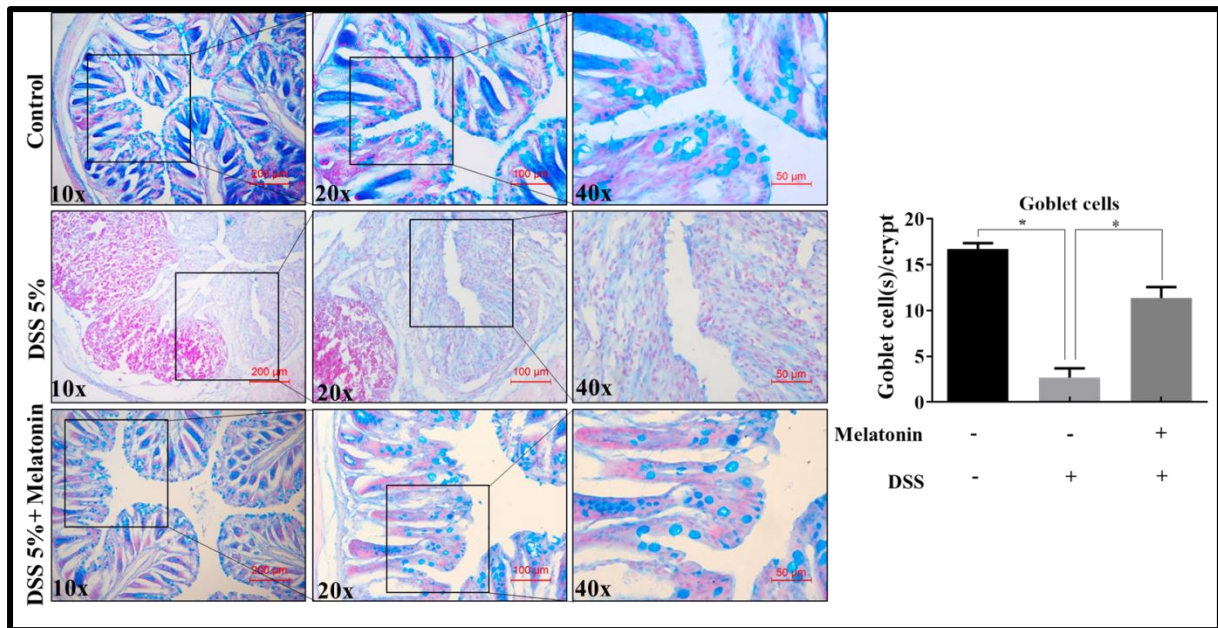


Figure 3.11: Goblet cells examination: Alcian Blue and Nuclear Fast staining for evaluation of colonic tissue section (5 μ M) for analysis of pathological alterations due inflammatory condition on specifically Goblets cells responsible for mucous secretion. (* $p \leq 0.05$) (Scale: 200 μ m, 100 μ m, 50 μ m)

A thorough histopathological analysis of DSS-treated mice colonic lesions exhibited significantly damaged crypt architecture, mucosal ulceration, profound immune cell infiltration, and swelling. Melatonin, on the other hand, has been documented to restore crypt structure and limit immune cell infiltration, and our findings back up previous results [35]. Indeed, mast cell activation and infiltration in the colonic epithelial layer causes a severe inflammatory response, resulting in an accumulation of immune cells in the colonic region. [36]. Mast cells can generate histamine, which promotes inflammation and immune cell infiltration. Mast cell recruitment in colonic tissue is higher in DSS-treated groups, indicating inflammatory aggravation [37]. Goblet cell loss is also a key indicator of colonic inflammatory disorders. Goblet cells secrete mucin, which acts as a protective covering for epithelial cells. The mucous layer serves as the first barrier layer against harmful external elements. Goblet cell depletion causes mucous layer depletion, which leads to ulcer development [38-40]. The current study found staining of goblet cells, indicating that melatonin has a therapeutic effect by shielding goblet cells from DSS-induced damages. As a result, histo-pathological analysis confirmed that melatonin has a substantial therapeutic efficacy in reducing the intensity of diseased conditions caused by inflammation.

3.2 Conclusion

We propose that LPS and DSS-induced UC inflammatory impairments in an *in vitro* and *in vivo* mouse model require macrophage activation and colon damage, which is rescued by melatonin. The investigation highlighted the significance of the epigenetic regulator EZH2 in the development of IBD. The present study establishes a physical link between EZH2 and NOS2, which mediates the advancement of IBD pathogenesis. Melatonin offers therapeutic potential because it inhibits EZH2-NOS2 signaling. Thus, our findings show that the therapeutic potential of melatonin with an inhibitory effect on EZH2 in the treatment of IBD may be an epigenetic therapeutic target in preclinical and translational clinical research.

Note:

*The following published works was included into the current thesis with the authors, corresponding author's, and publisher's permission. The following works is associated with this chapter:

1) Sardoiwala, M.N., et al., Melatonin mediated inhibition of EZH2-NOS2 crosstalk attenuates inflammatory bowel disease in preclinical *in vitro* and *in vivo* models. Life Sciences, 2022. 302: p. 120655.

3.3 References

- [1] S.H. Lee, J.E. Kwon, M.-L. Cho, *Intestinal research*, 16 (2018) 26-42.
- [2] S. Singh, R. Bhatia, P. Khare, S. Sharma, S. Rajarammohan, M. Bishnoi, S.K. Bhadada, S.S. Sharma, J. Kaur, K.K. Kondepudi, *Scientific Reports*, 10 (2020) 18597.
- [3] H. Takeshima, D. Ikegami, M. Wakabayashi, T. Niwa, Y.J. Kim, T. Ushijima, *Carcinogenesis*, 33 (2012) 2384-2390.
- [4] A.J. Watson, A.R. Hart, *Gastroenterology*, 141 (2011) 768-770.
- [5] R.J. Reiter, *Endocrine reviews*, 12 (1991) 151-180.
- [6] D.X. Tan, R.J. Reiter, L.C. Manchester, M.T. Yan, M. El-Sawi, R.M. Sainz, J.C. Mayo, R. Kohen, M. Allegra, R. Hardeland, *Current topics in medicinal chemistry*, 2 (2002) 181-197.
- [7] P.T. Pentney, G.A. Bubenik, 19 (1995) 31-39.
- [8] V. Nosál'ová, M. Zeman, S. Černá, J. Navarová, M. Zakálová, 42 (2007) 364-370.
- [9] E. Esposito, E. Mazzon, L. Riccardi, R. Caminiti, R. Meli, S. Cuzzocrea, 45 (2008) 166-173.
- [10] E. Marquez, S. Sánchez-Fidalgo, J.R. Calvo, C.A.I.d. Lastra, V. Motilva, 40 (2006) 48-55.
- [11] D. Pozo, R.J. Reiter, J.R. Calvo, J.M. Guerrero, *Life Sci*, 55 (1994) P1455-460.
- [12] M. Emet, H. Ozcan, L. Ozel, M. Yayla, Z. Halici, A. Hacimuftuoglu, *Eurasian J Med*, 48 (2016) 135-141.
- [13] A. Jenwitheesuk, C. Nopparat, S. Mukda, P. Wongchitrat, P. Govitrapong, *International journal of molecular sciences*, 2014, pp. 16848-16884.
- [14] A. Korkmaz, E.J. Sanchez-Barcelo, D.-X. Tan, R.J. Reiter, *Breast Cancer Research and Treatment*, 115 (2009) 13-27.
- [15] X. Zhang, Y. Wang, J. Yuan, N. Li, S. Pei, J. Xu, X. Luo, C. Mao, J. Liu, T. Yu, S. Gan, Q. Zheng, Y. Liang, W. Guo, J. Qiu, G. Constantin, J. Jin, J. Qin, Y. Xiao, *The Journal of experimental medicine*, 215 (2018) 1365-1382.
- [16] A. Herrera-Merchan, L. Arranz, J.M. Ligos, A. de Molina, O. Dominguez, S. Gonzalez, *Nat Commun*, 3 (2012) 623.
- [17] N.K. Boughton-Smith, S.M. Evans, C.J. Hawkey, A.T. Cole, M. Balsitis, B.J. Whittle, S. Moncada, *Lancet*, 342 (1993) 338-340.
- [18] Q. Xue, Y. Yan, R. Zhang, H. Xiong, *Int J Mol Sci*, 19 (2018).
- [19] G. Ray, M.S. Longworth, *Inflammatory bowel diseases*, 25 (2019) 235-247.
- [20] Kaundal, A. Srivastava, A. Dev, S. Mohanbhai, S. Karmakar, S. Roy Choudhury, *Molecular Pharmaceutics*, 17 (2020).

- [21] L.E. Targownik, C.N. Bernstein, *Am J Gastroenterol*, 108 (2013) 1835-1842, quiz 1843.
- [22] M.G. Goggins, S.A. Shah, J. Goh, A. Cherukuri, D.G. Weir, D. Kelleher, N. Mahmud, *Mediators Inflamm*, 10 (2001) 69-73.
- [23] Y. Noda, A. Mori, R. Liburdy, L. Packer, *J Pineal Res*, 27 (1999) 159-163.
- [24] H. Rafa, S. Benkhelifa, S. AitYounes, H. Saoula, S. Belhadeif, M. Belkhefha, A. Boukercha, R. Toumi, I. Soufli, O. Moralès, Y. de Launoit, H. Mahfouf, M. Nakmouche, N. Delhem, C. Touil-Boukoffa, *Mediators Inflamm*, 2017 (2017) 7353252.
- [25] S.S. Dhillon, L.A. Mastropaolo, R. Murchie, C. Griffiths, C. Thöni, A. Elkadri, W. Xu, A. Mack, T. Walters, C. Guo, D. Mack, H. Huynh, S. Baksh, M.S. Silverberg, J.H. Brumell, S.B. Snapper, A.M. Muise, *Clinical and translational gastroenterology*, 5 (2014) e46-e46.
- [26] W.-G. Dong, Q. Mei, J.-P. Yu, J.-M. Xu, L. Xiang, Y. Xu, *World journal of gastroenterology*, 9 (2003) 1307-1311.
- [27] Q. Mei, J.M. Xu, L. Xiang, Y.M. Hu, X.P. Hu, Z.W. Xu, *Postgraduate Medical Journal*, 81 (2005) 667.
- [28] H. Dreger, A. Ludwig, A. Weller, G. Baumann, V. Stangl, K. Stangl, *Genomics*, 107 (2016) 145-149.
- [29] T.J. Gross, K. Kremens, L.S. Powers, B. Brink, T. Knutson, F.E. Domann, R.A. Philibert, M.M. Milhem, M.M. Monick, *J Immunol*, 192 (2014) 2326-2338.
- [30] S. Wirtz, V. Popp, M. Kindermann, K. Gerlach, B. Weigmann, S. Fichtner-Feigl, M.F. Neurath, *Nature protocols*, 12 (2017) 1295-1309.
- [31] J. Däbritz, L. Judd, H. Chalinor, T. Menheniott, A. Giraud, *Scientific Reports*, 6 (2016) 20584.
- [32] A.M. Abdelmegid, F.K. Abdo, F.E. Ahmed, A.A.A. Kattaia, *Scientific Reports*, 9 (2019) 10176.
- [33] K. Paskaloglu, G. Sener, C. Kapucu, G. Ayanoglu-Dulger, *Life Sci*, 74 (2004) 1093-1104.
- [34] A.E. Neele, M.P.J. de Winther, *The Journal of experimental medicine*, 215 (2018) 1269-1271.
- [35] Y.-S. Park, S.-H. Chung, S.-K. Lee, J.-H. Kim, J.-B. Kim, T.-K. Kim, D.-S. Kim, H.-W. Baik, *Int J Mol Med*, 35 (2015) 979-986.
- [36] M. Kurosawa, H. Nagai, *Ulcers*, 2013 (2013) 714807.
- [37] M.O. Lansink, V. Patyk, H. de Groot, K. Effenberger-Neidnicht, *Journal of Surgical Research*, 211 (2017) 114-125.

[38] J.J. Kim, M.S. Shajib, M.M. Manocha, W.I. Khan, *J Vis Exp*, (2012).

[39] H.S. Cooper, S.N. Murthy, R.S. Shah, D.J. Sedergran, *Laboratory investigation; a journal of technical methods and pathology*, 69 (1993) 238-249.

[40] S.W. Kim, S. Kim, M. Son, J.H. Cheon, Y.S. Park, *Scientific Reports*, 10 (2020) 2232.

Chapter 4:

Melatonin-loaded chitosan nanoparticles endows nitric oxide synthase 2 mediated anti-inflammatory activity in inflammatory bowel disease model

4.0 Background

Inflammatory bowel disease (IBD) is a multifactorial disorder caused by an abnormal immune response to the host gut bacteria. Two major pathological conditions included in this category which includes Ulcerative Colitis (UC) and Crohn's Disease (CD). Ulcerative Colitis (UC) is a disorder characterised by ulcers in the mucosal and submucosal layers of colonic tissue, resulting in gut-epithelial layer damage localized to the colon and rectum portions of the gastrointestinal tract [1, 2]. Histological findings of UC are distinguished by acute and chronic inflammation of polymorphonuclear leucocytes, mononuclear cells, pus, crypt destruction, and goblet cell depletion [3]. Crohn's disease (CD) can affect any part of the gastrointestinal tract; however it is most typically seen in the ileocecal region in that case, the inflammation can spread to the serosa, resulting in sinus tracts (crohn like structure). Histological investigation may demonstrate submucosal inflammation as well as non-caseating granuloma development [3]. Rectal haemorrhage is more common in UC patients, whereas CD patients exhibit weight loss and perianal illness. Similarly, the risk of autoimmune illness is higher in people with CD than in healthy people [4].

The worldwide occurrence of IBD is rising, worsening the probability of getting colorectal cancer in the near future. According to a survey, 3.9 million females and 3 million males worldwide suffer from IBD [5]. Initially, it was thought that IBD was exclusively seen in developed countries. However, the prevalence of IBD is increasing in developing countries, raising doubts about the disease's threat.

Currently, pharmacological interventions used to manage IBD include salicylates, immunomodulators, corticosteroids, and anti-TNF-alpha drugs [6][7]. Despite their limited therapeutic efficacy, these medicines have undesirable adverse consequences, limiting their use as curative agents. Immunotherapy is also available for the treatment of IBD; however the cost of immunotherapy limits its application and feasibility to the average person. As a result, novel pharmacological drugs with improved therapeutic efficacy are required for IBD treatment.

Melatonin is a naturally synthesized neurohormone having anti-inflammatory, antioxidant, and neuroprotective properties [8, 9]. Melatonin is accessible over the counter (OTC), indicating its excellent safety profile. Melatonin has demonstrated promising anti-inflammatory properties in a murine model of ulcerative colitis (UC) [10]. Melatonin's therapeutic efficacy is reduced due to its poor solubility and burst drug release, which raises

its dosage interval and therapeutic dose [10]. To address this issue, we designed a chitosan-based nano-formulation of melatonin to augment its therapeutic potential.

Chitosan is a pharmaceutical excipient that is extremely biodegradable, biocompatible, and non-toxic. Chitosan is a naturally produced cationic polymer of glucosamine and N-acetylglucosamine with a pKa of 6.5, making it soluble in acidic conditions due to amine protonation [11]. Nanotherapeutic techniques based on nano-drug delivery systems have gained popularity in recent years. Chitosan nanoparticles-based drug delivery systems are also being investigated extensively in order to optimize the drug release profile and therapeutic efficacy of hydrophobic drug molecules [12].

As a result, we encapsulated melatonin in chitosan nanoparticles to improve melatonin release profile and hence improve therapeutic efficacy. We used anionic sodium tripolyphosphate (STPP) to synthesise melatonin-loaded chitosan nanoparticles to investigate their *in-vitro* and *in-vivo* therapeutic potential [13]. *In-vitro* therapeutic efficacy is assessed against LPS-stimulated macrophages, and the DSS-induced Ulcerative colitis mouse model is employed for assessing *in-vivo* therapeutic potential [14]. We have effectively demonstrated the therapeutic efficacy of a chitosan nanoformulation incorporating melatonin for the treatment of IBD in this study.

4.1 Results and discussion

4.1.1 Size and morphological analysis of nanoparticles

Dynamic light scattering (DLS) measurements revealed that the mean hydrodynamic size of CSNPs and Mel-CSNPs was 135 nm and 155 nm, respectively in **Figure 4.1a (A)**. The mean PDI was determined to be 0.133 ± 0.01 and 0.166 ± 0.022 , respectively. CSNPs ($36 \pm 2\text{mV}$) and Mel-CSNPs ($35 \pm 1\text{mV}$) showed positive zeta potential accredited due to cationic nature of Chitosan **Figure 4.1a (B)**. We witnessed a slight reduction in zeta potential in Mel-CSNPs which may be due to loading of melatonin. Because nanoparticles were designed for intravenous (*i.v.*) delivery, managing size was a crucial consideration, as revealed by TEM images. As a result, TEM pictures of our formulations' surfaces revealed their spherical and monodisperse character in **Figure 4.1a (C)**. FESEM pictures also demonstrate that nanoparticles are spherical and monodisperse in **Figure 4.1b**. Morphological and size study results demonstrate that melatonin-loaded chitosan nanoparticles with sizes ranging from 110 to 300 nm have a spherical form [13, 27].

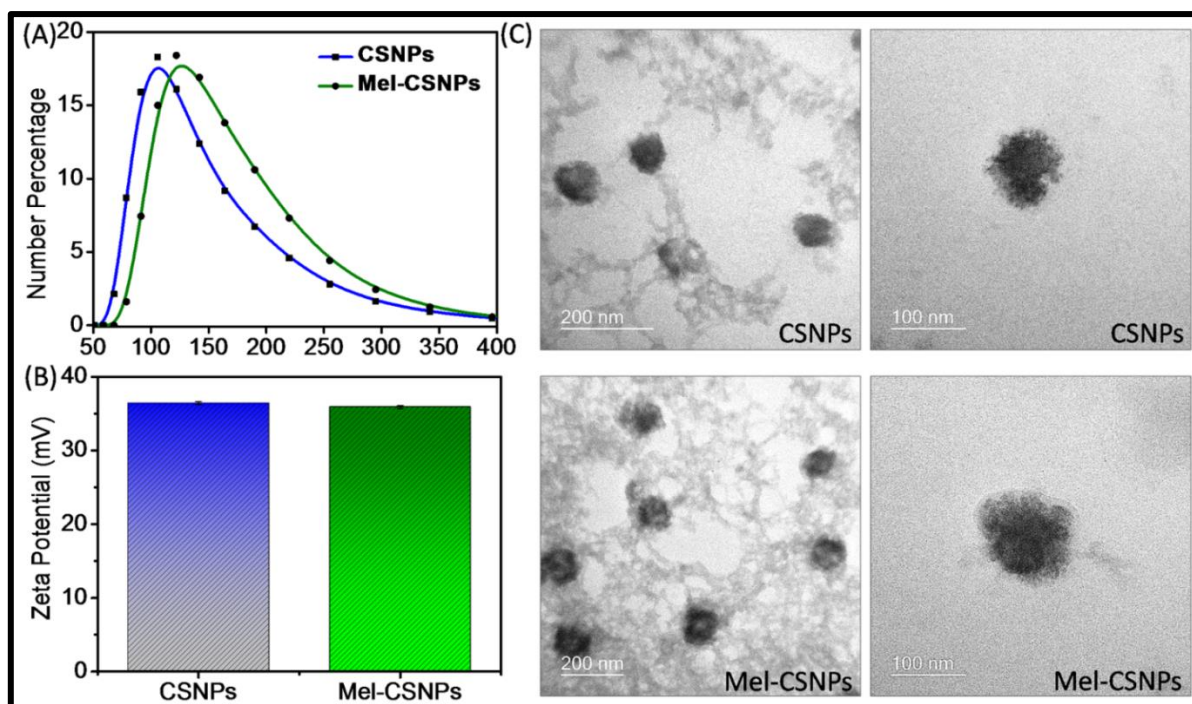


Figure 4.1a: Characterization of nanoparticles (A) Dynamic Light scattering measurement of mean hydrodynamic size of chitosan nanoparticles (CSNPs) and Melatonin loaded chitosan nanoparticles (Mel-CSNPs) (B)-Surface zeta potential measurement of CSNPs ($+ 36 \pm 2\text{mV}$) and Mel-CSNPs ($+35 \pm 1\text{mV}$) and (C)TEM images of CSNPs and Mel-CSNPS shows nano-sized particles.

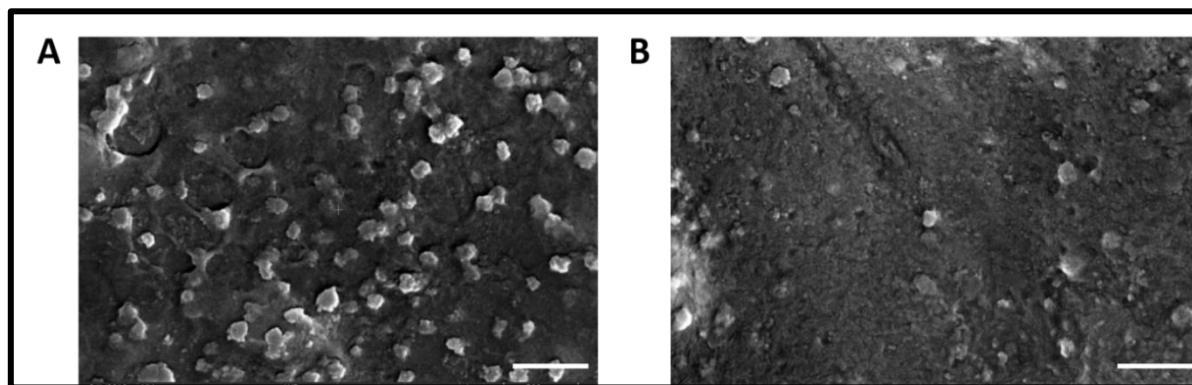


Figure 4.1b: Field emission scanning electron microscopy (FESEM) of CSNPS (A) and Mel-CSNPs (B). (Scale bar = 500nm)

4.1.2 Fourier transform infrared spectroscopy (FT-IR) and X-ray diffraction (XRD) analysis

Chitosan exhibited a large hydroxyl (-OH) absorption band obtained at 3400 cm^{-1} and free amino (-NH₂) at C2 position in glucosamine 1157 cm^{-1} peak obtained shows -C-O-C-bridge

that confirms the presence of chitosan [28]. a sharp peak for N-H bending at 3300 cm^{-1} and a peak for C-N stretching at 3078 cm^{-1} . Melatonin has peaks at 1495 cm^{-1} , 1556 cm^{-1} , and 1627 cm^{-1} for aromatic -C= and -C=O, respectively. CSNPs exhibited a wider -OH stretching peak at 3400 cm^{-1} , which might be attributed to nanoparticle production, and the difference between Mel-CSNPs and CSNPs spectrum, FTIR indicated full encapsulation of melatonin in **Figure 4.2 (A)**. An X-ray Diffraction (XRD) analysis was performed to determine the physical properties of chitosan, melatonin, CSNPs, and Mel-CSNPs. Chitosan exhibited large diffraction peaks at 10.43° and 20.31°, indicating a low degree of crystalline nature, which is consistent with earlier research [13]. Melatonin exhibited a prominent and intense peak at 10.75°, 11.42°, 14.76°, 16.45°, 18.89°, 20.48°, 22.53°, 24.14°, and 24.93°, showing that it is extremely crystalline [13, 29]. CSNPs had a wider diffraction peak at 20.31°, and Mel-CSNPs have a similar diffraction pattern with minute crystalline peaks of melatonin, confirming the presence of melatonin in chitosan nanocarriers [30]. The findings back the previous research that showed XRD analysis of chitosan nanoparticles and melatonin-loaded chitosan nanoparticles indicating amorphous nanoparticle structure [13, 31] in **Figure 4.2 (B)**. Furthermore, the drug loading efficiency of our nanoformulation was measured at three distinct drug polymer weight ratios: 1:10 (3.1%), 1:5 (8.5%), and 1:2 (20.4%). For our investigation, we utilised the optimal drug loading ratio of 1:2, which was 20.4%. The synthesized nanoformulation demonstrated higher loading efficiency (20.4%) than previous reports of melatonin-loaded lecithin/chitosan nanoparticles (7.2%), indicating that our nanoformulation has superior properties [32].

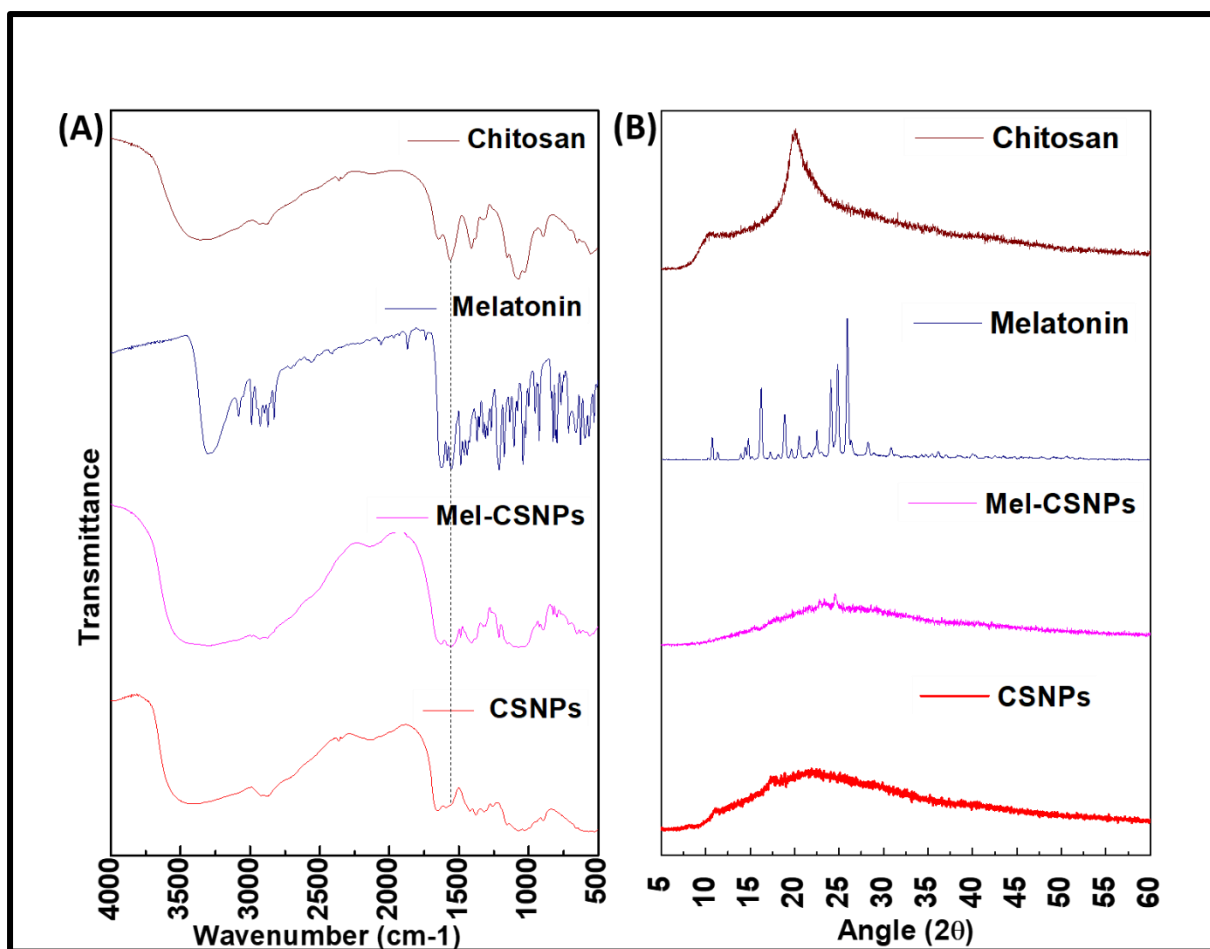


Figure 4.2: (A)-FTIR spectra of CSNPs, Mel-CSNPs, Melatonin and Chitosan (B) - X-RD diffraction spectra of CSNPs, Mel-CSNPs, Melatonin and Chitosan.

4.1.3 *In-vitro* drug release study

Mel-drug CSNP's release profile exhibited a biphasic pattern, with an initial burst release followed by prolonged release. Within 1 hour of the experiment, Mel-CSNP displayed a cumulative release of 22.05%, and at the end of 24 hours, it had increased to 76.35% cumulative release in PBS pH 7.4. According to earlier research, biphasic drug release from nanoparticles is one of the key reasons for boosting the therapeutic efficiency of melatonin, which has a low retention duration in the body [13] as shown in **Figure 4.3a (A)**. The drug release analysis in acidic conditions at pH 4.5 revealed a similar pattern as in PBS pH 7.4 but was faster and more drug release occurred at 24 hours, which is up to 96.22% in acidic conditions **Figure 4.3b**.

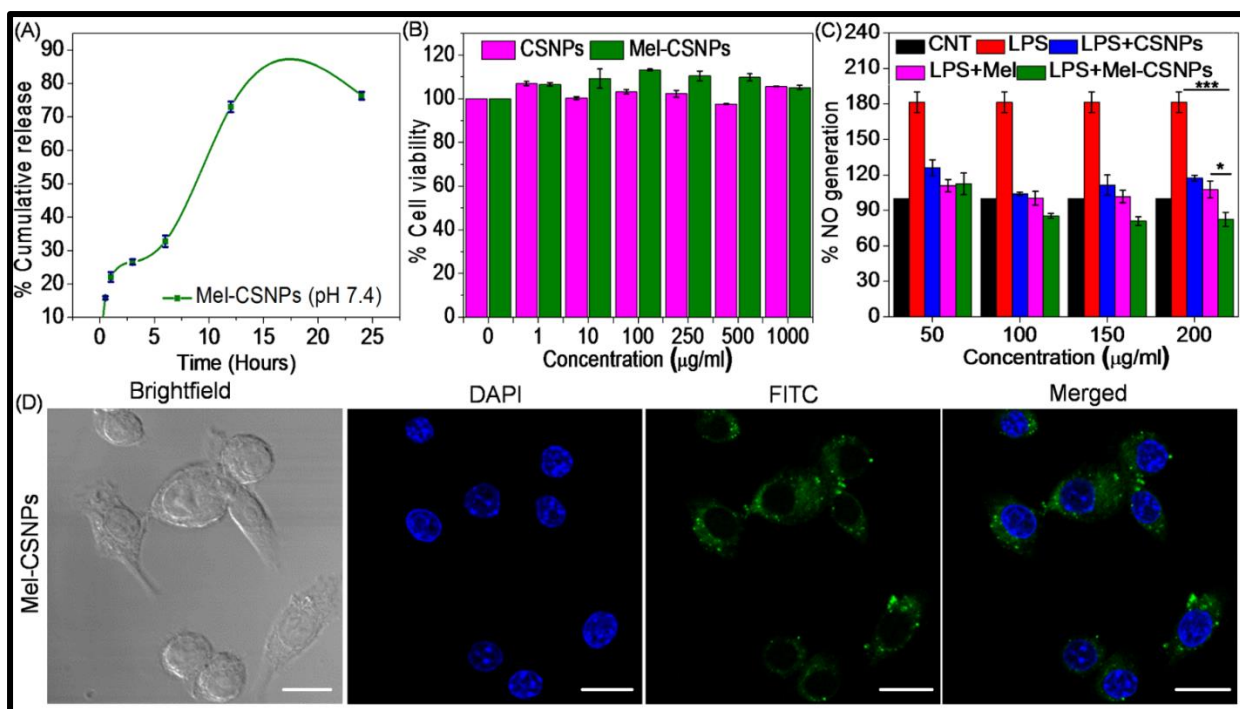


Figure 4.3a: (A) *In-vitro* drug release indicates biphasic release, (B) MTT assay for biocompatibility of nanoformulation, (C) Nitrite estimation for anti-inflammatory activity assessment, (D) Confocal laser microscopy (CLSM) images show major cytoplasmic accumulation of nanoparticles. (* $p \leq 0.05$, ** $p \leq 0.001$ and *** $p \leq 0.0001$) (Scale bar = 20 µm)

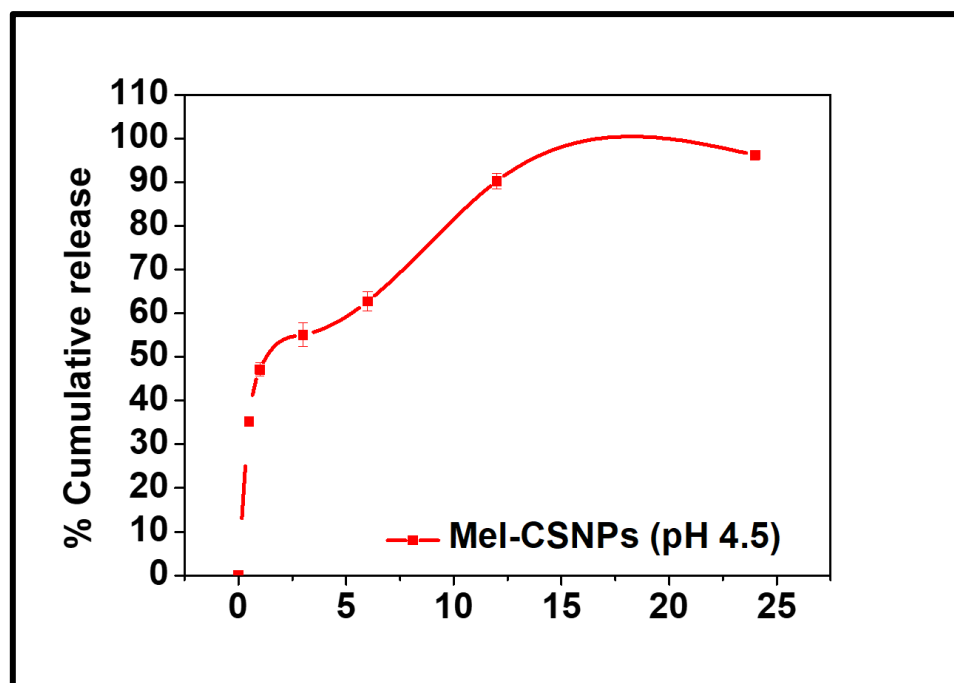


Figure 4.3b: *In-vitro* drug release indicating initial burst release followed by gradual release pattern at pH 4.5.

4.1.4 *In-vitro* cellular internalization of nanoparticles

One hour after treatment, FITC-tagged Mel-CSNP had higher cumulative cytoplasmic uptake in **Figure 4.3a (D)**. This suggests that nanoparticles have the ability to infiltrate cells and deliver drugs. RAW 264.7 murine macrophages, which have a basic physiological role of phagocytosis, could be explored as a plausible mechanism of nanoparticle cellular internalisation [18].

4.1.5 *In-vitro* anti-inflammation analysis

Chitosan is a non-toxic and biocompatible polymer. As a result, CSNPs and Mel-CSNPs exhibited negligible cytotoxicity. In **Figure 4.3a (B)** CSNPs and Mel-CSNPs used at several concentrations up to 1000 µg/mL did not show any major cytotoxicity which is in lieu to reports that demonstrated highly biocompatible nature of CSNPs [13, 32]. RAW 264.7 cells were treated with lipopolysaccharide (LPS) to create an inflammatory response in order to assess the anti-inflammatory properties of melatonin and Mel-CSNP. LPS can cause an inflammatory immune response by activating the TLR-4 receptor. Following previous reports, a 1µg/mL dosage of LPS, a bacterial endotoxin, was used to cause inflammation [33] Mel-CSNPs and melatonin were found to have anti-inflammatory properties, both in **Figure 4.3a (C)** by reducing 55% and 40% NO generation. In this study, we discovered that our nanoformulations surpassed prior melatonin studies that showed 10% nitrite reduction at 250 µM dosage [34]. Furthermore, they demonstrated a larger 60% reduction with a 2000 µM dosage. Indeed, with 200 µM dosage of melatonin, our nanoformulation reduced NO by 55%. It suggests that chitosan nanoformulation improves melatonin anti-inflammatory efficiency. It also has the advantage of lowering the required effective medication concentration in the treatment of inflammatory diseases.

4.1.6 Nuclear factor kappa-light-chain-enhancer of activated B (NF-kB) p65 - nuclear translocation study

NF-kB p65 is a transcription factor family that regulates a number of genes involved in immunological and inflammatory responses. LPS binds to macrophage TLR4 receptors, activating the redistribution of nuclear factor kappa B (NF-kB p65) transcription factor from the cytosol into the nucleus, leading in the transcription of target genes [35, 36]. Mel-CSNP (200 µg/ml) pre-treatment improved anti-inflammatory response by interfering with NF-kB nuclear translocation compared to bare melatonin and placebo CSNPs treatment group as

observed in the **Figure 4.4**. Our nanoformulation's ability to inhibit NF-kB nuclear translocation suggests that it has anti-inflammatory properties. As observed in **Figure 4.4 A** and **B** we can conclude that Mel-CSNPs exhibit significant reduction in inflammation by inhibiting activation of macrophages. Almost each cell was activated upon LPS stimulation which can be clearly concluded from **Figure 4.4 B**. These findings support previous findings that NF-kB nuclear translocation inhibition is an effective therapeutic potential of anti-inflammatory drugs [37, 38]. Immunofluorescence experiments with an activated RAW264.7 macrophage cell line treated with LPS (1 μ g/ml) exhibited active nuclear translocation in comparison to cells not treated with LPS. As a result, Mel-CSNPs reduce gene expression of several NF-kB target inflammatory genes, exacerbating the inflammatory response. The agreement of MTT assay, NO quantification, and NF-kB nuclear translocation data verifies our nanoformulation's anti-inflammatory and therapeutic potential.

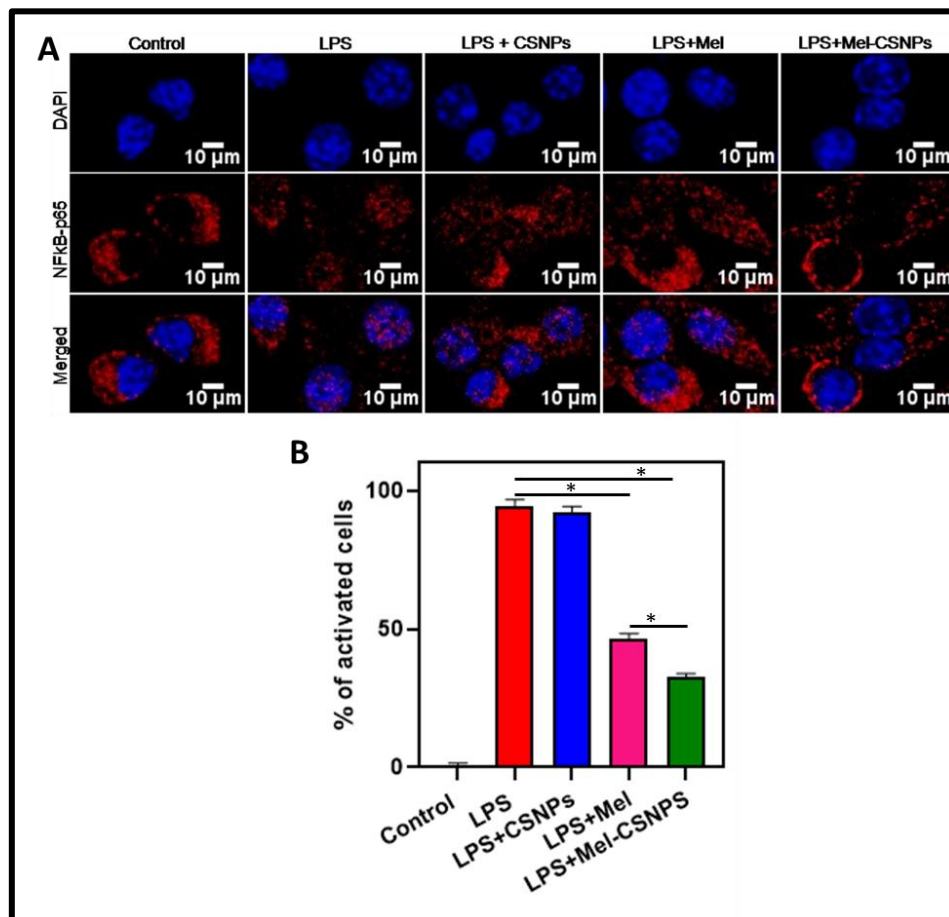


Figure 4.4: CLSM micrographs (A) anti-inflammatory action of Mel-CSNPs by showing reduction in nuclear translocation of NF-kB p65 against LPS stimulation. (B) Percentage of activated cells based on nuclear translocation of NF-kB

4.1.7 Haemolysis analysis

The haemolysis test was carried out to determine the biocompatibility of nanoparticles for safe intravenous administration. The haemolysis assay results showed no significant difference between Mel-CSNPs and CSNPs at doses of 1mg/ml and 5 mg/ml, respectively as observed in **Figure 4.5**. This confirms that our nanoformulation is safe for intravenous usage and does not cause red blood cell lyses. The findings are consistent with a previous study that found chitosan nanoparticles to be more hemocompatible [39]. Because of their composition, chitosan nanoparticles have exhibited selective targeting when administered intravenously.

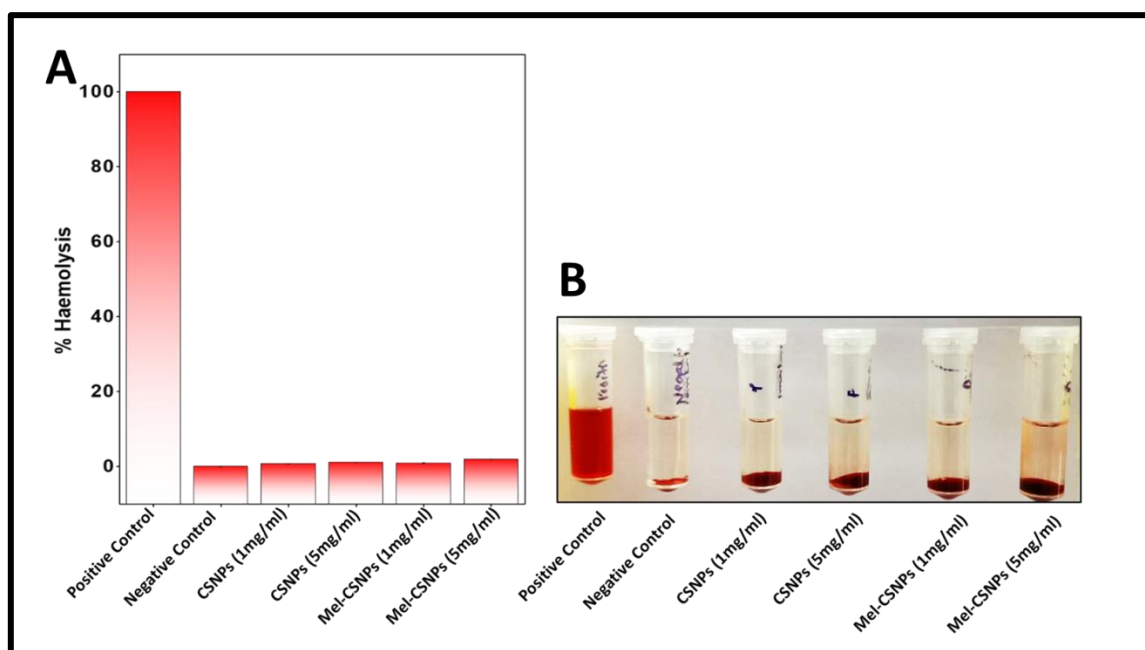


Figure 4.5: Haemolysis analysis (A) Percentage lysis of RBC upon treatment with nanoformulations (B) Images of blood sample after treatment with nanoformulations.

4.1.8 *In-vivo* bio distribution study

As depicted in **Figure 4.6**, an *in-vivo* biodistribution investigation of ICG-tagged Mel-CSNP revealed initial distribution in highly perfused tissue, namely the heart and liver. The decrease in fluorescence intensity was observed at later time points, showing that the nanoparticles were gradually cleared from the body. As a result, the fluorescence intensity in the kidney and liver rose as compared to the original time point, indicating the nanoparticle clearance path. The findings support previous reports indicating a liver and kidney-mediated clearance mechanism for nanoparticles [40, 41]. Ex-vivo imaging also revealed lower fluorescence intensity in important organs such as the brain, kidney, liver, heart, and spleen

due to low nanoparticle retention and removal from these tissues. High fluorescence intensity detected in target colonic tissue, on the other hand, indicates more retention of nanoparticles in colon. This could be owing to increased availability and expression of melatonin receptors, as well as a larger cumulative fraction of macrophages in the intestinal region [42, 43].

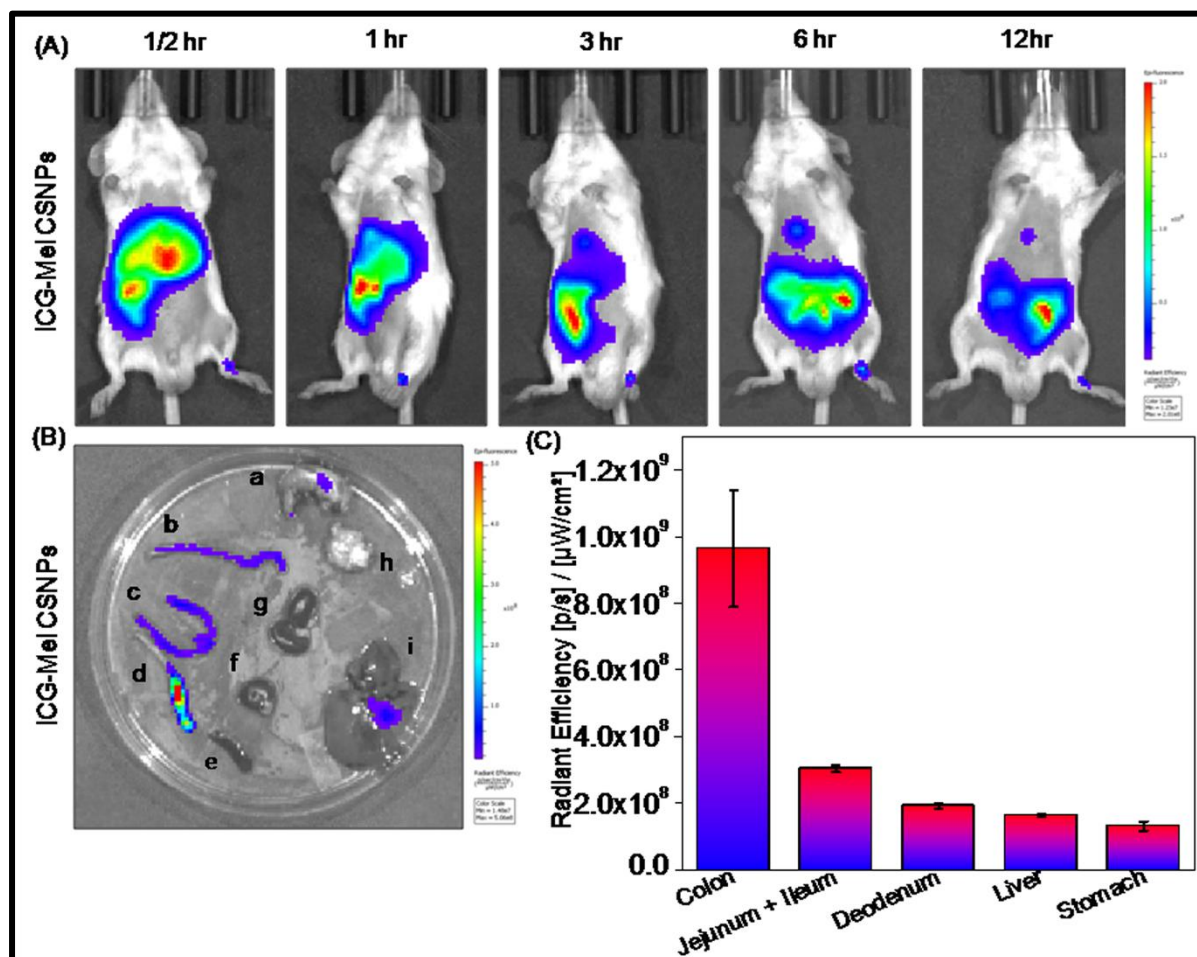


Figure 4.6: (A) *In-vivo* bio-distribution study of Indocyanine green (ICG)-tagged Mel-CSNPs and (B-C)–*Ex-vivo* bio-distribution of ICG-Mel-CSNPs, (a-stomach, b-deodenum, c-ileum+jejunum, d- colon, e- spleen, f- heart, g-kidney, h- brain and i-liver) show good bio-distribution and clearance path of nanoparticles.

4.1.9 *In-vivo* therapeutic efficacy study

Disease Activity Index was recorded for each experiment to evaluate the severity of disease produced by DSS treatment in order to estimate the therapeutic efficacy of nano-formulation. Melatonin and Mel-CSNPs were also tested for their therapeutic impact in DSS-induced ulcerative colitis in mice.

The increased DAI in DSS-induced colitic mice suggest severe inflammatory pathological states such as diarrhoea and bleeding, and considerable recovery has been observed with Mel-CSNPs in contrast to other treatment groups as observed in **Figure 4.7 (A)**. As indicated in **Figure 4.7 (A)**, no significant difference was seen between the melatonin and Mel-CSNPs groups, but after the fifth day, Mel-CSNPs exhibited a considerable improvement in therapeutic efficacy when compared to bare melatonin. Similarly, in **Figure 4.7 (B)**, Mel-CSNPs treatment significantly restored body weight compared to the melatonin treatment group against DSS-induced weight loss. Weight loss occurs as a result of decreased gut function caused by DSS exposure in mice with leaky gut pathological diseases.

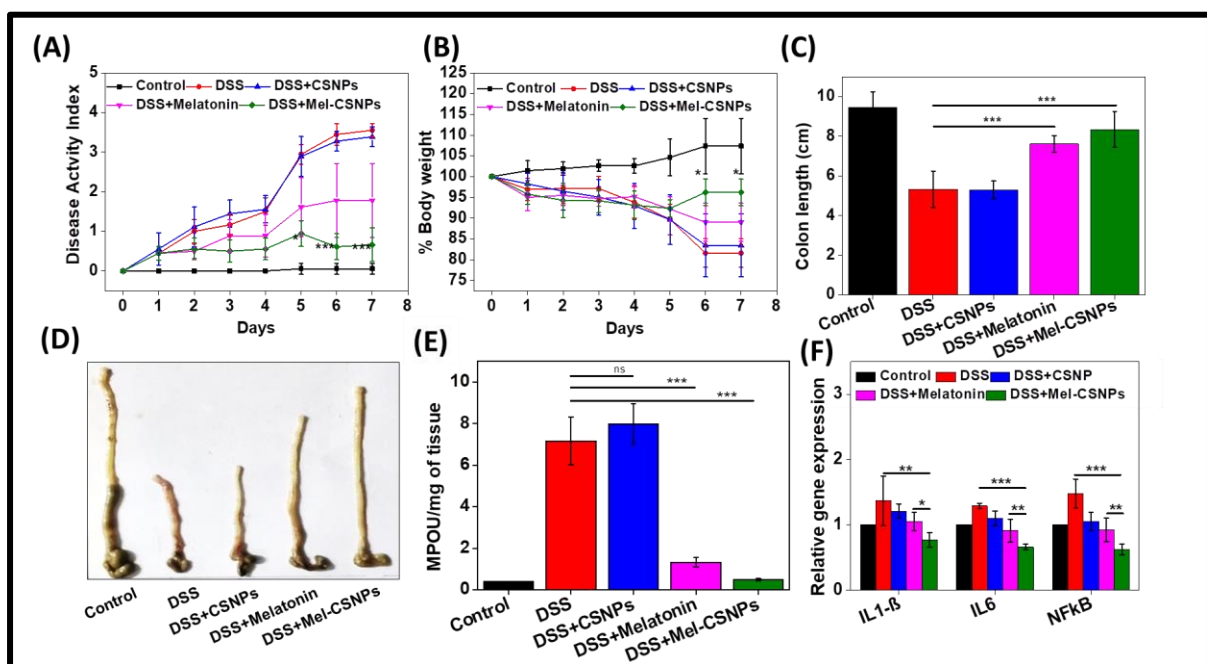


Figure 4.7: (A)- Disease Activity Index, (B) Percentage change in body weight,(C-D) Colon length evaluation, (E) Myeloperoxidase (MPO) assay in colonic tissue homogenates and(F)Gene expression of analysis in colonic tissue sample of mice confirms anti-inflammatory potential of Mel-CSNPs.(* $p \leq 0.05$, ** $p \leq 0.001$, *** $p \leq 0.0001$ and ns: non-significant)

In **Figure 4.7**, the curative effect of Mel-CSNPs was validated by noticing a negligible reduction in colon length compared to the control group vs DSS-induced colon damage (C-D). In terms of colon length parameter study, our Mel-CSNPs showed superior in-vivo therapeutic efficacy in comparison to bare melatonin [44]. As a result, our nanoformulation demonstrated therapeutic efficacy by improving health indices in mice with DSS-induced IBD symptoms. Because melatonin has a short plasma half-life in the body, it is taken out of

the system, which could explain why its anti-inflammatory effect is compromised. Mel-CSNPs significantly improved anti-inflammatory action, as evidenced by the results shown in **Figure 4.7**.

4.1.10 Myeloperoxidase assay (MPO)

A positive correlation exists between myeloperoxidase (MPO) activity and the degree of intestinal inflammation and neutrophil infiltration. During an inflammatory situation, there is a greater amount of neutrophilic infiltration [45]. MPO is found in neutrophils and can be utilised to determine the degree of neutrophilic infiltration and inflammation. The ability of the therapeutic drug to limit immune cell infiltration into disease sites demonstrates its anti-inflammatory potential. MPO activity was shown to be increased in groups 2: DSS and 3: DSS + CSNPs, however it was significantly lower in groups 4: DSS + Melatonin and 5: DSS+ Mel-CSNPs in **Figure 4.7 (E)**. The results of this study indicate that our nanoformulation lowers immune cell infiltration to the DSS-induced colon by two fold as compared to other anti-inflammatory drugs [46, 47]. Mel-CSNPs (MPO U/mg: 1.32) reduced MPO activity more than bare melatonin (MPO U/mg: 0.49), indicating an improvement in therapeutic efficiency via a nanotherapeutic method. Thus, MPO activity data demonstrated that our nano-formulation has anti-inflammatory effect. This claim has been confirmed by gene expression analysis of inflammatory genes.

4.1.11 qPCR analysis – gene expression study

There was a significant upsurge in gene expression of numerous inflammatory genes such as IL-1, IL-6, and NF- κ B in DSS induced mouse models of Ulcerative colitis were performed using colonic tissue [48, 49]. As a result, we examined the expression of IL-1 β , IL-6, and NF- κ B to corroborate the anti-inflammatory activity of our nanoformulation. As shown in **Figure 4.7(F)**, our nanoformulation significantly reduced the expression of inflammatory genes in response to DSS-induced insults. The results showed similar double fold declines when compared to previous reports that showed reductions in inflammatory markers as therapeutic action of anti-inflammatory drugs [24, 50]. There is a one-fold reduction in inflammatory indicators with Mel-CSNPs versus Melatonin against DSS induced expression, indicating an enhancement in therapeutic action due to nanoformulation versus bare melatonin.

4.1.12 Haematoxylin and Eosin staining

To assess protection against DSS-induced toxicological demarcation, colonic tissue sections were stained with Haematoxylin and Eosin (H&E). Microscopic pictures of colonic tissue sections from different treatment groups were stained with H&E, as shown in **Figure 4.8 (A)**. The control group had normal colonic tissue morphology, but the DSS group had total destruction to the colonic crypt and villi. Immune cell infiltration was shown to be greater in DSS-treated colonic tissue sections. The DSS + CSNPs exposed group did not show a reduction in immune cell infiltration, as shown in **Figure 4.8 (A)**, indicating a substantial difference between the bare Melatonin (Histological Score: 5.5) and Mel-CSNPs treated groups (Histological score: 3.1). Furthermore, the results are consistent with MPO activity, confirming that the nanoformulation has better anti-inflammatory action over bare Melatonin in the treatment of DSS-induced IBD. The gross pathological in-vivo therapeutic evaluation presented in **Figure 4.7** shows that Mel-CSNPs improved the anti-inflammatory therapeutic efficacy of melatonin. Additionally, histological examination performed H&E study highly corroborated and validated these findings. The histopathological study indicated noteworthy inflammatory pathological changes in a cross-section of colon, such as epithelial layer erosion, fibrotic changes, immune cell infiltration, goblet cell destruction, and so on, which were greatly reduced in Mel-CSNPs, implying therapeutic efficiency.

4.1.13 Alcian Blue and Nuclear Fast Red staining

Alcian blue staining was used to assess goblet cell loss and damage in mice during DSS-induced inflammatory conditions. In **Figure 4.8 (B)**, the control group had a normal amount of goblet cells (blue colour) in the crypt of colonic tissue sections. In DSS and DSS + CSNPs therapy groups, there is a significant decrease in goblets cell number per crypt, indicating the amount of severity and damage during inflammatory circumstances. Crypt destruction occurs in mice as a result of DSS-induced epithelial injury, which leads to the depletion of goblet cells, which are crucial for maintaining gut homeostasis and protecting the epithelial layer from pathogenic assaults by secreting mucin, a sticky protective material. In comparison to the DSS + Melatonin treated group, DSS + Mel-CSNPs showed improved protection of immune cell infiltration and little damage to the colonic crypt.

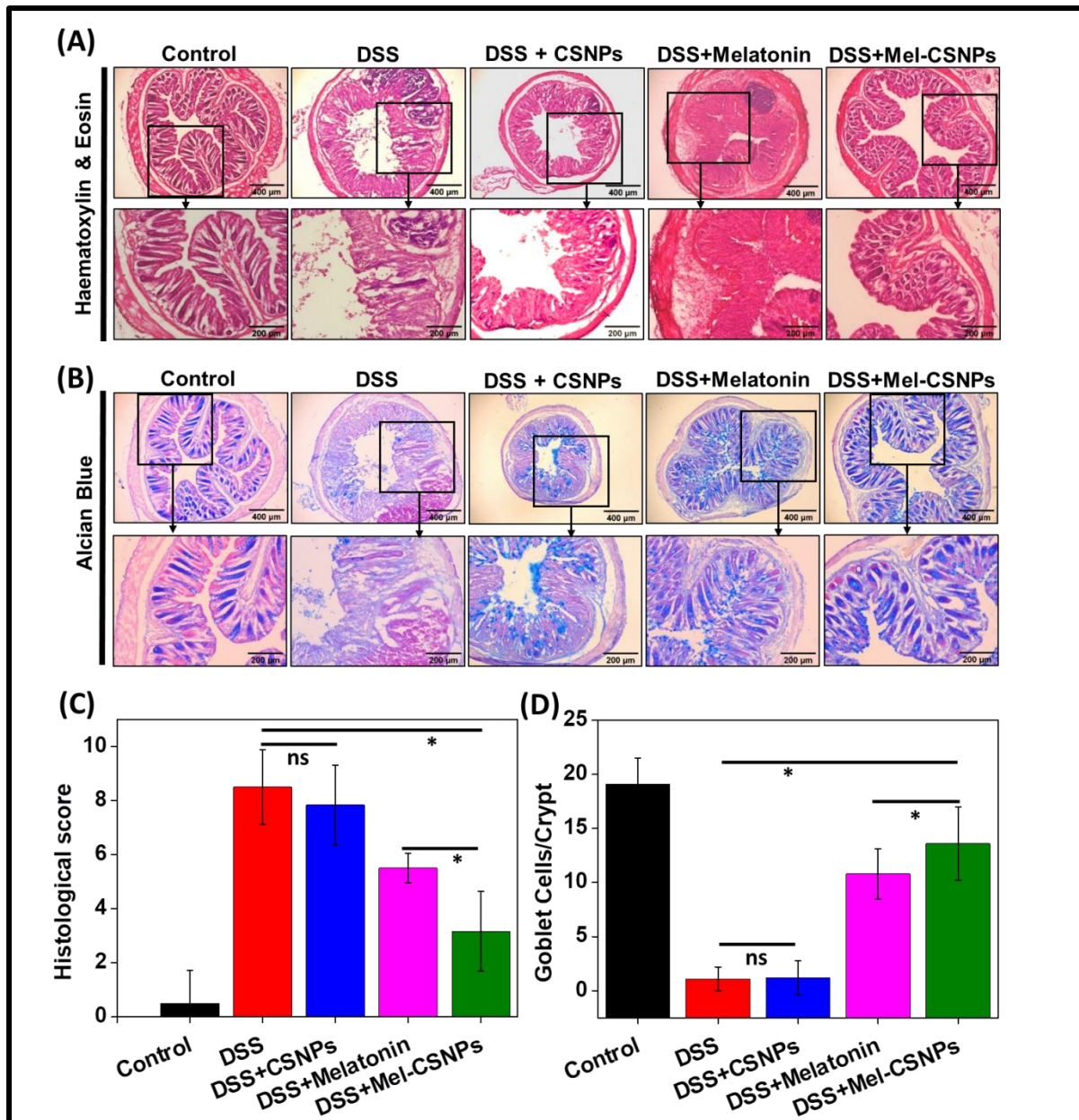


Figure 4.8: (A) - Haematoxylin and Eosin (H&E) staining of cross section of colon (7µm) indicates pathological demarcation. (B)- Alcian Blue and Nuclear Fast Red (AB-NR) staining of cross section of colon (7µm) for evaluating goblet cells (Blue) and epithelial cells (Red) (C) Histological score for H&E stained cross section of colon. (D) Goblet cell(s) count per crypt in cross section of colon. (* $p \leq 0.05$, ** $p \leq 0.001$, *** $p \leq 0.0001$ and ns: non-significant)

Goblet cells were detected in substantial numbers in colonic tissue sections from the DSS + Melatonin (10.8 goblet cell/crypt) and DSS + Mel-CSNP groups (13.6 goblet cell/crypt). This result also indicates Mel-CSNPs' superior therapeutic efficacy when compared to melatonin alone. Our findings imply that bare melatonin and Mel-CSNPs provide protection against DSS-induced epithelium damage, resulting in goblet cell depletion and crypt destruction,

which is consistent with previous research [51]. Furthermore, the current work adds that nanoformulations of melatonin greatly strengthen therapeutic potential, as illustrated in **Figure 4.8 (C) and (D)**.

4.1.14 Nitric Oxide Synthase 2 (NOS2) and Nitro-tyrosine

To confirm the mechanism of nanoformulation as an anti-inflammatory drug, immunohistochemical (IHC) examination was done. As a result, IHC analysis revealed that inflammatory biomarkers such as NOS2 and Nitro-tyrosine were up-regulated in DSS-induced inflammation in mice, as shown in **Figure 4.9. (A)**. NOS2 is an inflammatory biomarker associated with increased infiltrating inflammatory M1 macrophages in DSS-induced colitis [52]. As shown in **Figure 4.9(A)**, the DSS + Mel-CSNPs treated group had significantly lower NOS2 expression than the bare Melatonin treated group. The fluorescence intensity is quantified and found to be significantly lower in **Figure 4.9 (B)** of DSS+ Mel-CSNPs treated (fluorescence intensity=1.03) compared to the bare DSS+Melatonin treated (fluorescence intensity=1.51) group, indicating that the therapeutic potential of nanoformulations has improved. In murine ulcerative colitis models melatonin has exhibited ability to lower NOS2 expression [53]. We investigated the enhancement in anti-inflammatory activity of melatonin loaded nanoformulation, which resulted in improved melatonin therapeutic efficacy.

Melatonin can also influence host response by down regulating the innate immune system, resulting in a reduction in the inflammatory process [51]. Because macrophages are an important component of the innate immune response, melatonin reduces macrophage expression, resulting in anti-inflammatory effects. Melatonin's inhibition of NOS2 is connected to its effect on NF-kB expression [52]. We evaluated nuclear translocation of NF-kB, which is suppressed by melatonin, and melatonin loaded nanoformulations, which resulted in lower expression of NOS2 in colonic tissue. Melatonin-loaded nanoformulation exhibited a substantial reduction in NOS2 expression, resulting in increased therapeutic efficacy. Increased NOS2 expression results in higher nitrite radical generation, which aids in the generation of increased oxidative stress. These results in amplified level oxidative stress which causes uncontrolled inflammation and thereby causing pathological injury to colonic

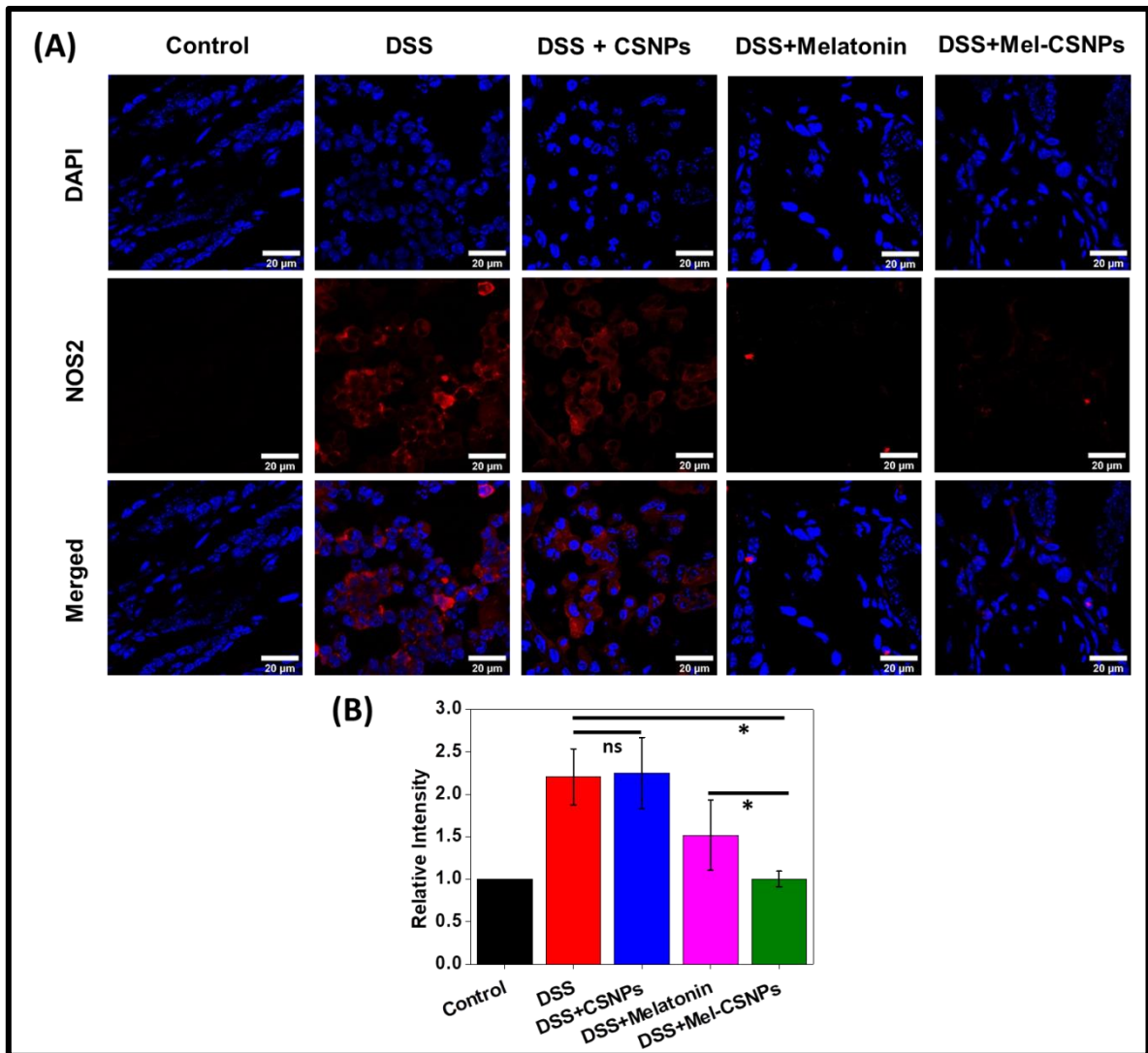


Figure 4.9: (A) Immuno-histochemical staining of Nitric Oxide synthase 2 (NOS2) indicates M1 macrophage infiltration due to inflammation (B) Quantification of the fluorescence intensity. (* $p \leq 0.05$, ** $p \leq 0.001$ and *** $p \leq 0.0001$)

tissue in mice as shown in histopathological analysis study in **Figure 4.8** where H&E staining done on DSS challenged mice results in increased pathological score compared to control where no damage is observed. Even when tested with DSS, melatonin and Mel-CSNPs dramatically improved pathology score.

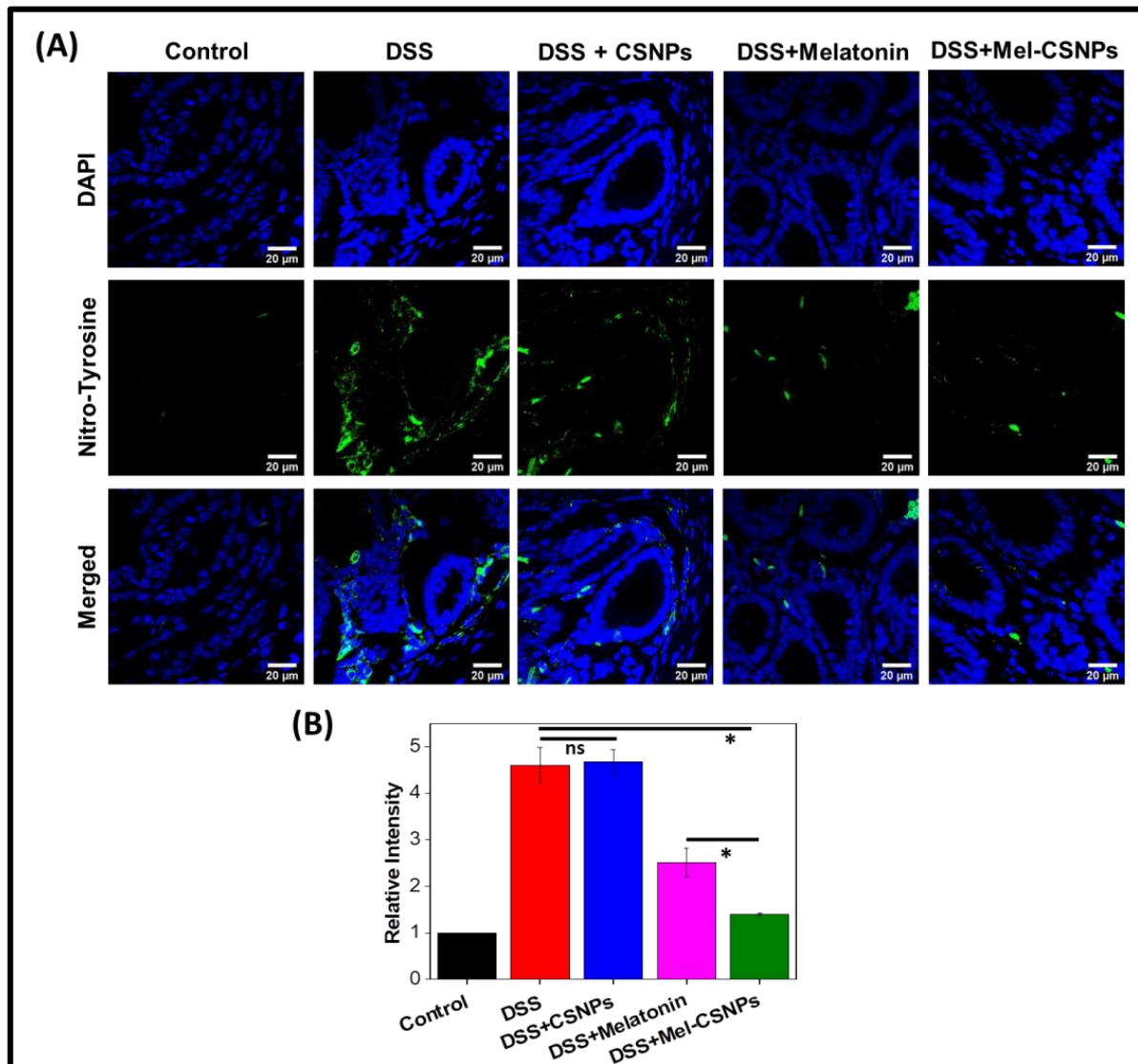


Figure 4.10: (A) Immuno-histochemical stained CLSM images for Nitro-tyrosine represents inflammatory condition (B) Quantification of the fluorescence intensity. (* $p \leq 0.05$, ** $p \leq 0.001$ and *** $p \leq 0.0001$)

Furthermore, immunohistochemical examination of Nitro-tyrosine was done to assess the degree of peroxynitrite-mediated protein nitrosylation that occurred in mice during DSS-induced colitis. Nitro-tyrosine expression was significantly increased in DSS-induced colitis

animals [54]. Tyrosine nitration occurs in biological systems as a result of oxidative damage or stress triggered by harmful conditions [55].

In **Figure 4.10 (A)**, a greater reduction in fluorescence intensity of nitro-tyrosine expression verifies our nanoformulations' superior therapeutic efficacy over bare Melatonin by reversing the DSS-induced pathological markers. As shown in **Figure 4.10 (B)**, the quantification of fluorescence intensity is evaluated for a comparative study of the efficacy of bare Melatonin treated (fluorescence intensity =2.51) group and nanoformulations treated (fluorescence intensity =1.41) group, which clearly indicates a significant reduction in expression of nitrosylation status in colonic tissue cross section, resulting in an improvement in Melatonin therapeutic efficacy.

Our results are in agreement with earlier studies accomplished using melatonin against inflammatory pathological condition [56]. Generally, Mel-CSNPs have demonstrated tremendous anti-inflammatory and therapeutic potential, as evidenced by numerous in-vivo therapeutic assessments. The fact that Mel-CSNPs outperform bare melatonin in terms of therapeutic efficacy demonstrates that they have anti-inflammatory activity in the prevention of IBD.

4.2 Conclusions

Mel-CSNPs significantly improve anti-inflammatory action both *in vitro* and *in vivo* when compared to bare melatonin, according to the results of a study. The reduction of NF-kB nuclear translocation and nitric oxide verifies Mel-CSNPs' anti-inflammatory potential in an in-vitro LPS-induced IBD model. The remarkable reduction in disease activity index (DAI) and Myeloperoxidase (MPO) activity demonstrates the in-vivo therapeutic efficacy of our nanoformulation by lowering immune cell infiltration to the disease site. Our nanoformulation's efficacy is revealed by the downregulation of IL-1 β , IL-6, NFkB gene markers, and NOS2, Nitro-tyrosine inflammatory hallmark molecules. Thus, the thorough examination of the in-vitro and in-vivo studies shows strong evidence for improved anti-inflammatory efficacy with the use of nanotherapeutic approach in IBD treatment as compared to bare melatonin.

Note:

*The following published works was included into the current thesis with the authors, corresponding author's, and publisher's permission. The following works is associated with this chapter:

1) Soni, J.M., et al., *Melatonin-loaded chitosan nanoparticles endows nitric oxide synthase 2 mediated anti-inflammatory activity in inflammatory bowel disease model*. Mater Sci Eng C Mater Biol Appl, 2021. **124**: p. 112038.

4.3 References

- [1] R.J. Xavier, D.K. Podolsky, *Nature*, 448 (2007) 427-434.
- [2] D.C. Baumgart, W.J. Sandborn, *Lancet*, 369 (2007) 1641-1657.
- [3] B.A. Hendrickson, R. Gokhale, J.H. Cho, *Clinical Microbiology Reviews*, 15 (2002) 79.
- [4] P.D. Castro, G. Harkin, M. Hussey, B. Christopher, C. Kiat, J.L. Chin, V. Trimble, D. McNamara, P. MacMathuna, B. Egan, B. Ryan, D. Kevans, M. Abuzakouk, R. Farrell, C. Feighery, V. Byrnes, N. Mahmud, R. McManus, *United European Gastroenterol J*, 8 (2020) 148-156.
- [5] G.B.D.I.B.D. Collaborators, *Lancet Gastroenterol Hepatol*, 5 (2020) 17-30.
- [6] M.A. Raad, N.H. Chams, A.I. Sharara, *Inflamm Intest Dis*, 1 (2016) 85-95.
- [7] A. Kumar, M. Auron, A. Aneja, F. Mohr, A. Jain, B. Shen, *Mayo Clin Proc*, 86 (2011) 748-757.
- [8] G. Negi, A. Kumar, S.S. Sharma, *Journal of Pineal Research*, 50 (2011) 124-131.
- [9] G. Negi, A. Kumar, R.K. Kaundal, A. Gulati, S.S. Sharma, *Neuropharmacology*, 58 (2010) 585-592.
- [10] J.R. Friedman, J. Nunnari, *Nature*, 505 (2014) 335-343.
- [11] V. Dehousse, N. Garbacki, A. Colige, B. Evrard, *Biomaterials*, 31 (2010) 1839-1849.
- [12] U. Garg, S. Chauhan, U. Nagaich, N. Jain, *Adv Pharm Bull*, 9 (2019) 195-204.
- [13] S. Kumar Yadav, A. Kumar Srivastava, A. Dev, B. Kaundal, S. Roy Choudhury, S. Karmakar, *Nanotechnology*, 28 (2017) 365102.
- [14] J.J. Kim, M.S. Shajib, M.M. Manocha, W.I. Khan, *J Vis Exp*, (2012) 3678.
- [15] P. Calvo, C. Remuñan-López, J.L. Vila-Jato, M.J. Alonso, *Pharmaceutical Research*, 14 (1997) 1431-1436.
- [16] M. Sun, Z. Deng, F. Shi, Z. Zhou, C. Jiang, Z. Xu, X. Cui, W. Li, Y. Jing, B. Han, W. Zhang, S. Xia, *Biomaterials Science*, 8 (2020) 912-925.
- [17] P. Calvo, C. Remunan-Lopez, J.L. Vila-Jato, M.J.J.o.A.P.S. Alonso, 63 (1997) 125-132.
- [18] L.Q. Jiang, T.Y. Wang, T.J. Webster, H.-J. Duan, J.Y. Qiu, Z.M. Zhao, X.X. Yin, C.L. Zheng, *Int J Nanomedicine*, 12 (2017) 6383-6398.
- [19] S. Mao, J. Chen, Z. Wei, H. Liu, D. Bi, *International Journal of Pharmaceutics*, 272 (2004) 37-43.

- [20] J. Benevides Bahiense, F.M. Marques, M.M. Figureueira, T.S. Vargas, T.P. Kondratyuk, D.C. Endringer, R. Scherer, M. Fronza, *Pharm Biol*, 55 (2017) 991-997.
- [21] A.V. Bagaev, A.Y. Garaeva, E.S. Lebedeva, A.V. Pichugin, R.I. Ataulakhanov, F.I. Ataulakhanov, *Scientific reports*, 2019, pp. 4563.
- [22] A. Dev, S.J. Mohanbhai, A.C. Kushwaha, A. Sood, M.N. Sardoiwala, S.R. Choudhury, S. Karmakar, *Acta Biomaterialia*, 109 (2020) 121-131.
- [23] L.A. Dieleman, A.S. Peña, S.G. Meuwissen, E.P. van Rees, *Scandinavian journal of gastroenterology. Supplement*, 223 (1997) 99-104.
- [24] A.M. Abdelmegid, F.K. Abdo, F.E. Ahmed, A.A.A. Kattaia, *Scientific Reports*, 9 (2019) 10176.
- [25] A. Arbab, G. Yocum, M. Rad, A. Khakoo, V. Fellowes, E. Read, J. Frank, *NMR in biomedicine*, 18 (2005) 553-559.
- [26] X. Wang, X. Kong, Y. Qin, X. Zhu, W. Liu, J. Han, *Food Funct*, 10 (2019) 4608-4619.
- [27] M. Shokrzadeh, N. Ghassemi-Barghi, *Pharmacology*, 102 (2018) 74-80.
- [28] M. Queiroz, K. Melo, D. Sabry, G. Sasaki, H. Rocha, *Marine drugs*, 13 (2014) 141-158.
- [29] B. Topal, D. Cetin Altindal, M. Gümüşderelioğlu, *International Journal of Pharmaceutics*, 496 (2015).
- [30] F. Noori Siahdasht, N. Farhadian, M. Karimi, L. Hafizi, *RSC Advances*, 10 (2020) 9462-9475.
- [31] M. Ali, M. Aboelfadl, A. Seliem, H. Khalil, G. Elkady, *Separation Science and Technology*, (2018).
- [32] A. Hafner, J. Lovrić, I. Pepić, J. Filipovic-Grcic, *Journal of microencapsulation*, 28 (2011) 807-815.
- [33] T. Joo, K. Sowndhararajan, S. Hong, J. Lee, S.-Y. Park, S. Kim, J.-W. Jhoo, *Saudi J Biol Sci*, 21 (2014) 427-435.
- [34] C. Phiphatwatcharaded, A. Topark-Ngarm, P. Puthongking, P. Mahakunakorn, *Drug Dev Res*, 75 (2014) 235-245.
- [35] R. Moreno, J.-M. Sobotzik, C. Schultz, M.L. Schmitz, *Nucleic Acids Res*, 38 (2010) 6029-6044.
- [36] O. Sharif, V.N. Bolshakov, S. Raines, P. Newham, N.D. Perkins, *BMC Immunology*, 8 (2007) 1.

- [37] S. Ikeguchi, Y. Izumi, N. Kitamura, S. Kishino, J. Ogawa, A. Akaike, T. Kume, *Journal of Pharmacological Sciences*, 138 (2018).
- [38] A. Grodzki, B. Poola, N. Pasupuleti, M. Nantz, P. Lein, F. Gorin, *The Journal of pharmacology and experimental therapeutics*, 352 (2014).
- [39] R. Nadesh, D. Narayanan, R.S. P, S. Vadakumpully, U. Mony, M. Koyakkutty, S.V. Nair, D. Menon, *J Biomed Mater Res A*, 101 (2013) 2957-2966.
- [40] M.N. Sardoiwala, A.K. Srivastava, B. Kaundal, S. Karmakar, S.R. Choudhury, *Nanomedicine*, 24 (2019) 102088.
- [41] M.N. Sardoiwala, A.C. Kushwaha, A. Dev, N. Shrimali, P. Guchhait, S. Karmakar, S. Roy Choudhury, *ACS Biomaterials Science & Engineering*, 6 (2020) 3139-3153.
- [42] C.-Q. Chen, J. Fichna, M. Bashashati, Y.-Y. Li, M. Storr, *World J Gastroenterol*, 17 (2011) 3888-3898.
- [43] C.C. Bain, A. Schridde, 9 (2018).
- [44] V.G. Kokich, *American Journal of Orthodontics and Dentofacial Orthopedics*, 143 (2013) S11.
- [45] J.E. Krawisz, P. Sharon, W.F. Stenson, *Gastroenterology*, 87 (1984) 1344-1350.
- [46] M. Davaatseren, J.-T. Hwang, J. Park, M.-S. Kim, S. Wang, M. Sung, *Mediators of inflammation*, 2013 (2013) 982383.
- [47] T. Bui Thanh, H. Thanh, H. Le Thi Thu, D. Huong, *Merit Research Journal of Medicine and Medical Sciences*, 2 (2014) 216-224.
- [48] M. Perše, A. Cerar, *J Biomed Biotechnol*, 2012 (2012) 718617-718617.
- [49] R.M. Gadaleta, K.J. van Erpecum, B. Oldenburg, E.C.L. Willemsen, W. Renooij, S. Murzilli, L.W.J. Klomp, P.D. Siersema, M.E.I. Schipper, S. Danese, G. Penna, G. Laverny, L. Adorini, A. Moschetta, S.W.C.v. Mil, *Gut*, 60 (2011) 463.
- [50] J. Däbritz, L. Judd, H. Chalinor, T. Menheniott, A. Giraud, *Scientific Reports*, 6 (2016) 20584.
- [51] S.W. Kim, S. Kim, M. Son, J.H. Cheon, Y.S. Park, *Scientific Reports*, 10 (2020) 2232.
- [52] G. Kolios, V. Valatas, S.G. Ward, *Immunology*, 113 (2004) 427-437.
- [53] G. Negi, A. Kumar, S.S. Sharma, *J Pineal Res*, 50 (2011) 124-131.
- [54] D.N. Seril, J. Liao, G.Y. Yang, *Mol Carcinog*, 46 (2007) 341-353.
- [55] J.S. Beckman, *Chem Res Toxicol*, 9 (1996) 836-844.

[56] S. Cuzzocrea, E. Mazzon, I. Serraino, V. Lepore, M.L. Terranova, A. Ciccolo, A.P. Caputi, J Pineal Res, 30 (2001) 1-12.

Chapter 5:

Colon targeted chitosan-melatonin nanotherapy for preclinical Inflammatory Bowel Disease

5.0 Background

Inflammatory Bowel Disease (IBD) is a broad term that encompasses two pathological conditions: Ulcerative Colitis (UC) and Crohn's Disease (CD). The precise cause of this condition is unknown. UC is characterised by inflammation that results in ulcers in the colonic and rectum regions of the gastrointestinal system (GIT) [1]. In UC, inflammation develops and primarily destroys the mucosal layer, resulting in superficial damage to the gut surface. UC is also characterized by severe diarrhoea with blood. Inflammation in CD is characterised by patchy lesions that can appear anywhere in the GIT [2]. Transmural inflammation causes fibrosis, stricture, and fistula throughout the GIT in CD.

5-aminosalicylates, immunosuppressants, and antibiotics are among the medications used to treat UC, and they can provide symptomatic relief [3]. Until the discovery of corticosteroids in 1955, moderate to severe UC had a devastating effect on the patient's health, with mortality rates of more than 50% [4]. Nonetheless management with the corticosteroid for longer period give rise to secondary infections [5], osteoporosis [6], depression, type 2 diabetes mellitus [7] and cataract [8]. As a result, novel treatments that can induce remission and prevent illness relapse are urgently needed. Melatonin (N-acetyl-methoxytryptamine) is a neurohormone produced by the pineal gland and excreted during the night [9] possessing pleiotropic effects that can be employed as an anti-inflammatory, antioxidant, anti-aging, and neuroprotectant in addition to maintaining circadian rhythm [10]. Melatonin's chemical structure includes an indole ring and an amide group, which can be deprotonated to get acidity constant values (pKa). Melatonin's pKa values in totally secure aqueous mediums were discovered to be 5.777 0.011 and 10.201 0.024 [11]. Precursor of melatonin is tryptophan which is converted to 5-hydroxy tryptophan by enzyme tryptophanhydroxylase. Serotonin is synthesized from 5-hydroxytryptophan by decarboxylation using enzyme decarboxylase. N-acetyl transferase converts serotonin to N-acetyl serotonin. Finally this N-acetyl serotonin is converted melatonin by hydroxyindole-O-methyltra Precursor of melatonin is tryptophan which is converted to 5-hydroxy tryptophan by enzyme tryptophanhydroxylase. Serotonin is synthesized from 5-hydroxytryptophan by decarboxylation using enzyme decarboxylase. N-acetyl transferase converts serotonin to N-acetyl serotonin. Finally this N-acetyl serotonin is converted melatonin by hydroxyindole-O-methyltransferase (HIOMT) [12]. Inflammation is caused by a cascade of inflammatory gene overexpression. Nuclear transcription factor-kappa B (NF-kB) has been shown to over-express in inflammatory responses. NF-kB reaches the nucleus and activates other

inflammatory genes [12]. Melatonin suppresses NF- κ B nuclear translocation, which lowers NF- κ B DNA binding and so inhibits the inflammatory process [13]. Melatonin has immunosuppressive effect via influencing the Th17 subgroup of T-helper cells, which is important in the pathophysiology of autoimmune disorders [14].

Melatonin's pharmacokinetic parameters are poor, forcing frequent dosages to maintain consistent plasma concentration in the body. Melatonin's plasma half-life ($T_{1/2}$) in experimental animals ranges from 18 to 35 minutes [15, 16]. Melatonin's oral bioavailability is also poor, limiting its use as a therapeutic agent [17].

As a result, targeted drug delivery systems come into play to target and maintain prolonged drug release, reducing dose intervals and maximizing melatonin therapeutic efficacy. Because of their physicochemical features, polymeric nanoparticles are commonly used in the synthesis of targeted nano-drug delivery systems to overcome the limitations of active pharmacological agents [18]. Carbohydrate polymers such as chitosan, chitin, starch, and others have been widely used in the production of nanocarriers for drug delivery applications [19]. Nanotechnology offers customized and site-specific drug delivery systems, which improve a medicine's therapeutic potential while minimizing any unwanted effects connected with it through dose reduction and site-specific release [20]. Chitosan is the most appropriate option for use as a nanocarrier system because to its high biocompatibility, and it is also permitted as a food dietary ingredient by the US FDA [21]. Chitosan can improve permeation by opening epithelial tight junctions. In acidic pH, the main amine group interacts with negatively charged mucin but fails when pH is raised above its pKa, limiting its mucoadhesive function. Due to this mucoadhesive nature, it tends to adhere in the upper GIT and cannot access the distal location where Ulcerative Colitis originates. Traditional chitosan nanoparticles' targeting efficacy is hampered when given orally for particular delivery to the colon due to their mucoadhesive characteristic and tendency to remain in the upper GIT [22]. To address this drawback of chitosan nanoparticles, a pH-dependent drug delivery method was developed in which the nanoparticles are coated or synthesized from pH-sensitive. The pH-sensitive methacrylic acid copolymers are frequently employed for oral drug administration to distal areas of the gut [23]. When coated with the colon-specific polymer Eudragit-S-100, nanoparticles enable effective sustained release and directed delivery of medication at the desired region of inflammation, preventing premature release, which results in superior drug activity [24].

In this study, we developed, characterized, and assessed the therapeutic efficacy of colon-targeted chitosan nanoparticles for drug delivery to the specific colon region to treat UC in mice. Chitosan nanoparticles and colon-targeted nanoparticles have exhibited remarkable anti-inflammatory activity against LPS-stimulated macrophages. Furthermore, colon-targeted nanoparticles provided greater protection in an *in-vivo* DSS-induced UC mouse model. Colon-targeted nanoparticles provide improved protection against body weight loss, colon shortening, and disease activity index. In addition, colon-targeted nanoparticles inhibited myeloperoxidase activity more effectively. Furthermore, histopathological findings suggest that colon targeted nanoparticles augment therapy efficacy. Whenever given orally to mice, colon-targeted nanoparticles greatly improve the *in-vivo* therapeutic potential of melatonin compared to basic chitosan nanoparticles.

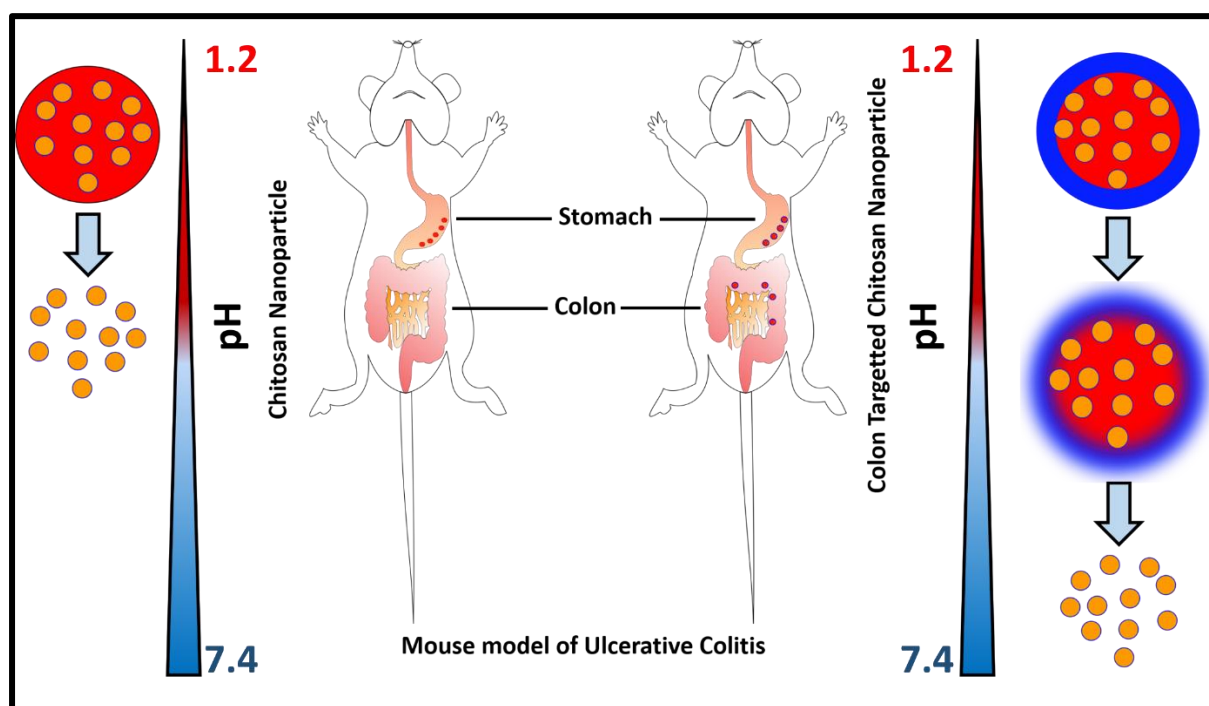


Figure 5.1: Scheme elucidates better targeting potential of Eudragit-S-100 coated colon targeted chitosan of nanoparticles. (red= CSNP, blue- Eudragit coat and orange-melatonin)

5.1.0 Results and Discussion

5.1.1 Size and morphological examination of nanoparticles

Mean hydrodynamic size of chitosan nanoparticles synthesized by ionotropic gelation was 255.2 nm, with a Polydispersity Index (PDI) of 0.22 ± 0.06 measured by dynamic light scattering (**Figure 5.2C**). Similarly, Eudragit-S-100 coated chitosan nanoparticles showed an increase in mean hydrodynamic size due to the creation of a coating of pH-sensitive polymer

used for colon targeting. Eudragit-S-100 coated chitosan nanoparticles have size of 342 nm and a PDI of 0.36 ± 0.08 . (**Figure 5.2C**). Increase in mean hydrodynamic size clearly shows the surface change caused by the Eudragit-S-100 coating on the surface of the chitosan nanoparticles. Chitosan nanoparticles have limitations for oral administration to the distal region of the colon, as depicted in the bio-distribution study in **Figure 5.7**. Chitosan nanoparticles aggregate in the stomach, limiting its use as a nanocarrier for treating Ulcerative Colitis via the oral route. The mucoadhesive nature of chitosan nanoparticles (CSNPs) is desirable for their use in drug delivery via the oral route, which leads to increased absorption and reduced dose frequency [25]. Protonated amino groups in CSNPs can react with epithelial cells and disrupt tight junctions between cells, enhancing drug transport [26]. Chitosan has considerable mucoadhesive activity at low pH and a low mucoadhesive value at high pH, indicating that it accumulates in the upper GIT. To circumvent this limitation of chitosan nanoparticles, several surface modifications are used. Eudragit-S-100 and other enteric soluble polymers do not dissolve in acidic pH and can aid in drug delivery to distant targeted GIT locations. Chitosan nanoparticles coated with Eudragit-S-100 have been designed to deliver drugs to colon areas for targeted delivery [27, 28]. Furthermore, to verify the coating, we conducted Transmission Electron microscopy imaging of nanoparticles, which presented a strong coating of pH-sensitive polymer, Eudragit-S-100 on the surface of chitosan nanoparticles, causing an increase in size (87 nm) of chitosan nanoparticles (**Figure 5.2D-E**), whereas simple chitosan nanoparticles do not have any coating on the surface, as shown in TEM images TEM pictures support the coating on chitosan nanoparticles.

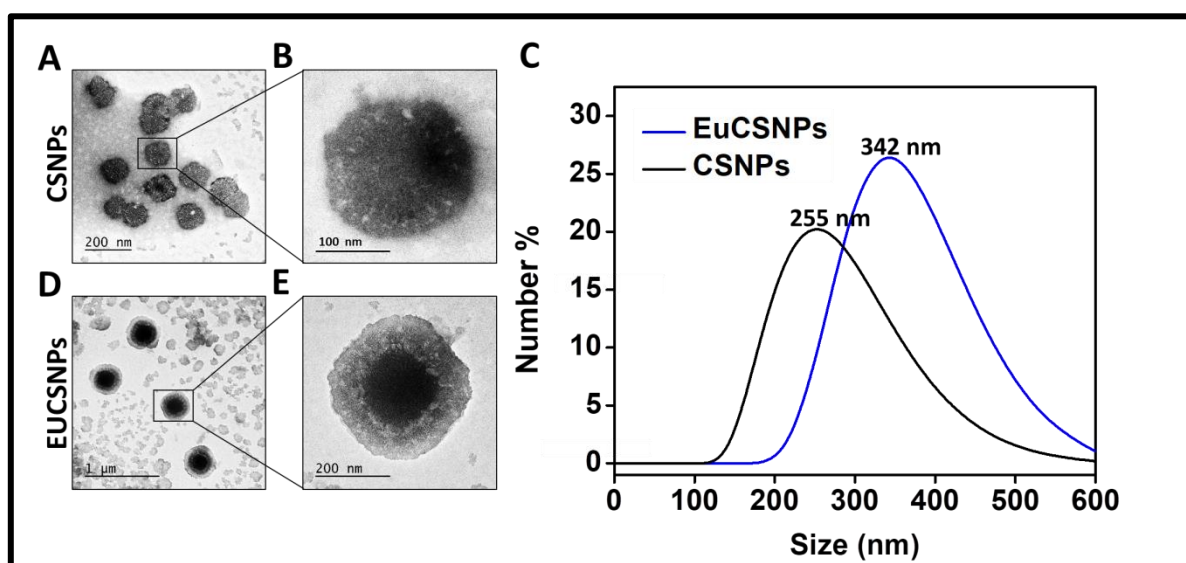


Figure 5.2: Size and morphology analysis: (A-B) Transmission Electron Micrograph of Chitosan nanoparticles (CSNP) (D-E) Eudragit-S-100 coated Chitosan nanoparticle (EU-CSNPs) (C) Mean hydrodynamic size of Chitosan nanoparticles (CSNPs) and) Eudragit-S-100 coated Chitosan nanoparticle (Eu-CSNPs).

5.1.2 Fourier transform infrared spectroscopy (FT-IR)

FTIR investigation demonstrates a characteristic peak of hydroxyl (-OH) group at 3342 cm^{-1} and free amino group (-NH₂) at C2 position in glucosamine at 1018 cm^{-1} representing -C-O-C- bridge, which validates chitosan, as previously reported [29]. In **Figure 5.3**, chitosan nanoparticles showed a broad hydroxyl (-OH) peak at 3342 cm^{-1} , while Mel-CSNPs showed a comparable broad -OH peak. The narrowing of the OH transmittance peak in CSNPs and Mel-CSNPs relative to bare chitosan suggests involvement in nanoparticle production. Melatonin had transmittance peaks at 3269 cm^{-1} and 3315 cm^{-1} , which corresponded to the amine vibration peak found in melatonin. Melatonin also showed bending vibration of amines at 1552 cm^{-1} and 1623 cm^{-1} . Melatonin is confirmed by the observed peaks matching with previously reported FTIR transmittance studies [30]. The OH peak at 2948 cm^{-1} of carboxylic acid in Eudragit-S-100 matched the peak disclosed in an earlier research [31]. EU-CSNPs and Mel-EUCSNPs exhibited a carboxylic acid -OH peak at 2848 cm^{-1} . At 1712 cm^{-1} , a moderate narrow transmittance peak of C=O stretching is found in Eudragit-S-100 [32] which is not observed upon its coating on CSNPs. Mel-CSNPs and CSNPs exhibited broad OH peaks between 3200 and 3400 cm^{-1} . Transmittance peaks at 1537 cm^{-1} were observed in CSNPs and Mel-CSNPs, indicating amide band 1 of chitosan. According to the FTIR measurement, the production of chitosan nanoparticles induces a decrease in the strength of the OH peak detected at 3342 cm^{-1} , implying its function in nanoparticle formation. Furthermore, when chitosan nanoparticles were coated with Eudragit-S-100, the C=O peak at 1712 cm^{-1} was observed, indicating that this bond is involved in the development of coating layers on CSNPs. The drop in intensity of the carboxyl group of Eudragit S-100 at 1712 cm^{-1} suggests a reduction in the number of carboxyl groups involved in the production of the amide bond, N-H stretch peak at 3683 cm^{-1} . According to the FTIR study, the reduced peak intensity at 1700 cm^{-1} could be due to the interaction of chitosan and Eudragit S-100, which contrasts with previous findings that demonstrate a similar decreasing intensity of the peak which indicates the chitosan and Eudragit S-100 interaction [31, 33].

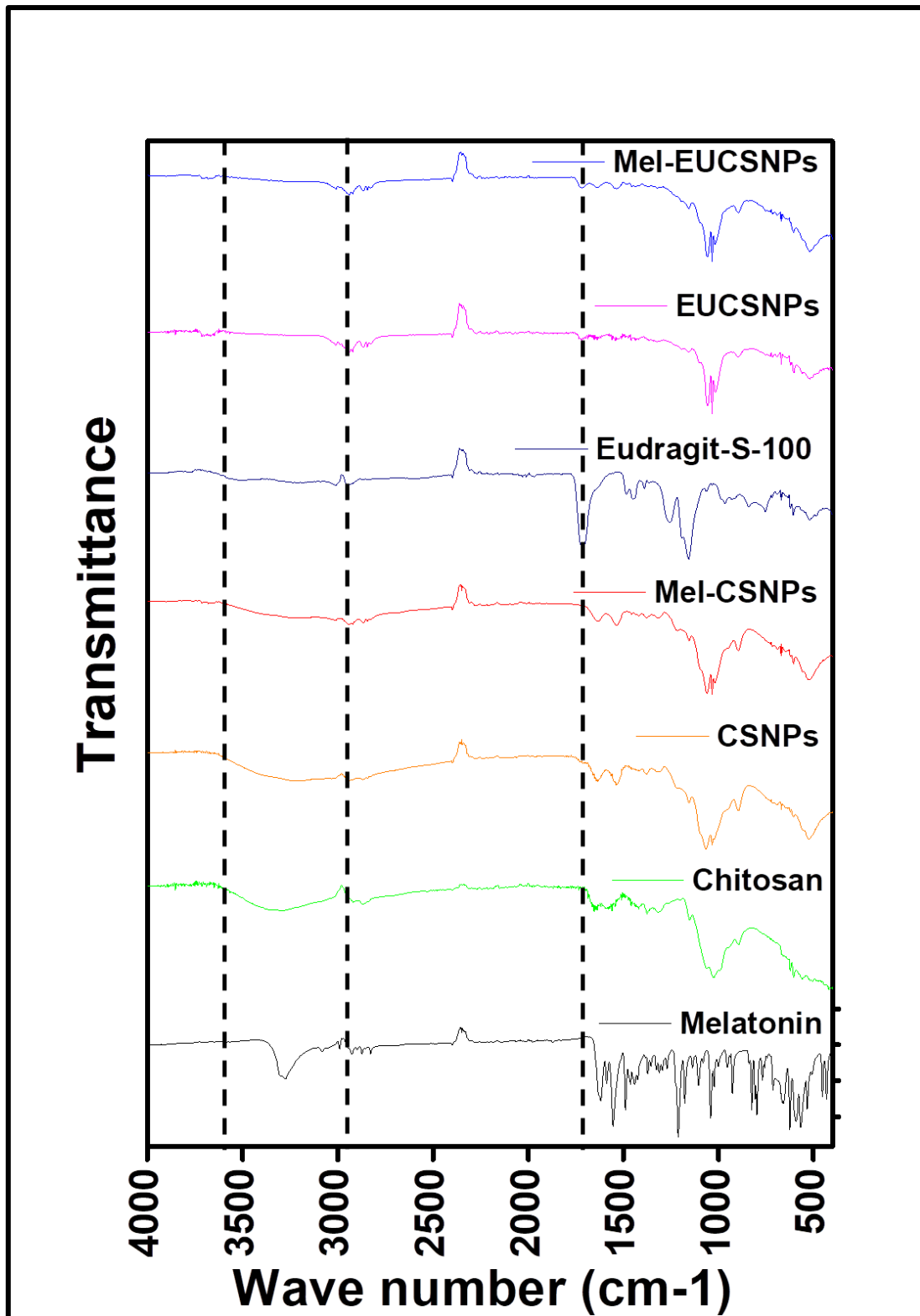


Figure 5.3: Functional group interaction analysis: Fourier transform infrared (FT-IR) analysis of Melatonin, Chitosan, CSNPs, Mel-CSNPs, Eudragit-S-100, EuCSNPs, Mel-Eu-CSNPs.

5.1.3 Drug loading and *In-vitro* drug release study:

Drug loading of Mel-CSNPs was found to 18.9 % w/w at ratios of drug to polymer (1:2) and Mel-EUCSNPs was observed to be 10.8 % w/w assessed by taking absorbance of melatonin

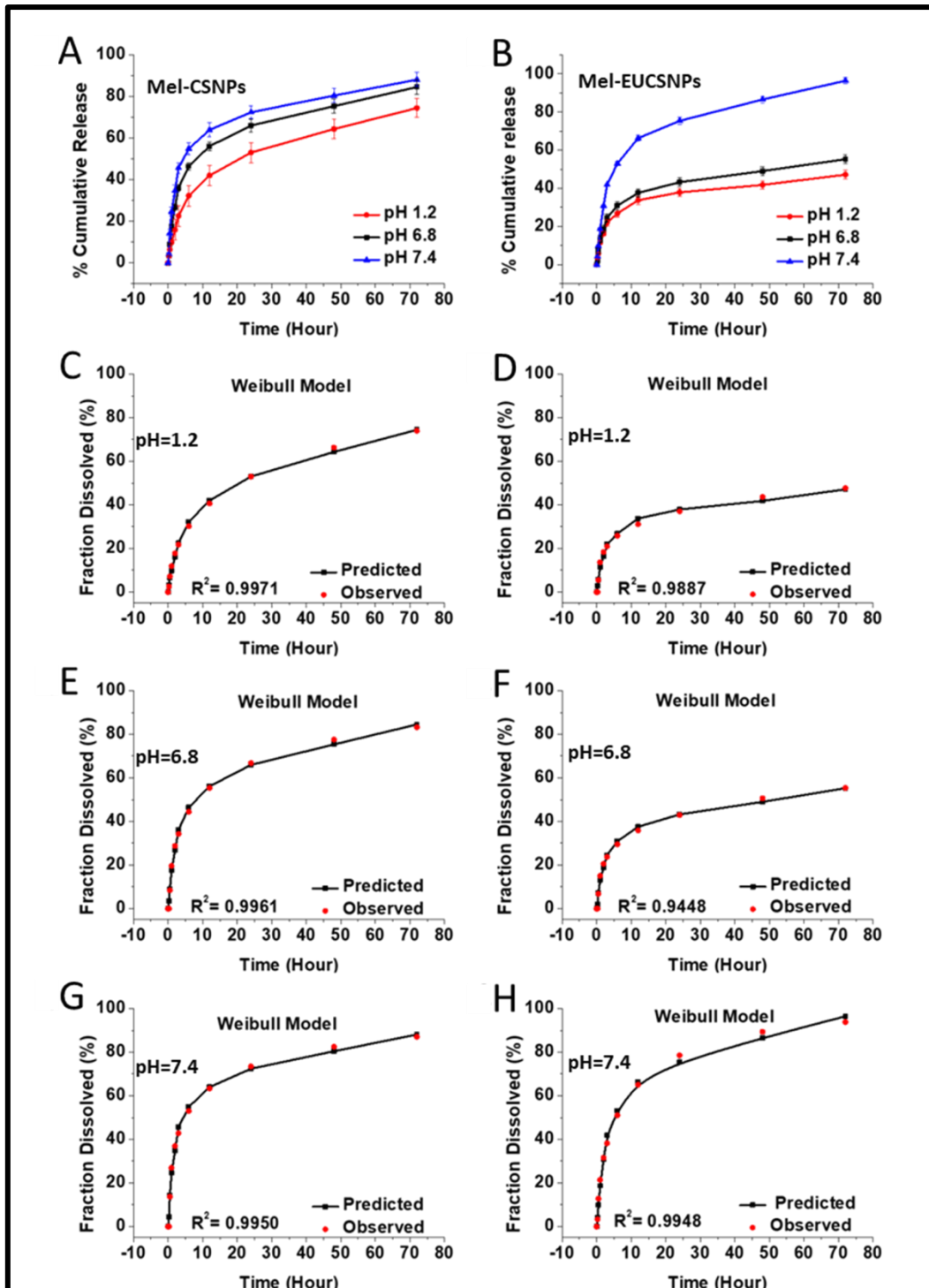


Figure 5.4: *In vitro* drug release (4A) pH dependent release of Melatonin from Chitosan nanoparticle (Mel-CSNPs) (4) pH dependent release of Melatonin from Eudragit-S-100

coated Chitosan nanoparticle (Mel-EUCSNPs) (C, E, G) Best fitted Weibull mathematical model for dissolution of Mel-CSNPs at pH 1.2, 6.8, and 7.4 (D, F, H) Best fitted Weibull mathematical model for dissolution of Mel-EUCSNPs at pH 1.2, 6.8, and 7.4.

at 278 nm. Targeted nano-drug delivery system enables regulated and site-specific drug release from nanoparticles, making them more efficient and appropriate for the treatment of Ulcerative Colitis than conventional drug delivery methods. The anti-inflammatory efficacy of melatonin-loaded conventional chitosan nanoparticles is limited by rapid and premature release (Mel-CSNPs). The drug was released *in vitro* from melatonin-loaded chitosan nanoparticles (Mel-CSNPs) and melatonin-loaded Eudragit-S-100coated chitosan nanoparticles (Mel-EUCSNPs) at pH 1.2, 6.8, and 7.4 to replicate the fluctuations that occur during nanoparticle passage through the gastrointestinal tract (GIT) [27, 34]. A pH-dependent drug release study would allow us to evaluate its performance in delivering pharmaceuticals to the targeted colonic site based on changes in GIT pH and increase its efficacy in treating Ulcerative Colitis in an *in-vivo* mouse model.

Here, in **Figure 5.4A**, we found that simple chitosan nanoparticles released drug (melatonin) about $74.43 \pm 4.5\%$ at pH 1.2, $84.53 \pm 3.4\%$ at pH 6.8 and $88.11 \pm 3.35\%$ at pH 7.4 and in **Figure 5.4B** which is $47.14 \pm 2.19\%$ at pH 1.2, $55.27 \pm 2.34\%$ at pH 6.8 and at pH 7.4, $96.47 \pm 3.35\%$ cumulative release. As shown in **Figure 5.4B** with increasing pH there is increase in quantity of drug release which designates that the developed targeted drug delivery system is following pH-dependent drug release. Because chitosan is a cationic polymer, it tends to interact with negatively charged mucus and adhere in the upper GIT due to its acidic nature, preventing drug delivery to the targeted region in Ulcerative Colitis, where the true pathological damage occurs [35] To improve Melatonin's anti-inflammatory activity, which is impaired due to the above qualities of chitosan since it fails to reach the target site. As a result, we expected that covering chitosan nanoparticles with pH-sensitive colon targeting material will enhance melatonin therapeutic efficacy and hence aid to reduce disease severity. Eudragit-S-100coated chitosan nanoparticles would aid in drug delivery and release. We believe that by developing a colon-targeted nano-drug delivery system, we will be able to manage UC disease therapy more efficiently. There are also previously published reports that support our theory that by establishing a colon targeting system, we can more effectively treat the condition [20, 36]. The pH-sensitive nano-delivery system released the drug higher amount of drug at higher pH which is in line with earlier

published report [37] and is more capable in ameliorating UC in mice compared to simple chitosan nanoparticle.

DDsolver software was used to apply multiple mathematical models to understand release kinetics from nano-formulation through dissolution. We investigated drug release for Mel-CSNPs and Mel-EUCSNPs at pH 1.2, 6.8, and 7.4 using the best fitted dissolution models of the Weibull model, namely Mel-CSNPs ($R^2=0.9971$ pH1.2, $R^2= 0.9961$ pH6.8, $R^2=0.9950$ pH7.4) and Mel-EUCSNPs ($R^2= 0.9887$ pH1.2, $R^2= 0.9948$ pH6.8, $R^2=$ This method could more precisely explain the release kinetics from both formulations than other known mathematical models, as illustrated in **Figure 5.4 C-5.4 E-5.4 G** and **5.4D-5.4G-5.4H**. The shape parameter of the Weibull method is β whose value is used to determine whether the dissolution profile is exponential ($\beta =1$), sigmoidal S-shaped with upward curvature followed by turning point ($\beta >1$), or parabolic with high starting slope ($\beta <1$) [38]. Here, in our study we have measured β value values for analysis of dissolution profile which was $\beta= 0.391$ Mel-CSNP and $\beta= 0.540$ Mel-EUCSNPs at pH 7.4. As a result, the shape parameter derived after using the Weibull mathematical model suggests a parabolic and steep site specific dissolving profile of drug from both formulations at different pH levels, as shown in **Figure 5.4**.

5.1.4 Nitrite estimation

Nitric oxide ($\text{NO}\bullet$) is a signaling molecule that functions as a mediator in a variety of physiological processes. It is produced by nitric oxide synthase isoforms that mediate the immunological process. $\text{NO}\bullet$ is essential in the advancement of inflammatory signaling that leads to pathogenic infiltration of the immune system [39]. Nitrite (NO_2^-) is a later outcome of $\text{NO}\bullet$ that can be utilized to measure the degree of inflammation created by macrophages in response to bacterial lipopolysaccharide activation, as well as the anti-inflammatory activity of various pharmacological treatments. In **Figure 5.5** Mel-CSNPs and Mel-EUCSNPs presented marked drop in NO_2^- production upon treatment with formulation. As shown in **Figure 5.5** Mel-CSNPs showed significantly improved NO_2^- scavenging compared to Mel-EUCSNPs. Melatonin facilitates anti-inflammatory activity by NO scavenging which is supported by earlier published literature [40]. The NO scavenging activity of Mel-CSNPs is better compared to bare melatonin which is stated in our earlier work [41]. Mel-CSNPs' enhanced potency could be attributed to the cationic nature of chitosan nanoparticles, which are readily absorbed by macrophages. Furthermore, when coated with negatively charged Eudragit-S-100, the cationic nature is compromised, resulting in lower *in-vitro* efficacy.

However, Eudragit-S-100's limitation proves advantageous in an *in-vivo* system, resulting in delayed pH dependant release.

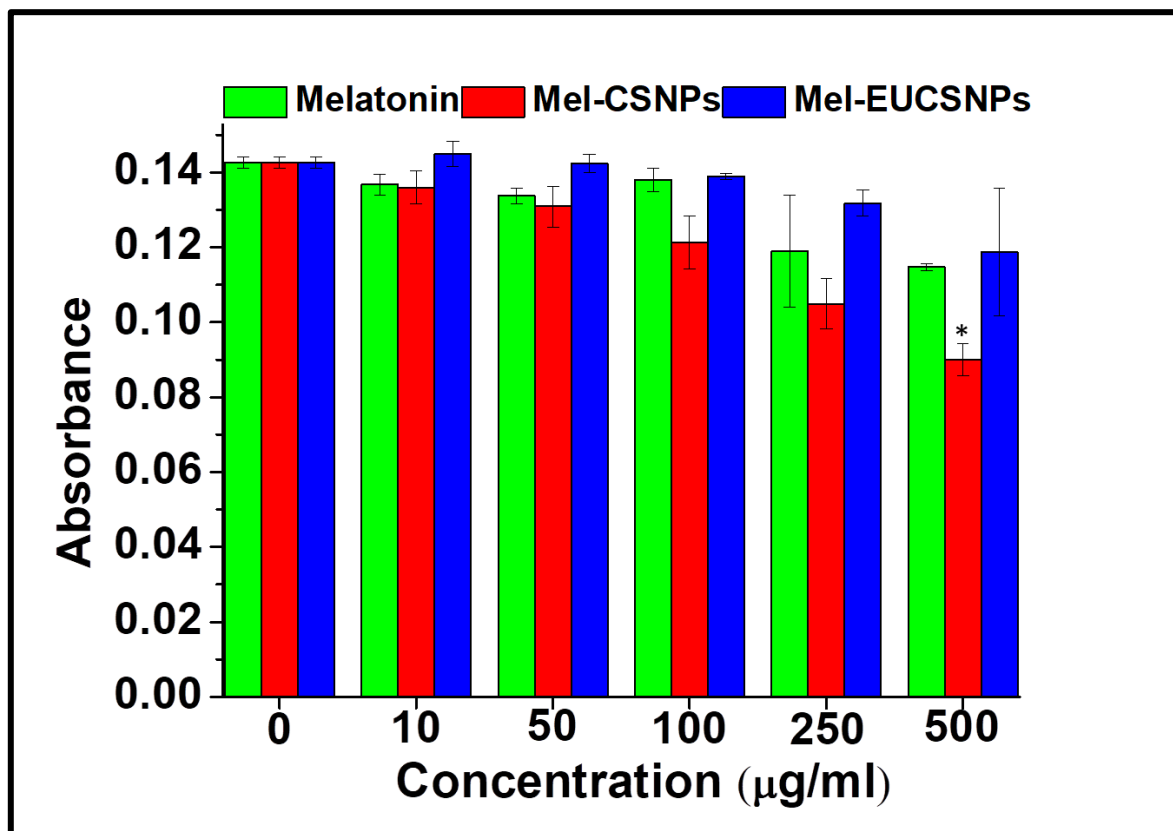


Figure 5.5: Nitric Oxide (NO) scavenging activity of Melatonin, Mel-CSNPs and Mel-EUCSNPs in LPS stimulated RAW 264.7 macrophages.

5.1.5 Bio-distribution study

In order to inspect whether the nanoparticle system is competent to reach the preferred target colonic site when given orally, we have conducted a bio-distribution study. To conduct this experiment, we loaded nanoparticles with Indocyanine Green, a near-infrared fluorescent dye (ICG). ICG is an amphiphilic dye that emits fluorescence in the near-infrared spectral region (700-900 nm), allowing for deep signal extraction from tissues with minimal interference from auto-fluorescence [42]. Apart from this, it has several clinical applications in the realm of diagnostics, such as assessing cardiac output, ocular angiography, and liver clearance [43-45].

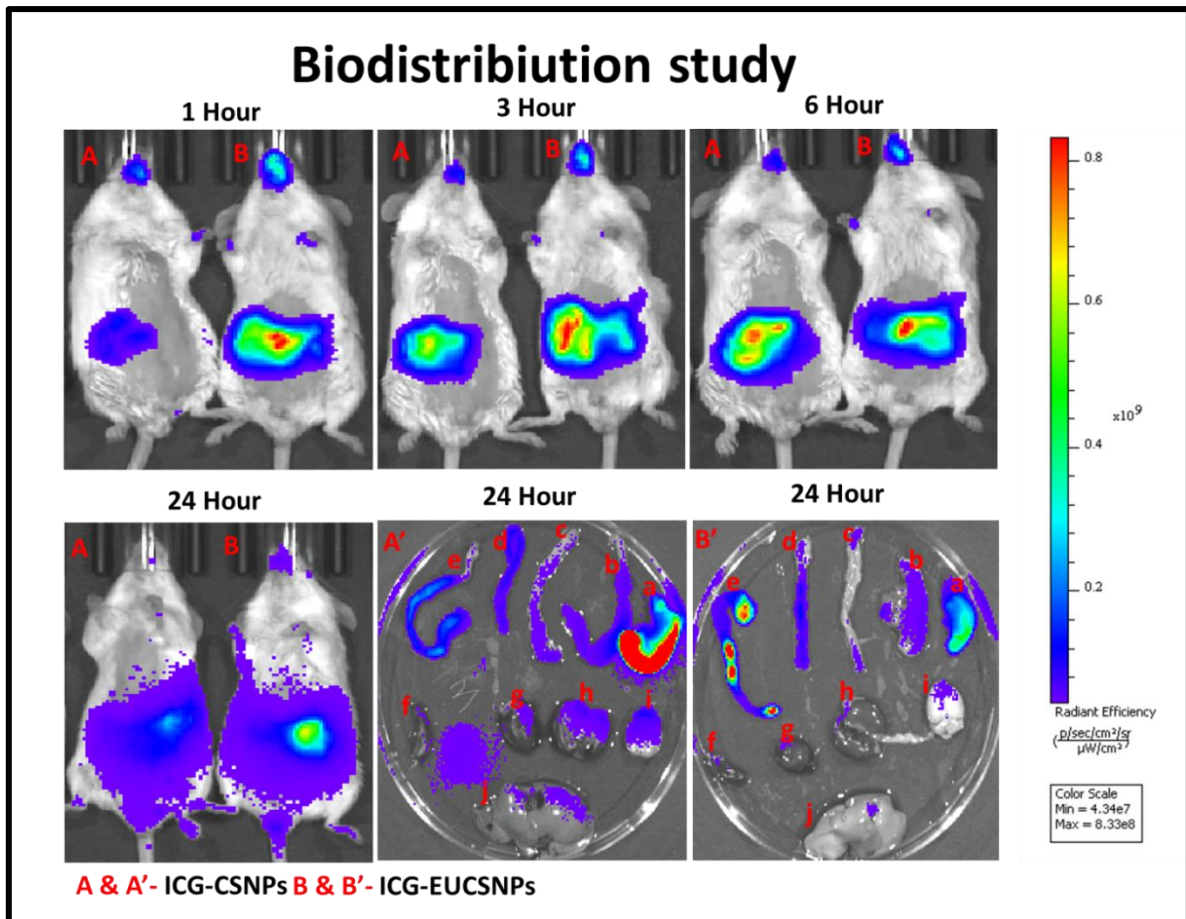


Figure 5.6: Biodistribution study: (A) In-vivo & (A') ex-vivo bio-distribution analysis of Indocyanine green-Chitosan nanoparticle (ICG-CSNPs); (B) & (B') In-vivo bio-distribution analysis of Indocyanine green- Eudragit-S-100 coated Chitosan nanoparticle (ICG-EUCSNPs)(a=stomach, b=duodenum, c=jejunum, d= ileum, e=colon, f=spleen, g=heart, h=kidney, i=brain and j=liver).

In **Figure 5.6**, we found that ICG-loaded chitosan nanoparticles accumulated in the upper gastrointestinal tract GIT when imaged with a fluorescence whole body animal imager IVIS (Perkin Elmer), whereas ICG-loaded colon targeted nanoparticles reached the desired target site, as evidenced by a robust radiant efficiency signal in mouse organs when imaged ex-vivo after sacrificing the mice after 24 hours of administration. After sacrificing mice, all essential organs were scanned for radiant efficiency signal assessment. The stomach (for CSNPs) and colon (for ICG-EUCSNPs) showed the strongest expression for radiant efficiency. As a result, the findings demonstrate that the developed colon-targeted nanoparticle system has met the criterion for a targeted nanocarrier system to treat Ulcerative colitis in mice.

5.1.6 *In-vivo* therapeutics

The murine model of Ulcerative colitis was established using earlier reported protocol with Dextran Sulphate Sodium (DSS, 36-50 kDa) for 5 days in drinking water at 5% (w/v, 200 ml given initially) to evaluate the therapeutic efficacy of Mel-CSNPs and Mel-EUCSNPs [46, 47]. Daily bodyweights were measured for each group to check for gross changes in order to evaluate the efficacy of nano-formulations for oral delivery in the UC mice model. Weight loss is the most noticeable symptom in UC patients due to low dietary status [48]. As seen in **Figure 5.7A**, percentage changes in body weight have been provided to measure disease severity. It is obvious that the DSS group lost weight significantly more than the control groups who solely received drinking water. When UC mice were given Melatonin nano-formulations, they improved significantly from 5 to 7 days. On day 7, the DSS group lost 23.7% of their body weight. On day 7, the DSS + Melatonin loaded chitosan nanoparticles (Mel-CSNPs) groups lost 19.17% of their body weight. DSS+ Melatonin loaded Eudragit-S-100 coated chitosan nanoparticles reduced body weight by 6.33%. The enhanced protection against body weight loss in Mel-EUCSNPs supports our theory that chitosan nanoparticle coating may effectively strengthen melatonin's therapeutic potential to reduce inflammatory pathology in UC mice. This is also supported by data from days 5 to 7 when Mel-EUCSNPs showed a considerable improvement in pathological severity compared to Mel-CSNPs. Our findings imply that melatonin protects against DSS-induced UC pathology, which is consistent with previous research [49, 50]. Furthermore, Mel-CSNPs, when administered intravenously, provide greater protection than melatonin alone [41]. However, because the intravenous route has several disadvantages such as sterility, isotonicity, and patient compliance, we designed a targeted oral nano-formulation that can overcome the aforementioned drawbacks. Furthermore, as shown in **Figure 5.7A**, the colon-targeted nano-delivery system provides greater protection when compared to simple chitosan nanoparticles (Mel-CSNPs).

Based on different gross pathological parameters, the Disease Activity Index (DAI) is calculated to assess the degree of UC pathology in mice. In **Figure 5.7B**, the group getting only 5% DSS had a significant increase in DAI of roughly 3.3 on the final day, but the control group receiving only drinking water had no such value. When we examined Mel-CSNPs with Mel-EUCSNPs, we discovered substantial differences, with Mel-EUCSNPs providing stronger protection than Mel-CSNPs, as shown in **Figure 5.7B**. On the final day, Mel-CSNPs had a DAI of 2.3, whereas Mel-EUCSNPs had a DAI of 0.8, which is

considerably superior in protection than the previous day, confirming our theory and can be applied to clinical therapy of UC.

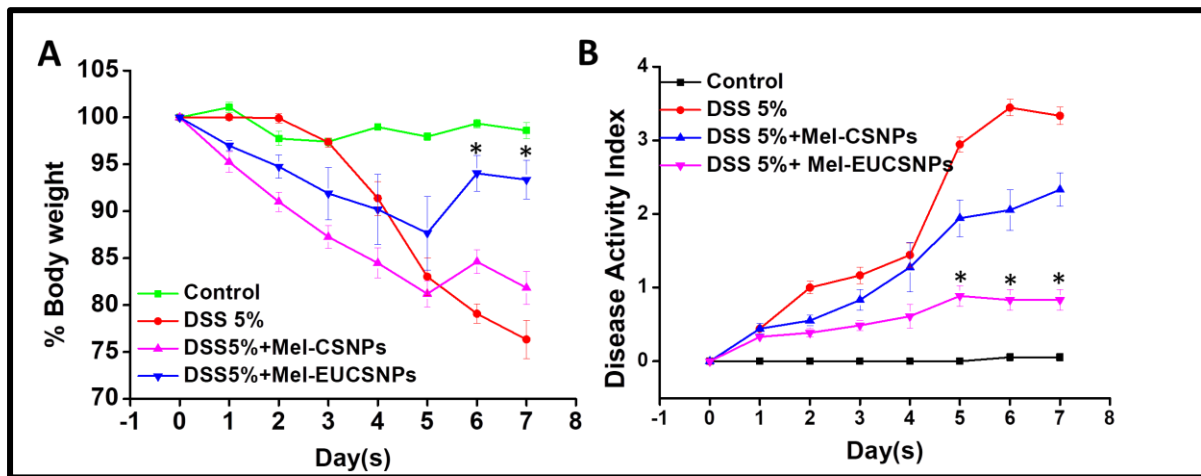


Figure 5.7: (A) Percentage body weight (daily) (B) Disease Activity Index analysis for assessing the inflammatory pathology.

5.1.7 Myeloperoxidase (MPO) Assay

MPO activity can be used to determine the level of invasion of granulocytes such as neutrophils, which express this enzyme. Enhanced neutrophilic infiltration worsens disease severity. As a result, the MPO assay can be used to calculate the extent of inflammation and infiltration. There is a large body of clinical data that HOCL/OCL- and hypochlorite synthesized by MPO induces lipid peroxidation, which leads to inflammation and associated pathologies [51, 52]. Melatonin suppresses MPO which can be more useful in mitigating the inflammatory pathogenesis [53]. In this investigation, we observed that Mel-EUCSNPs revealed higher efficacy by reducing MPO expression and activity, which is a major marker of inflammatory response in colonic tissue (**Figure 5.8**). MPO activity was considerably reduced in **Figure 5.8**, indicating that Mel-EUCSNPs (0.59 U/mg) outperformed Mel-CSNPs (1.16 U/mg). The aforesaid findings support the idea that it has superior anti-inflammatory efficacy due to colon targeting as a drug available at the site of pathology owing to an enhanced nano-delivery mechanism. As a result, as compared to Mel-CSNPs, the colon targeted nanoparticle approach has outstanding MPO reduction activity via reducing neutrophilic infiltration to reduce UC in mice.

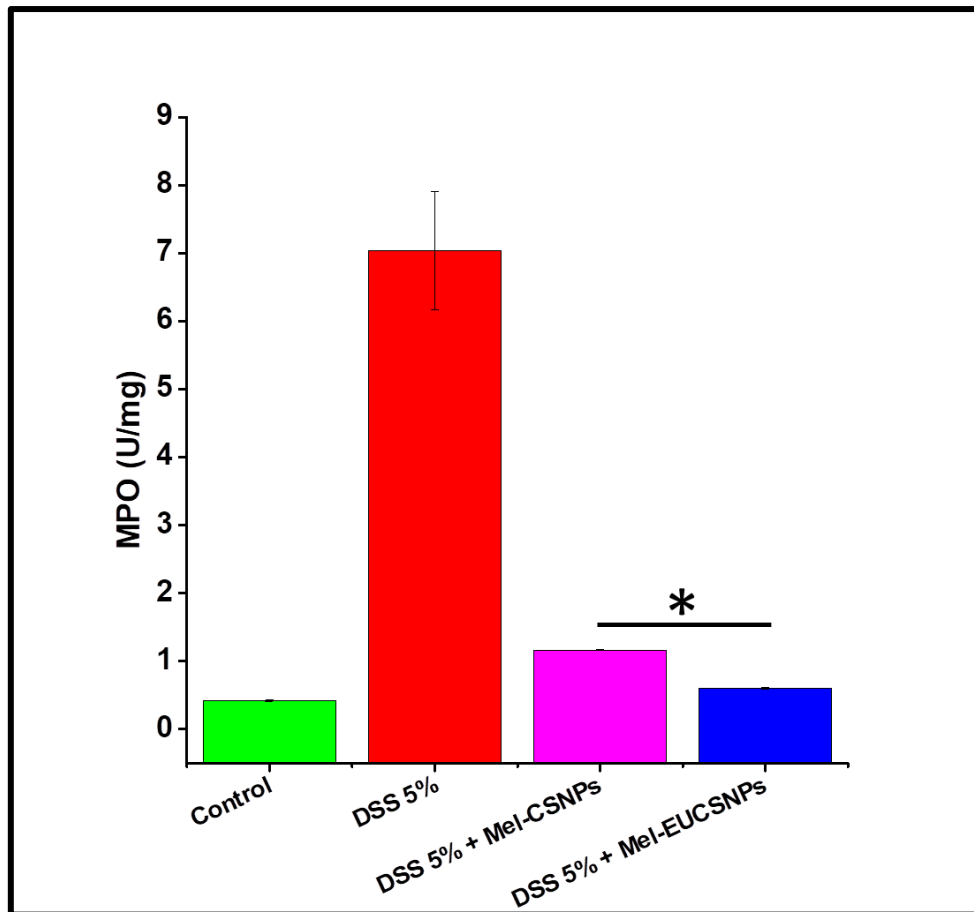


Figure 5.8: Myeloperoxidase assay in colon tissue homogenates to determine degree of neutrophilic infiltration.

5.1.8 Western Blot

Nitric Oxide Synthase 2 (NOS2) is involved in the acute inflammatory phase in macrophages, which is important in disease progression. NOS2 produces $\text{NO}\bullet$, which is mutagenic and can promote nitrosative and oxidative damage [39]. NOS2 up regulation leads to an increase in inflammatory pathophysiology. NOS2 is abundantly expressed in M1 macrophages and can serve as a unique marker for macrophages when activated by bacterial lipopolysaccharide. Because NOS2 is activated by lipopolysaccharide, it is also known as inducible nitric oxide synthase (iNOS) in macrophages. Furthermore, in the case of UC, M1 macrophages infiltrate, causing an acute inflammatory response and worsening the pathophysiology [54]. Melatonin is known to suppress NOS2 through suppressing NF- κ B activity and nuclear translocation [55].

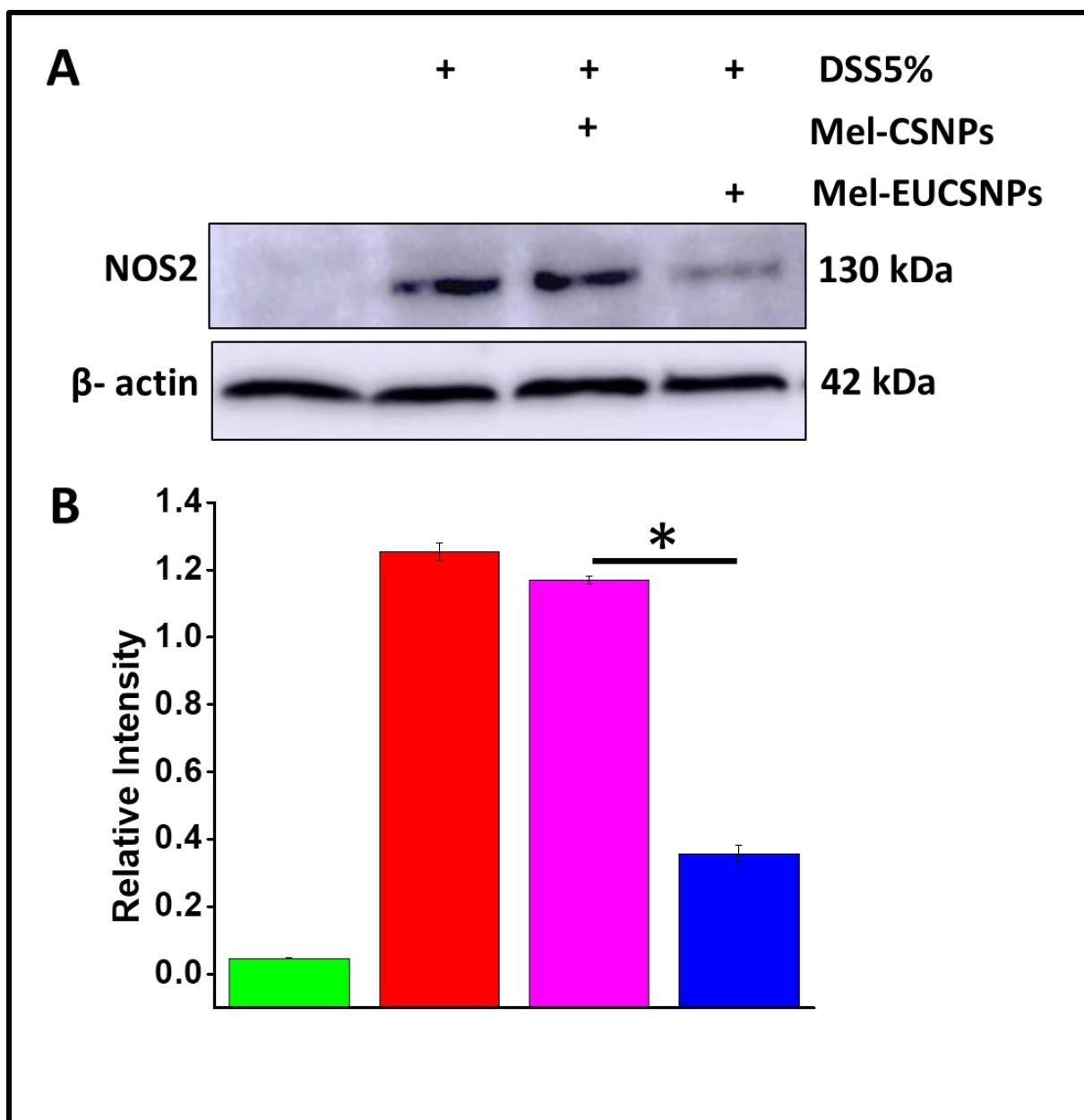


Figure 5.9: (A) Expression of Nitric oxide synthase 2 (NOS2) in colon tissue lysate (B) Densitometry analysis of Nitric oxide synthase 2 (NOS2) in colon tissue lysate Western Blot expression of Nitric oxide synthase 2 (NOS2).

DSS-treated colonic tissue homogenate has a high level of NOS2 expression, as seen in **Figure 5.9**, whereas groups treated with Mel-CSNPs and Mel-EUCSNPs had a significant decrease in NOS2 expression. Furthermore, Mel-EUCSNPs outperformed Mel-CSNPs in terms of protection due to their colon-targeted drug release.

5.1.9 Histology

Haematoxylin and Eosin (H&E) staining offers a thorough examination of histo-architectural changes that occur during disease states. Pathological characteristics such as crypt damage, neutrophil infiltration, epithelial damage, and so on are obviously visible. We examined the damage that occurs in UC in **Figure 5.10A** to determine the efficacy of colon-targeted nano-formulation. The group which received only DSS presented a histological score of 8.5 ± 0.71 , indicating extremely severe tissue damage. Furthermore, this score was lowered in the DSS + Mel-CSNPs group to 5.16 ± 0.30 and in the DSS + Mel-EUCSNPs group to 2.5 ± 0.34 indicating their efficacy in attenuating tissue damage in the UC condition. Histological scoring is done to evaluate the degree of inflammatory pathology that has occurred during the UC condition in mice, like crypt damage, muscle thickening, immune cell infiltration etc.,[56].

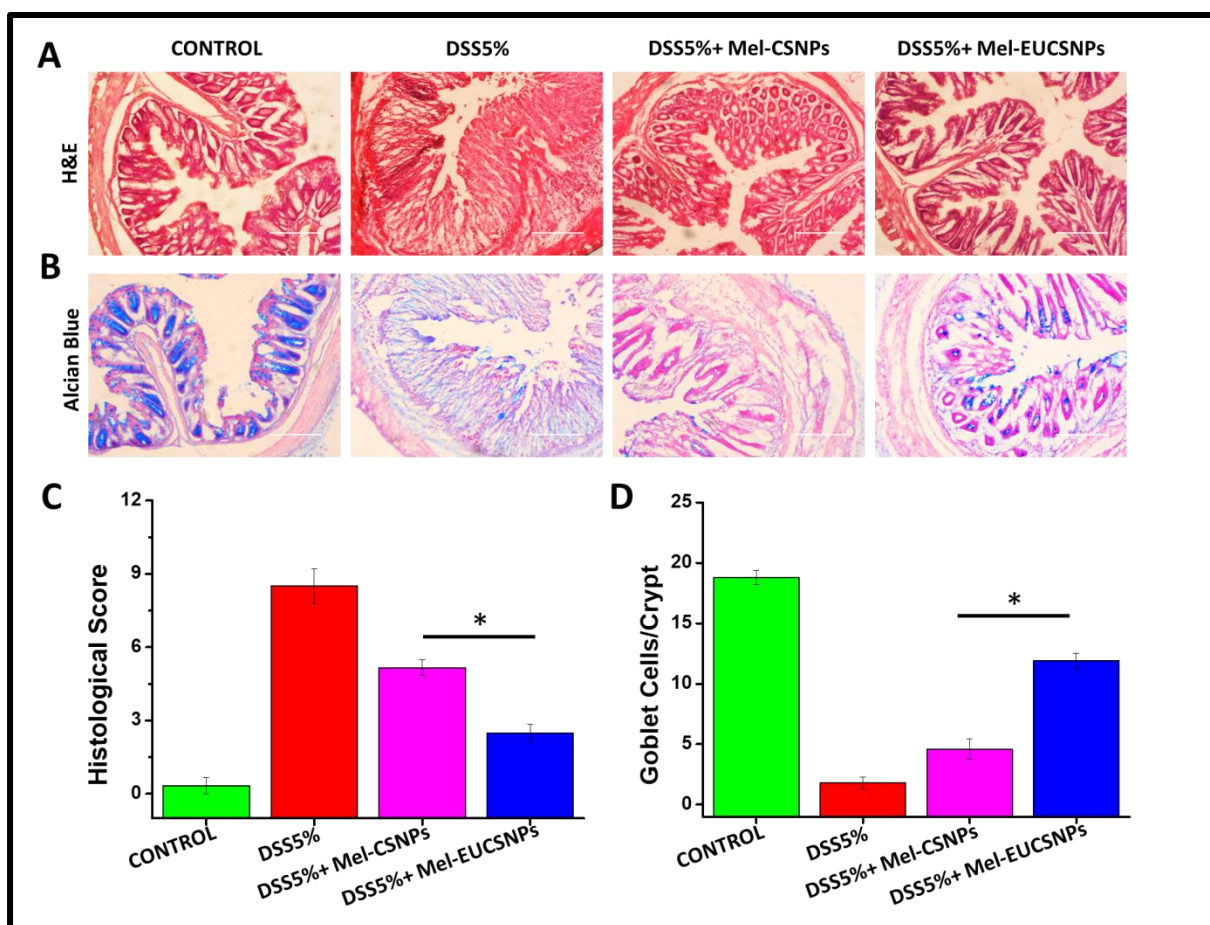


Figure 5.10: (A) Haematoxylin & Eosin (H&E) stain of colon sections (B) Alcian blue stain for goblet cells stain (C) Histological score for determining degree of inflammation in H&E

stained cross section (10 μ m) of colon (D) Goblet cell number per crypt in cross section (10 μ m) of colon.

Goblet cells play an important role in the maintenance of gut homeostasis by generating a defensive mucosal layer on the epithelial surface, establishing the first line of defense in the gut. However, during UC disease, this barrier is almost reduced owing to epithelial layer washout, which allows bacteria and other pathogenic agents to come into direct contact with the epithelial layer. Because the epithelium layer is already injured, this toxic agent induces disease exacerbation, resulting in increased disease severity. Goblet cell alterations or depletion are linked to UC pathophysiology [57]. As depicted in **Figure 5.10B**, goblet cells were almost depleted in only the DSS-treated group (1.8 \pm 0.48 cells/crypt), but treatment with colon-targeted nano-formulation reduced severity (11.9 \pm 0.64 cells/crypt), indicating the efficacy of nano-formulation against DSS-induced goblet cell depletion.

5.1.10 Immuno-histochemical analysis

Activation of the pro-inflammatory cytokine interleukin-1 β (IL-1 β), which play an important in the onset of pain, inflammation, and autoimmune diseases [58]. Cells such as monocytes, macrophages, natural killer cells, activated T and B cells release cytokines from the IL-1 family [59]. IL-1 β immunohistochemistry expression can be employed to determine the extent of inflammatory damage exhibited in colonic tissue cross-sections during disease progression [60]. Melatonin's anti-inflammatory properties have been shown to suppress the expression of pro-inflammatory cytokines such as IL-1 β [61]. Melatonin-loaded nano-formulation suppressed IL-1 β expression, which is consistent with previously published findings [62, 63]. In **Figure 5.11**, higher IL-1 β fluorescence intensity indicates a greater severity of inflammatory pathology after the DSS challenge. Mel-EUCSNPs reduce fluorescence intensity more than Mel-CSNPs, indicating their therapeutic potential as UC treatment in mice.

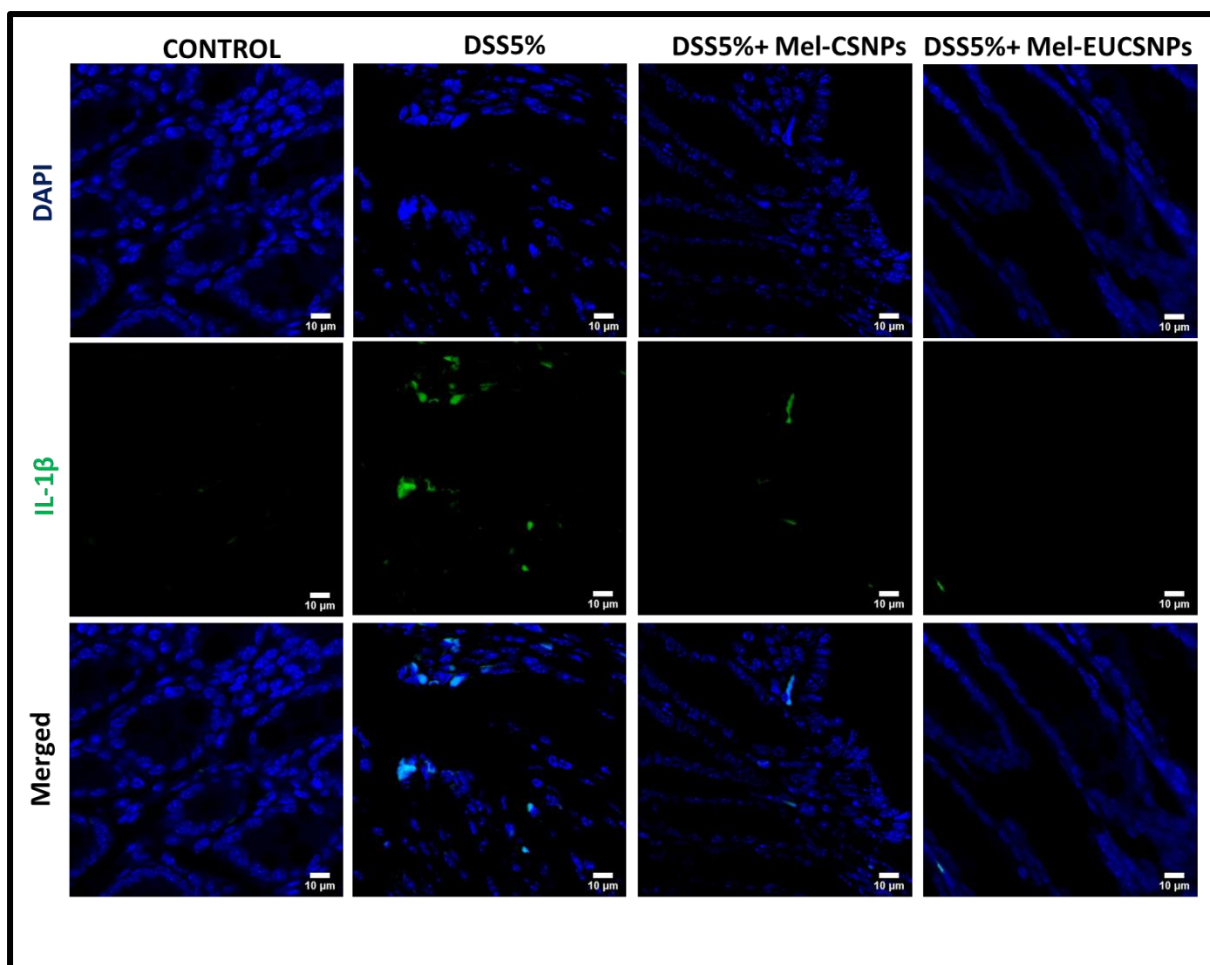


Figure 5.11: Immuno-histochemical expression analysis of Interleukin 1- β (IL-1 β) in cross section (10 μ m) of colon tissue.

5.2 Conclusion

In this investigation, we found that CSNPs coated with colon targeting polymer (Eudragit-S-100) showed pH-dependent and prolonged drug release, potentially enhancing melatonin's efficacy due to prolonged release to the target colon region. If administered orally, CSNPs fail to reach the intended colonic region, but when coated with Eudragit-S-100, they reach the target site, as proven by a bio-distribution study. The colon-targeted nanoparticles also demonstrated a pH-dependent release profile, indicating that drug is released in the colonic region when pH is 6-8. We evaluated the therapeutic efficacy of Mel-CSNPs and Mel-EUCSNPs in an in-vivo UC mouse model, and the results show that colon-targeted nanoparticles outperform Mel-CSNPs. We propose that the preclinical results of colon-targeted nanoparticle systems indicate the potential for future drug delivery systems for UC management.

Note:

*The following published works was included into the current thesis with the authors, corresponding author's, and publisher's permission. The following works is associated with this chapter:

1) Mohanbhai, S.J., et al., *Colon targeted chitosan-melatonin nanotherapy for preclinical Inflammatory Bowel Disease*. *Biomaterials Advances*, 2022. **136**: p. 212796.

5.3 References

- [1] T. Kobayashi, B. Siegmund, C. Le Berre, S.C. Wei, M. Ferrante, B. Shen, C.N. Bernstein, S. Danese, L. Peyrin-Biroulet, T. Hibi, *Nature Reviews Disease Primers*, 6 (2020) 74.
- [2] T. Hibi, H. Ogata, *J Gastroenterol*, 41 (2006) 10-16.
- [3] G.A. Akerkar, M.A. Peppercorn, *Drugs Aging*, 10 (1997) 199-208.
- [4] K. Matsuoka, T. Kobayashi, F. Ueno, T. Matsui, F. Hirai, N. Inoue, J. Kato, K. Kobayashi, K. Kobayashi, K. Koganei, R. Kunisaki, S. Motoya, M. Nagahori, H. Nakase, F. Omata, M. Saruta, T. Watanabe, T. Tanaka, T. Kanai, Y. Noguchi, K.I. Takahashi, K. Watanabe, T. Hibi, Y. Suzuki, M. Watanabe, K. Sugano, T. Shimosegawa, *J Gastroenterol*, 53 (2018) 305-353.
- [5] N.C. Klein, C.H. Go, B.A. Cunha, *Infectious disease clinics of North America*, 15 (2001) 423-432, viii.
- [6] I.R. Reid, *Clinical endocrinology*, 30 (1989) 83-103.
- [7] J. Upadhyay, N. Trivedi, A. Lal, *Lung*, 198 (2020) 525-533.
- [8] E.R. James, *Journal of ocular pharmacology and therapeutics : the official journal of the Association for Ocular Pharmacology and Therapeutics*, 23 (2007) 403-420.
- [9] V. Srinivasan, W.D. Spence, S.R. Pandi-Perumal, R. Zakharia, K.P. Bhatnagar, A. Brzezinski, *Gynecological endocrinology : the official journal of the International Society of Gynecological Endocrinology*, 25 (2009) 779-785.
- [10] S.R. Pandi-Perumal, A.S. BaHammam, G.M. Brown, D.W. Spence, V.K. Bharti, C. Kaur, R. Hardeland, D.P. Cardinali, *Neurotoxicity Research*, 23 (2013) 267-300.
- [11] A. Zafra-Roldán, S. Corona-Avenidaño, R. Montes-Sánchez, M. Palomar-Pardavé, M. Romero-Romo, M.T. Ramírez-Silva, *Spectrochimica Acta Part A: Molecular and Biomolecular Spectroscopy*, 190 (2018) 442-449.
- [12] R.J. Reiter, J.R. Calvo, M. Karbownik, W. Qi, D.X. Tan, *Annals of the New York Academy of Sciences*, 917 (2000) 376-386.
- [13] N. Mohan, K. Sadeghi, R.J. Reiter, M.L. Meltz, *Biochemistry and molecular biology international*, 37 (1995) 1063-1070.
- [14] Jacob S. Lee, Daniel J. Cua, *Cell*, 162 (2015) 1212-1214.
- [15] K. Yeleswaram, L.G. McLaughlin, J.O. Knipe, D. Schabdach, *J Pineal Res*, 22 (1997) 45-51.
- [16] F.P. Gibbs, J. Vriend, *Endocrinology*, 109 (1981) 1796-1798.
- [17] R.L. DeMuro, A.N. Nafziger, D.E. Blask, A.M. Menhinick, J.S. Bertino, Jr., *J Clin Pharmacol*, 40 (2000) 781-784.
- [18] R.H. Prabhu, V.B. Patravale, M.D. Joshi, *Int J Nanomedicine*, 10 (2015) 1001-1018.

- [19] S. Gim, Y. Zhu, P.H. Seeberger, M. Delbianco, *Wiley Interdiscip Rev Nanomed Nanobiotechnol*, 11 (2019) e1558.
- [20] M. Naeem, M.A. Oshi, J. Kim, J. Lee, J. Cao, H. Nurhasni, E. Im, Y. Jung, J.W. Yoo, *Nanomedicine*, 14 (2018) 823-834.
- [21] J. Sarvaiya, Y.K. Agrawal, *Int J Biol Macromol*, 72 (2015) 454-465.
- [22] C. Feng, Z. Wang, C. Jiang, M. Kong, X. Zhou, Y. Li, X. Cheng, X. Chen, *Int J Pharm*, 457 (2013) 158-167.
- [23] L. Lu, G.X. Chen, Y.Y. Qiu, M.W. Li, D.H. Liu, D.H. Hu, X.J. Gu, Z.Y. Xiao, *Sci Bull*, 61 (2016) 670-681.
- [24] M. Naeem, J. Lee, M.A. Oshi, J. Cao, S.P. Hlaing, E. Im, Y. Jung, J.W. Yoo, *Acta Biomater*, 116 (2020) 368-382.
- [25] M. Collado-Gonzalez, Y. Gonzalez Espinosa, F.M. Goycoolea, *Biomimetics (Basel)*, 4 (2019).
- [26] F.Y. Su, K.J. Lin, K. Sonaje, S.P. Wey, T.C. Yen, Y.C. Ho, N. Panda, E.Y. Chuang, B. Maiti, H.W. Sung, *Biomaterials*, 33 (2012) 2801-2811.
- [27] S. Chen, F. Guo, T. Deng, S. Zhu, W. Liu, H. Zhong, H. Yu, R. Luo, Z. Deng, *AAPS PharmSciTech*, 18 (2017) 1277-1287.
- [28] M.B. Subudhi, A. Jain, A. Jain, P. Hurkat, S. Shilpi, A. Gulbake, S.K. Jain, *Materials (Basel)*, 8 (2015) 832-849.
- [29] M. Queiroz, K. Melo, D. Sabry, G. Sasaki, H. Rocha, *Marine drugs*, 13 (2014) 141-158.
- [30] C.M. Cristache, E.E. Totu, G. Cristache, A.C. Nechifor, I.I. Pintilie, *Rev Chim-Bucharest*, 70 (2019) 1089-1093.
- [31] R. Mehta, A. Chawla, P. Sharma, P. Pawar, *J Adv Pharm Technol Res*, 4 (2013) 31-41.
- [32] M. Sharma, V. Sharma, A.K. Panda, D.K. Majumdar, *Int J Nanomedicine*, 6 (2011) 2097-2111.
- [33] A. Sood, A. Dev, S.J. Mohanbhai, N. Shrimali, M. Kapasiya, A.C. Kushwaha, S. Roy Choudhury, P. Guchhait, S. Karmakar, *ACS Applied Nano Materials*, 2 (2019) 6409-6417.
- [34] M. Naeem, J. Bae, M.A. Oshi, M.S. Kim, H.R. Moon, B.L. Lee, E. Im, Y. Jung, J.W. Yoo, *Int J Nanomedicine*, 13 (2018) 1225-1240.
- [35] M.W. TM, W.M. Lau, V.V. Khutoryanskiy, *Polymers (Basel)*, 10 (2018).
- [36] I.O. Tekeli, A. Atessahin, F. Sakin, A. Aslan, S. Ceribasi, M. Yipel, *Inflammopharmacology*, (2018).
- [37] Y. Serkan, A. Kazime Gonca, K. Result, E. Deniz, A. Fusun, *Research Square*, (2021).
- [38] F. Langenbacher, *J Pharm Pharmacol*, 24 (1972) 979-981.
- [39] T. Okamoto, K. Gohil, E.I. Finkelstein, P. Bove, T. Akaike, A. van der Vliet, *Am J Physiol Lung Cell Mol Physiol*, 286 (2004) L198-209.
- [40] Y. Noda, A. Mori, R. Liburdy, L. Packer, *J Pineal Res*, 27 (1999) 159-163.

- [41] J.M. Soni, M.N. Sardoiwala, S.R. Choudhury, S.S. Sharma, S. Karmakar, *Mater Sci Eng C Mater Biol Appl*, 124 (2021) 112038.
- [42] T.K. Hill, A. Abdulahad, S.S. Kelkar, F.C. Marini, T.E. Long, J.M. Provenzale, A.M. Mohs, *Bioconjug Chem*, 26 (2015) 294-303.
- [43] J.M. Maarek, D.P. Holschneider, J. Harimoto, J. Yang, O.U. Scremin, E.H. Rubinstein, *Anesthesiology*, 100 (2004) 1476-1483.
- [44] A. Invernizzi, M. Pellegrini, E. Cornish, K. Yi Chong Teo, M. Cereda, J. Chabblani, *Asia Pac J Ophthalmol (Phila)*, 9 (2020) 335-348.
- [45] L. Lau, C. Christophi, M. Nikfarjam, G. Starkey, M. Goodwin, L. Weinberg, L. Ho, V. Muralidharan, *HPB Surg*, 2015 (2015) 757052.
- [46] M. Perse, A. Cerar, *J Biomed Biotechnol*, 2012 (2012) 718617.
- [47] J.J. Kim, M.S. Shajib, M.M. Manocha, W.I. Khan, *J Vis Exp*, (2012).
- [48] Y. Elsherif, C. Alexakis, M. Mendall, *Gastroenterol Res Pract*, 2014 (2014) 762191.
- [49] X.-W. Liu, C.-D. Wang, *International Immunopharmacology*, 73 (2019) 108-117.
- [50] P.P. Trivedi, G.B. Jena, *Digest Dis Sci*, 58 (2013) 3460-3474.
- [51] D.I. Pattison, M.J. Davies, *Curr Med Chem*, 13 (2006) 3271-3290.
- [52] S.J. Klebanoff, *J Leukoc Biol*, 77 (2005) 598-625.
- [53] S. Galijasevic, I. Abdulhamid, H.M. Abu-Soud, *Biochemistry*, 47 (2008) 2668-2677.
- [54] J.D. Abron, N.P. Singh, R.L. Price, M. Nagarkatti, P.S. Nagarkatti, U.P. Singh, *PLoS One*, 13 (2018) e0199631.
- [55] E. Gilad, H.R. Wong, B. Zingarelli, L. Virág, M. O'Connor, A.L. Salzman, C. Szabó, *Faseb j*, 12 (1998) 685-693.
- [56] H.S. Cooper, S.N. Murthy, R.S. Shah, D.J. Sedergran, *Laboratory investigation; a journal of technical methods and pathology*, 69 (1993) 238-249.
- [57] C.K. Heazlewood, M.C. Cook, R. Eri, G.R. Price, S.B. Tauro, D. Taupin, D.J. Thornton, C.W. Png, T.L. Crockford, R.J. Cornall, R. Adams, M. Kato, K.A. Nelms, N.A. Hong, T.H. Florin, C.C. Goodnow, M.A. McGuckin, *PLoS medicine*, 5 (2008) e54.
- [58] K. Ren, R. Torres, *Brain Res Rev*, 60 (2009) 57-64.
- [59] H.E. Barksby, S.R. Lea, P.M. Preshaw, J.J. Taylor, *Clin Exp Immunol*, 149 (2007) 217-225.
- [60] T. Kanda, A. Nishida, M. Ohno, H. Imaeda, T. Shimada, O. Inatomi, S. Bamba, M. Sugimoto, A. Andoh, *PLoS One*, 11 (2016) e0159705.
- [61] Y.S. Park, S.H. Chung, S.K. Lee, J.H. Kim, J.B. Kim, T.K. Kim, D.S. Kim, H.W. Baik, *Int J Mol Med*, 35 (2015) 979-986.

- [62] T.K. Kim, Y.S. Park, H.W. Baik, J.H. Jun, E.K. Kim, J.W. Sull, H.J. Sung, J.W. Choi, S.H. Chung, M.C. Gye, J.Y. Lim, J.B. Kim, S.H. Kim, *World J Gastroenterol*, 22 (2016) 7559-7568.
- [63] W. Qin, W. Lu, H. Li, X. Yuan, B. Li, Q. Zhang, R. Xiu, *J Endocrinol*, 214 (2012) 145-153.

Chapter 6:

Summary and conclusion

Summary and conclusions

In the context of ulcerative colitis, this thesis investigates and explores the anti-inflammatory effects of melatonin using an epigenetic molecular mechanism. This thesis also presents a nanotherapeutic strategy for the development of polymeric size and pH-dependent nanocarrier systems to enhance the therapeutic effectiveness of melatonin. Utilizing *in-vitro* and *in-vivo* systems, the physicochemical characterization of nanoparticles and the assessment of their anti-inflammatory activity are carried out.

In **Chapter 1** of the thesis, the literature on inflammation and the disorders associated with it is introduced and reviewed. It largely focuses on one of the most common inflammatory illnesses, ulcerative colitis, including its pathophysiology, epidemiology, current therapeutic strategy, and understanding of melatonin as a potential novel anti-inflammatory alternative. The limitations of the present therapeutic agents utilized in the treatment of UC are a major emphasis of the article. Additionally, it emphasizes how inflammation affects both diseases brought on by untreated inflammation as well as the physiological systems that are typical for humans. There has been discussion on the role of epigenetics in UC and the possibility of inhibitors in UC management..

Chapter 2 of the thesis deals with various materials, methods, and techniques executed in the experiments. Protocols for synthesis and characterization of nanoparticles, methods for developing inflammatory models *in vitro* and *in vivo*, etc. have been discussed in this chapter in detail.

Chapter 3 of thesis deals with role melatonin anti-inflammatory effect against *in vitro* (RAW 264.7 murine macrophage) and *in vivo* (DSS induced colitis in mice) models. Investigating the role of melatonin in regulating inflammation via enhancer of zeste homolog 2 (EZH2) in managing Ulcerative colitis has been explored. Exploring molecular interaction between EZH2 and NOS2 has been carried out. In this chapter, melatonin anti-inflammatory activity has been evaluated by estimating nitrite level, gene expression, protein expression, gross pathological features and histological changes in colonic tissue etc. Melatonin was used at a concentration up to 0, 1, 10, 100, 250 and 500 µg/ml against LPS-stimulated RAW 264.7 murine macrophages. The expression of protein biomarkers like EZH2, NOS2, and H3k27me3 has been investigated. It focuses highly on the role of NOS2 in the inflammatory response in macrophages and colitic mice. Interlink between NOS2-EZH2 and their

connection in the progression of inflammation leading to Ulcerative Colitis. Physical interaction between EZH2-NOS2 and the binding of EZH2 on the promoter region of NOS2 has been explored in this chapter. Body weight loss, disease activity index and colon length have been investigated. Hematoxylin and eosin, alcian blue-nucleus red and toluidine blue staining have been performed for evaluating histo-architecture alterations. For the purpose of assessing their expression, immunofluorescence labeling of EZH2 and NOS2 was done.

Chapter 4 of the thesis deals with the formulation of chitosan nanoparticles for the delivery of melatonin in *in-vitro* and *in-vivo* inflammatory model. Chitosan nanoparticles were prepared by ionic gelation method and loaded with an anti-inflammatory agent to evaluate its anti-inflammatory efficacy. Characterization of nanoparticles was carried out by dynamic light scattering measurement for estimating the mean hydrodynamic size of nanoparticles, zeta potential to confirm a charge on the surface of nanoparticles, and transmission electron microscopy for confirming their spherical morphology. *In-vitro* cumulative release, cell viability, nitrite level, and cellular uptake for nanoparticles have been discussed in this chapter. Nuclear translocation of NF- κ B has been also performed to check its migration from cytosol to nucleus. Moreover, a bio-distribution study of chitosan nanoparticles has been discussed. Gross pathological changes like disease activity index, weight loss, colon length, gene expression, myeloperoxidase assay, and histological studies have been discussed for the same. An immunofluorescence study for evaluating the expression of NOS2 and nitro-tyrosine in the colon has been explored in this chapter.

Chapter 5 of the thesis deals with the formulation of the colon targeted chitosan nanoparticles for a specific colon delivery of melatonin in the colitic mice. Chitosan nanoparticles were prepared using ionic gelation method as mentioned earlier and were coated with enteric coating polymer like Eudragit-S-100. Characterization of nanoparticles was carried out by dynamic light scattering measurement for estimating the mean hydrodynamic size of nanoparticles, and transmission electron microscopy for confirming their spherical morphology and enteric coating on the surface of chitosan nanoparticles and FTIR to confirm any changes in its chemical nature. *In vitro* drug release studies at various physiological pH and their best-fitted models have been discussed. Bio-distribution study to confirm the specific colon targeting has been discussed. Gross pathological changes like disease activity index, weight loss, colon length, myeloperoxidase assay and histological studies have been discussed for the same. An immunofluorescence study for evaluating the expression of IL-1 β and immune blot for NOS2 in colon has been explored in this chapter.

In light of this, we can say that the thesis contributes to our understanding of how epigenetic regulation in inflammatory macrophages contributes to melatonin's anti-inflammatory effect. By overcoming the limitations of premature drug release and nonspecific drug targeting, colon-targeted nanodelivery systems might lessen the severity of ulcerative colitis more efficiently than bare drugs alone. If expanded to human research, this colon-targeted nanodelivery method indicates positive insight to be extremely successful.

Curriculum Vitae

Soni Jignesh Mohanbhai

Ph.D. Research Scholar,

Institute of Nanoscience and Technology (INST),

Indian Institute of Science Education and Research (IISER),

Mohali, Punjab- India.



Soni Jignesh Mohanbhai is a Ph.D. research scholar at the Institute of Nanoscience and Technology and registered under the Indian Institute of Science Education and Research, Mohali (Punjab). His research is focused on developing a melatonin-mediated therapeutic approach for the treatment of Inflammatory Bowel Disease (IBD). After completing his M.S. in Pharmacology and Toxicology from NIPER-Raebareli, he came to Mohali to pursue his dream of completing his doctoral research. Initially, he joined as a project-JRF that was later converted into a doctoral degree program. He has co-authored several research articles and presented his work on various platforms. His current research focuses on understanding epigenetic molecular mechanisms and developing targeted nano-carriers to alleviate IBD.